

**Igor Rafael Correia Rocha**

**Estudo dos Efeitos da Fotobioestimulação sobre a Neuropatia  
Diabética Periférica**

**Tese apresentada ao Programa em Biologia de Sistemas do  
Instituto de Ciências Biomédicas da Universidade de São  
Paulo, para obtenção do Título Doutor em Ciências.**

**São Paulo  
2023**

**Igor Rafael Correia Rocha**

**Estudo dos Efeitos da Fotobioestimulação sobre a Neuropatia  
Diabética Periférica**

**Tese apresentada ao Programa em Biologia de Sistemas  
do Instituto de Ciências Biomédicas da Universidade de  
São Paulo, para obtenção do Título Doutor em Ciências.**

**Área de concentração:** Biologia Morfofuncional

**Orientador:** Prof.<sup>a</sup> Dr.<sup>a</sup>. Marucia Chacur

**Versão Corrigida**

**São Paulo  
2023**

CATALOGAÇÃO NA PUBLICAÇÃO (CIP)  
Serviço de Biblioteca e informação Biomédica  
do Instituto de Ciências Biomédicas da Universidade de São Paulo

Ficha Catalográfica elaborada pelo(a) autor(a)

Correia Rocha , Igor Rafael  
Estudo dos Efeitos da Fotobioestimulação sobre a  
Neuropatia Diabética Periférica / Igor Rafael  
Correia Rocha ; orientador Marucia Chacur. -- São  
Paulo, 2023.  
100 p.

Tese (Doutorado) -- Universidade de São Paulo,  
Instituto de Ciências Biomédicas.

1. Citocinas. 2. Diabetes . 3. Estrepto-zotocina.  
4. Neuropatia . 5. Rato. I. Chacur, Marucia ,  
orientador. II. Título.

Candidato(a): **Igor Rafael Correia Rocha**

Título da Dissertação/Tese: **Estudo dos Efeitos da Fotobioestimulação sobre a Neuropatia Diabética Periférica**

Orientador: Prof(a) Dr(a) **Marucia Chacur**

A Comissão Julgadora dos trabalhos de Defesa da Dissertação de Mestrado/Tese de Doutorado, em sessão pública realizada a ...../...../....., considerou o(a) candidato(a):

(    ) **Aprovado(a)**            (    ) **Reprovado(a)**

Examinador(a):                      Assinatura: .....  
Nome: .....  
Instituição: .....

Examinador(a):                      Assinatura: .....  
Nome: .....  
Instituição: .....

Examinador(a):                      Assinatura: .....  
Nome: .....  
Instituição: .....

Presidente:                              Assinatura: .....  
Nome: .....  
Instituição: .....



## CERTIFICADO

Certificamos que a proposta intitulada "Estudo dos efeitos da fotobioestimulação sobre a neuropatia diabética periférica", protocolada sob o CEUA nº 2269190619, sob a responsabilidade de **Marucia Chacur e equipe; Igor Rafael Correia Rocha; Nathalia Lopes Ferreira; Matheus Cerussi de Souza; Ariela de Oliveira Pedro Bom** - que envolve a produção, manutenção e/ou utilização de animais pertencentes ao filo Chordata, subfilo Vertebrata (exceto o homem), para fins de pesquisa científica ou ensino - está de acordo com os preceitos da Lei 11.794 de 8 de outubro de 2008, com o Decreto 6.899 de 15 de julho de 2009, bem como com as normas editadas pelo Conselho Nacional de Controle da Experimentação Animal (CONCEA), e foi **aprovada** pela Comissão de Ética no Uso de Animais da Instituto de Ciências Biomédicas (Universidade de São Paulo) (CEUA-ICB/USP) na reunião de 11/10/2019.

We certify that the proposal "Study of the effects of photobiostimulation on peripheral diabetic neuropathy", utilizing 120 Heterogenics rats (120 males), protocol number CEUA 2269190619, under the responsibility of **Marucia Chacur and team; Igor Rafael Correia Rocha; Nathalia Lopes Ferreira; Matheus Cerussi de Souza; Ariela de Oliveira Pedro Bom** - which involves the production, maintenance and/or use of animals belonging to the phylum Chordata, subphylum Vertebrata (except human beings), for scientific research purposes or teaching - is in accordance with Law 11.794 of October 8, 2008, Decree 6899 of July 15, 2009, as well as with the rules issued by the National Council for Control of Animal Experimentation (CONCEA), and was **approved** by the Ethic Committee on Animal Use of the Biomedical Sciences Institute (University of São Paulo) (CEUA-ICB/USP) in the meeting of 10/11/2019.

Finalidade da Proposta: **Pesquisa (Acadêmica)**

Vigência da Proposta: **48 meses**

Depto/Setor: **Anatomia**

Origem: **Biotério de Produção de Ratos da Rede de Biotérios da USP - Profa. Dra. Zuleica Bruno Fortes**

Espécie: **Ratos heterogênicos**

sexo: **Machos**

Idade ou peso: **50 a 60 dias**

Linhagem: **Rattus norvegicus/Wistar**

**N amostral: 120**

São Paulo, 30 de janeiro de 2021



Profa. Dra. Luciane Valéria Sita

Coordenadora da Comissão de Ética no Uso de Animais  
Instituto de Ciências Biomédicas (Universidade de São Paulo)



Dr. Alexandre Ceroni

Vice-Coodenador da Comissão de Ética no Uso de Animais  
Instituto de Ciências Biomédicas (Universidade de São Paulo)

## **Agradecimentos**

À Deus e ao Nosso Senhor Jesus Cristo por ter tornado todos os meus sonhos realidade e por Ser Presente em Minha Vida.

Ao Departamento de Anatomia, Instituto de Ciências Biomédicas da Universidade de São Paulo (ICB-USP), e aos Programas de Pós-Graduação em Ciências Morfofuncionais e Biologia de Sistemas, minha casa por 10 anos, por toda infraestrutura oferecida para o desenvolvimento deste trabalho e por todas as oportunidades que surgiram a partir dele.

À minha orientadora, Profa. Dra. Marucia Chacur por ter me acolhido em seu laboratório por todos esses 10 anos. Sou imensamente grato.

Aos técnicos de laboratório Kelly Patrícia, Marta Maria, Marina Fevereiro, Sônia Regina e Ricardo Bandeira. Muito grato por terem sempre me recebido com braços e sorrisos abertos em seus laboratórios. Esse carinho, cuidado e confiança em mim tem grande contribuição no desenvolvimento do meu projeto de pesquisa. Aos técnicos do complexo didático Everton Luis, Fabio França, Milton Ferreira e Nilson Silva que grandemente contribuíram para meu aprendizado em anatomia humana. A todos que compõem a equipe da secretaria do Departamento de Anatomia, em especial Patrícia Rocha.

Aos meus colegas de laboratório, os de ontem e os de hoje. Gratidão.

Aos meus amigos Aline Kelly, Rodolpho Ornitz e Fábio Martinez. Pessoas especialíssimas que desejo ter sempre por perto.

Aos Professores (as) Ariel Silber, Edson Liberti, Renata Frazão, Patrícia Castelucci, Katiucia Batista, Cecília Gouveia, Maria Inês, Camila Dalle.

Com TODO meu carinho, admiração e respeito, meu mais que especial agradecimento à Profa. Dra. Maria Luiza Moraes Barreto de Chaves.

À Comissão Examinadora da minha defesa de doutorado, Professor Dr. Adriano Polican Ciena, Professora Dra. Andréa da Silva Torrão e Professora Dra. Maria Luiza Moraes Barreto de Chaves (membros titulares) e ao Pesquisador Dr. Rodolpho Ornitz Oliveira, Professora Dra. Alice Cristina Rodrigues e a Professora Dra. Patrícia Castelucci (membros suplentes).

Obrigado a todos por toda contribuição técnico-científica, por todo respeito e carinho e por compartilharem comigo momentos tão especiais para minha formação e carreira.

**OBRIGADO.**

### **Agradecimento à agência de fomento**

O presente trabalho foi realizado em sua totalidade com apoio da **Fundação de Amparo à Pesquisa do Estado de São Paulo (FAPESP)**. Processo FAPESP 2017/25554-0.

## RESUMO

**Rocha, I.R.C.** Estudo dos Efeitos da Fotobioestimulação sobre a Neuropatia Diabética Periférica. 2023. Número de folhas (100f). Tese (Doutorado em: Departamento de Anatomia) – Instituto de Ciências Biomédicas, Universidade de São Paulo, 2023.

O dano celular primário oriundo das células de Schwann em situação de hiperglicemia é um aspecto em grande parte esquecido em termos de neuropatia diabética periférica (NDP). Em contrapartida, os mecanismos pelos quais a fotobioestimulação (FBE) gera seus efeitos promissores ainda é campo de extensa investigação. Pouco se sabe sobre os efeitos da FBE sobre a NDP. A partir disso, o objetivo deste estudo foi investigar os possíveis mediadores envolvidos no efeitos anti-hiperalgésico / anti-inflamatório da FBE em ratos com NDP induzida por estreptozotocina (STZ), assim como, os efeitos da FBE sobre a respiração celular de células de Schwann. Os experimentos foram aprovados pela Comissão de Ética no Uso de Animais (CEUA/ICB-USP), protocolo 2269190619. Ratos Wistar, machos, 200-250 g, 8-9 semanas, receberam dose única de STZ (85 mg/kg) ou veículo (salina) por via intraperitoneal (i.p). O diabetes tipo I foi determinado por glicemia  $\geq 250$  mg/dL. Os animais foram submetidos ao teste de von Frey eletrônico 72 horas após a injeção de STZ ou veículo (salina) e em dias alternados ao tratamento com a FBE. Ratos diabéticos hiperalgésicos foram submetidos à FBE (AsGa, 904 nm; 6 J; 45 mW; 18 s) aplicada sobre a região do nervo isquiático. As células de Schwann foram cultivadas em meio fisiológico e hiperglicêmico de glicose (5.5 e 55 mM) e a partir da passagem 3 foram submetidas à FBE (AsGa, 904 nm; 6 J; 45 mW; 18 s). Os ratos foram eutanasiados e foram coletados: nervo isquiático, gânglios da raiz dorsal (GRD) e adicionalmente, medula espinal e córtex anterior cingular para experimentos de Western blot. As células de Schwann foram submetidas a ensaios de viabilidade celular por MTT e aos ensaios de respiração celular. A FBE reverteu a hiperalgesia mecânica nos ratos com NDP. A FBE atuou de forma significativa na modulação de citocinas pró e anti-inflamatórias no nervo isquiático e GRD de ratos diabéticos, assim como modulou o produto de glicação avançada carboximetilisina (CML) e seu receptor (RAGE) nos referidos tecidos. Foi observado também que a FBE foi capaz de modular o fator de transcrição nuclear kappa B (NFkB) no nervo isquiático e GRD de ratos diabéticos. Quanto a dinâmica mitocondrial, a FBE modulou de maneira expressiva os processos de fusão e fissão mitocondrial no nervo isquiático e GRD de ratos diabéticos. A FBE também atuou na modulação de proteínas relacionadas a dor e aos processos de excitação e inibição no sistema nervoso central (medula espinal e córtex anterior cingular) dos ratos diabéticos. A FBE aumentou a viabilidade celular das células de Schwann assim como, melhorou a respiração celular quando em meio hiperglicêmico (55 mM). Estes resultados podem ser influentes para o desenvolvimento de novas formas de terapias complementares que visem à restauração do sistema nervoso periférico em condição de hiperglicemia.

**Palavras-chave:** Citocinas, Diabetes, Estreptozotocina, Neuropatia, Rato

## ABSTRACT

**Rocha, I.R.C.** Study of the Photobiostimulation Effects on Peripheral Diabetic Neuropathy. 2023. Number of pages (100 p.) Ph.D. Thesis (Department of Anatomy) – Instituto de Ciências Biomédicas, Universidade de São Paulo, 2023.

The primary cellular damage arising from Schwann cells in hyperglycemia is a largely overlooked aspect in terms of diabetic peripheral neuropathy (DPN). Furthermore, the mechanisms by which photobiostimulation (PBS) generates its promising effects is still a field of extensive investigation. Little is known about the mechanisms of PBS effects on DPN. The aim of this study was to investigate the mechanisms involved in anti-hyperalgesic / anti-inflammatory effects of PBS in rats with streptozotocin (STZ) – induced DPN, as well as the effects of PBS Schwann cells respiration. The experiments were approved by the Animal Ethics Commission (CEUA/ICB-USP), protocol 2269190619. Male Wistar rats, 200-250 g, 4-8 weeks old, received a single dose of STZ (85 mg/kg) or vehicle (saline) intraperitoneally (i.p). Type I diabetes was determined by blood glucose  $\geq 250$  mg/dL. The animals were submitted to the electronic von Frey test 72 hours after the injection of STZ or vehicle (saline) and on days interspersed with the treatment with PBS. Hyperalgesic diabetic rats were submitted to PBS (AsGa, 904 nm; 6 J; 45 mW; 18 s) applied over the region of the sciatic nerve. Schwann cells were cultured in physiological and hyperglycemic glucose medium (5.5 and 55 mM) and from passage 3 onwards they were subjected to PBS (AsGa, 904 nm; 6 J; 45 mW; 18 s). The rats were euthanized and the sciatic nerve, dorsal root ganglia (DRG) and, additionally, spinal cord and anterior cingulate cortex were collected for Western blot experiments. Schwann cells were subjected to MTT cell viability assays and cell respiration assays. PBS reversed mechanical hyperalgesia in DPN rats. PBS modulated pro and anti-inflammatory cytokines in the sciatic nerve and DRG of diabetic rats, as well as modulated the advanced glycation end product carboxymethyl lysine (CML) and its receptor (RAGE) in those tissues. It was also observed that PBS was able to modulate nuclear transcription factor kappa B (NFkB) in the sciatic nerve and DRG of diabetic rats. PBS significantly modulated mitochondrial fusion and fission processes in the sciatic nerve and DRG of diabetic rats. PBS also modulated proteins related to pain and excitation and inhibition processes in the central nervous system (spinal cord and anterior cingulate cortex) of diabetic rats. PBS increased Schwann cells viability as well as improved cellular respiration when in hyperglycemic medium (55 mM). These results may be influential for the development of new forms of complementary therapies aimed at restoring the peripheral nervous system in hyperglycemic conditions.

**Keywords:** Cytokines, Diabetes, Neuropathy, Rat, Streptozotocin

## Lista de Abreviaturas

ACC	Córtex cingulado anterior
AGE	Produtos de glicação avançada
ATCC	American Type Culture Collection
ATP	Adenosina trifosfato
BCRJ	Banco de células do Rio de Janeiro
BDNF	Fator neurotrófico derivado do cérebro
CB <sub>1</sub>	Receptor endocanabinóide 1
CB <sub>2</sub>	Receptor endocanabinóide 2
CML	Carboximetilisina
CO <sub>2</sub>	Dióxido de carbono
DM	Diabetes mellitus
DRP-1	<i>Dynamin related protein 1</i>
DNA	Ácido desoxirribonucleico
FADH	Flavina adenina dinucleotídeo
FBE	Fotobioestimulação
FCCP	Cianeto de carbonila para-trifluoro-metil fenil hidrazina
GDNF	Fator neurotrófico derivado de linhagem de células gliais
GFAP	Proteína ácida fibrilar glial
GRD	Gânglio da raiz dorsal
i.p.	Intraperitoneal
ipGTT	Teste de tolerância à glicose (intraperitoneal)
MAPK	Proteína quinase ativado por mitógeno
MET	Microscopia eletrônica de transmissão
MFN-2	Mitofusina 2
NADH	Nicotinamida adenina dinucleotídeo
NDP	Neuropatia diabética periférica
NFKB	Fator nuclear kappa B.
NGF	Fator de Crescimento do Nervo
NT3	Neurotrofina 3
PIK3	Fosfatidilinositol-3 quinase
PLC	Fosfolipase C

RAGE	Receptor para os produtos de glicação avançada
STZ	Estreptozotocina
SNP	Sistema Nervoso Periférico
SNC	Sistema Nervoso Central

## Lista de Figuras

<b>Figura 1.</b> Desenvolvimento das células de Schwann.	18
<b>Figura 2.</b> Morfologia mitocondrial.	22
<b>Figura 3.</b> Cadeia transportadora de elétrons e ATP sintase.	23
<b>Figura 4.</b> Esquema representativo da terapia com a fotobioestimulação.	32
<b>Figura 5.</b> Delineamento experimental ao longo de oitenta e cinco (85) dias.	33
<b>Figura 6.</b> Aparelho emissor de laser (904 nm) e Oxígrafo de alta resolução.	35
<b>Figura 7.</b> Parâmetros metabólicos.	39
7. A. Glicemia.	
7. B. Peso.	
<b>Figura 8.</b> Teste de tolerância à glicose intraperitoneal (ipGTT).	40
<b>Figura 9.</b> Hiperalgisia mecânica.	41
9. A. Limiar de dor (retirada da pata).	
9. B. Intensidade de dor.	
<b>Figura 10.</b> Efeitos da fotobioestimulação sobre proteínas envolvidas nos processos pró e anti-inflamatórios no nervo isquiático de ratos diabéticos hiperalgésicos.	42
10.A. CML.	
10.B. RAGE.	
10.C. NF-KB.	
<b>Figura 11.</b> Efeitos da fotobioestimulação sobre citocinas anti e pró-inflamatórias no nervo isquiático de ratos diabéticos hiperalgésicos.	43
11.A. TNF-alfa.	
11.B. IL-1Beta.	
11.C. IL-6.	
11.D IL-10.	
<b>Figura 12.</b> Efeitos da fotobioestimulação sobre a dinâmica mitocondrial no nervo isquiático de ratos diabéticos hiperalgésicos.	44
12.A. Mitofusina-2.	
12. B. DRP-1.	



**Figura 13.** Efeitos da fotobioestimulação sobre proteínas envolvidas nos processos pró e anti-inflamatórias no gânglio da raiz dorsal de ratos diabéticos hiperalgésicos. 45

- 13.A. CML.
- 13.B. RAGE.
- 13.C. NF-KB.

**Figura 14.** Efeitos da fotobioestimulação sobre citocinas anti e pró-inflamatórias no gânglio da raiz dorsal de ratos diabéticos hiperalgésicos. 46

- 14.A. TNF-alfa.
- 14.B. IL-1Beta.
- 14.C. IL-6.
- 14.D IL-10.

**Figura 15.** Efeitos da fotobioestimulação sobre a dinâmica mitocondrial no gânglio da raiz dorsal de ratos diabéticos hiperalgésicos. 47

- 15.A. Mitofusina-2.
- 15. B. DRP-1.

**Figura 16.** Ensaios de viabilidade celular por redução do MTT. 48

**Figura 17.** Efeitos da fotobioestimulação sobre a respiração mitocondrial de células de Schwann. 49

**Figura 18.** Efeitos da fotobioestimulação sobre a medula espinal de ratos diabéticos hiperalgésicos. 50

- 18.A. Receptor endocanabinóide CB1.
- 18.B. Receptor endocanabinóide CB2.

**Figura 19.** Efeitos da fotobioestimulação sobre o córtex anterior cingulado de ratos diabéticos hiperalgésicos. 51

- 19.A. GAD65/67.
- 19.B. GLUR 1.
- 19.C. GFAP.
- 19.D. MOR.

## **Lista de tabelas**

<b>Tabela 1.</b> Parâmetros da fotobioestimulação.	33
<b>Tabela 2.</b> Anticorpos primários para Western Blotting.	37

## Sumário

<b>1. Introdução e revisão de literatura</b>	
1.1 <i>Diabetes mellitus: considerações gerais.</i>	16
1.2 <i>Neuropatia diabética periférica.</i>	16
1.3 <i>Células de Schwann.</i>	19
1.4 <i>Mitocôndrias – dinâmica mitocondrial e diabetes mellitus.</i>	23
1.5 <i>Fotobioestimulação e sistema nervoso.</i>	27
2. Justificativa	29
<b>3. Objetivos</b>	30
3.1 <i>Objetivo geral</i>	30
3.2 <i>Objetivos específicos</i>	30
<b>4. Materiais e métodos</b>	31
4.1 <i>Animais.</i>	31
4.2 <i>Indução do diabetes mellitus tipo 1.</i>	31
4.3 <i>Fotobioestimulação.</i>	32
4.4 <i>Teste comportamental de Von Frey Eletrônico.</i>	33
4.5 <i>Cultura celular – Células de Schwann linhagem RT4D6P2T</i>	34
4.6 <i>Viabilidade celular.</i>	34
4.7 <i>Respiração mitocondrial.</i>	35
4.8 <i>Coleta de tecidos: Nervo isquiático, gânglios da raiz dorsal, medula espinal e córtex anterior cingulado para análise de expressão proteica por Western Blotting.</i>	36
4.9 <i>Análise de expressão proteica – Western Blotting.</i>	37
4.10 <i>Análise de dados.</i>	38
<b>5. Resultados</b>	39
5.1 <i>Eficácia da indução do diabetes tipo 1 induzido por única dose de estreptozotocina (STZ).</i>	39
5.2 <i>Efeitos da estreptozotocina sobre o teste ipGTT.</i>	40

<i>5.3 Efeitos da fotobioestimulação sobre o limiar e intensidade de dor em ratos diabéticos hiperalgésicos.</i>	41
<i>5.4 Efeitos da fotobioestimulação sobre proteínas envolvidas nos processos pró e anti-inflamatórios no nervo isquiático de ratos diabéticos hiperalgésicos.</i>	42
<i>5.5 Efeitos da fotobioestimulação sobre citocinas pró e anti-inflamatórias no nervo isquiático de ratos diabéticos hiperalgésicos.</i>	43
<i>5.6 Efeitos da fotobioestimulação sobre a dinâmica mitocondrial no nervo isquiático de ratos diabéticos hiperalgésicos.</i>	44
<i>5.7 Efeitos da fotobioestimulação sobre proteínas envolvidas nos processos pró e anti-inflamatórios no gânglio da raiz dorsal de ratos diabéticos hiperalgésicos.</i>	45
<i>5.8 Efeitos da fotobioestimulação sobre citocinas pró e anti-inflamatórias no gânglio da raiz dorsal de ratos diabéticos hiperalgésicos.</i>	46
<i>5.9 Efeitos da fotobioestimulação sobre a dinâmica mitocondrial no gânglio da raiz dorsal de ratos diabéticos hiperalgésicos.</i>	47
<i>5.10 Ensaio de viabilidade celular – Células de Schwann.</i>	48
<i>5.11 Efeitos da fotobioestimulação sobre o metabolismo mitocondrial (respiração celular) em cultura de células de Schwann.</i>	49
<i>5.12 Efeitos da fotobioestimulação sobre os receptores endocanabinóide CB1 e CB2 na medula espinal de ratos diabéticos hiperalgésicos.</i>	50
<i>5.13 Efeitos da fotobioestimulação sobre o córtex anterior cingulado de ratos diabéticos hiperalgésicos.</i>	51
<b>6. Discussão</b>	52
<b>7. Conclusão</b>	56
<b>8. Referências</b>	57
<b>9. Trajetória no Departamento de Anatomia do Instituto de Ciências Biomédicas. Universidade de São Paulo (ICB/USP).</b>	62
<b>10. Artigos publicados ao longo da pós-graduação.</b>	64

## 1. Introdução e revisão da literatura

### 1.1 *Diabetes mellitus: considerações gerais*

O diabetes *mellitus* é considerado hoje um dos maiores problemas de saúde mundial do século XXI e o custo global do tratamento anual retira dos cofres públicos em torno de 825 milhões de dólares de acordo com um estudo publicado pela revista *The Lancet* em 2016 [1]. Além disso, segundo dados do International Diabetes Federation (IDF), até 2021, o número de adultos diabéticos era de 537 milhões e a estimativa prevista para 2045 será de aproximadamente 783 milhões de casos [2]. Cabe ressaltar ainda que, uma pessoa morre a cada seis segundos decorrente das complicações crônicas ocasionadas pelo diabetes *mellitus*, e em 2015 o número total de mortes foi de 5 milhões de pessoas [2].

O diabetes *mellitus* tipo 1 é uma doença crônica autoimune caracterizada por níveis elevados de glicose na circulação sanguínea (hiperglicemia) devido a deficiência na produção de insulina [3]. Tal deficiência se desenvolve a partir da perda expressiva de células  $\beta$  pancreáticas [3] e é uma das condições endócrinas e metabólicas mais comuns que ocorrem em crianças e em adultos jovens [3]. A hiperglicemia crônica causa danos irreversíveis aos tecidos corporais, em especial o sistema nervoso, levando aqueles acometidos por tal doença a uma vida cheia de complicações e incapacidades.

As pessoas com esta forma de diabetes precisam de insulina todos os dias de suas vidas de modo a controlar os níveis de glicose na circulação sanguínea. Com ou sem o uso de insulina, pessoas com diabetes *mellitus* tipo 1 desenvolvem suas complicações mais debilitantes e incapacitantes ao longo da vida.

### 1.2 *Neuropatia diabética periférica*

A neuropatia diabética periférica (NDP) é a complicação crônica mais comum do diabetes *mellitus* tipo 1, com grande variedade de manifestações clínicas. Afeta atualmente 60% daqueles acometidos por este tipo de diabetes [4] e é caracterizada por expressivo dano aos nervos periféricos. O tipo mais comum e prevalente é o que apresenta uma disfunção sensitiva – motora dos membros inferiores, apresentando quadro severo de dor decorrente da neuropatia crônica desenvolvida pelo quadro de hiperglicemia [5].

A grande vulnerabilidade do sistema nervoso periférico (SNP) quanto às complicações decorrentes do diabetes *mellitus* tipo 1 em relação aos demais tecidos ocorre provavelmente devido à sua estrutura, função e/ou a exclusivas necessidades metabólicas[6]. Cabe mencionar que a principal função do SNP é a de comunicação com

o sistema nervoso central por meio de sinais elétricos transmitidos por fibras mielínicas (fibras A $\delta$ , A $\beta$ ) e amielínicas (fibras C).

Há quatro hipóteses que estão relacionadas com as complicações decorrentes da hiperglicemia crônica no diabetes *mellitus*: 1 – ativação excessiva da via dos polióis; 2 - ativação excessiva da proteína C quinase; 3 – ativação excessiva da via das hexosaminas; 4 -aumento na formação dos produtos finais de glicação avançada (AGE) e consequentemente aumento na expressão e ativação dos receptores para os produtos finais de glicação avançada (RAGE) [7].

A Hiperglicemia ativa a via da aldose redutase, um dos metabolismos alternativos para a glicose [8]. A aldose redutase catalisa a formação de sorbitol a partir da glicose, e posteriormente, a sorbitol desidrogenase catalisa a formação de frutose a partir do sorbitol [8]. Uma vez que a frutose não pode ser metabolizada devido à falta de frutoquinase no tecido nervoso, e o sorbitol apresenta lento processo de difusão, estes então se acumulam nas células, levando ao aumento da pressão osmótica [9]. Como consequência, há desequilíbrio no efluxo de Inositol e taurina nas células nervosas [10].

Devido a semelhança estrutural entre a glicose e o inositol, a glicose inibe a absorção de inositol nas células nervosas em estado de hiperglicemia [8]. O inositol é um composto importante no metabolismo dos fosfolípidos dos nervos e também um cofator nas reações químicas envolvidas na eliminação de radicais livres [8]. A deficiência de inositol inibe a eliminação de radicais livres, causando estresse oxidativo e dano celular [8]. Ainda, a deficiência de inositol interfere no metabolismo dos fosfolípidos, reduzindo a atividade da Na<sup>+</sup>-K<sup>+</sup>-ATPase, consequentemente retardando a velocidade de condução do nervo e o transporte axonal [11].

Já a ativação excessiva das proteínas C quinases (PCK) devido a hiperglicemia e suas contribuições na neuropatia diabética, ainda é campo de intensa investigação [12]. A PCK é uma proteína quinase relacionada a serina/treonina que desempenha papel chave em múltiplas funções celulares e afeta diversas vias de transdução de sinal [13]. A PCK contribui para o desenvolvimento da neuropatia diabética através de mecanismos neurovasculares, como alteração de fluxo sanguíneo e alteração de condução do nervo [12]. Estudos mostram que em ratos diabéticos, tratados com inibidores seletivos e não seletivos de PCK, há melhora da função neural [14]. Há evidências que apontam para a redução da atividade da Na<sup>+</sup>K<sup>+</sup>-ATPase, resultando na diminuição da condução do nervo assim como na participação em processo de regeneração nervosa [15].

Embora menos explorado, o fluxo das hexosaminas tem sido proposto como um contribuinte adicional para a patogênese da neuropatia diabética [16]. O excesso de glicose aumenta a glicólise e a conversão de glicose – 6 – fosfato em frutose – 6 – fosfato. Aproximadamente, 5% do fosfato – 6 – frutose é desviado para a via da hexosamina, por meio da conversão em glicosamina – 6 – fosfato [17]. A glicosamina é então convertida irreversivelmente para o produto final da via da hexosamina, UDP-N-acetilglicosamina, que serve como substrato para a modificação pós traducional de proteínas [17]. A glicação excessiva de proteínas nucleares e citosolicas no diabetes tem sido relacionada a resistência insulínica e ao dano celular [16].

Embora os mecanismos precisos subjacentes a neuropatia diabética permaneçam incertos, há evidências de que os produtos finais de glicação avançada (AGEs) induzido por hiperglicemia está relacionado com a modificação de proteínas de mielina nas fibras periféricas, que se tornam suscetíveis a fagocitose por macrófagos [18], favorecendo desta maneira a degeneração de fibras nervosas periféricas [18]. Ainda, a modificação das proteínas do citoesqueleto axonal, como por exemplo, tubulina, neurofilamento e actina pelos AGEs, resulta em atrofia, degeneração e ainda compromete o transporte axonal [18]. Outro fato importante é a co-localização dos receptores para os AGEs (RAGE) nos nervos periféricos. A presença dos RAGEs nos nervos periféricos diabéticos, sugere estresse oxidativo, resultando na ativação do fator nuclear kappa B (NFkB) e de vários genes pró-inflamatórios, contribuindo desta forma para a exacerbação dos processos degenerativos e alteração do componente sensorial, como por exemplo, a geração de dor [18].

Sabe-se hoje que a produção aumentada de superóxidos pela cadeia transportadora de elétrons nas mitocôndrias é uma provável ideia que une as quatro hipóteses anteriormente citadas, uma vez que vários estudos indicam que a hiperglicemia crônica aumenta significativamente o estresse oxidativo [7]. A hiperglicemia induz mudanças mitocondriais, como a liberação de citocromo c, alteração na biogênese e fissão mitocondrial e conseqüentemente a morte celular [19]. A entrada excessiva de glicose nas células causa sobrecarga na cadeia transportadora de elétrons, gerando oxidantes na mitocôndria e conseqüentemente redução no potencial de membrana mitocondrial e diminuição na síntese de ATP [20].

Nos últimos anos, as células de Schwann (células responsáveis pela formação da bainha de mielina no SNP) têm ganhado destaque como as principais protagonistas na produção de espécies reativas de oxigênio e conseqüentemente como as células

responsáveis pelo processo nocivo ocasionado aos axônios em situação de hiperglicemia [21].

### ***1.3 Células de Schwann***

As células de Schwann são originárias das células migratórias da crista neural que dão origem a uma grande variedade de células polarizadas, incluindo células tão diversas como neurônios periféricos, melanócitos e células endócrinas [22, 23]. A cascata precisa de sinais moleculares que a célula da crista neural direciona para entrar na linhagem de células de Schwann *in vivo* ainda não é totalmente elucidada. Porém, o fator de transcrição Sox10 é o regulador essencialmente necessário para a geração das primeiras células da linhagem de células de Schwann [24]. A expressão do referido fator é crucial também para que as células de Schwann se diferenciem em células de Schwann mielinizantes [24].

Durante o desenvolvimento do sistema nervoso, as células de Schwann se associam a feixes de axônios à medida que se estendem para a periferia, inicialmente cercando as margens externas dos referidos feixes de fibras [25] (Figura 1). As células de Schwann suportam o crescimento axonal através de uma variedade de fatores de crescimento, como por exemplo, o fator de crescimento do nervo (NGF), o fator neurotrófico derivado do cérebro (BDNF), o fator neurotrófico derivado da linha de células gliais (GDNF) e ainda pela neurotrofina NT3 [26]. Com o acentuado processo de divisão celular pelas células de Schwann e de extensão do processo celular (axônios) dos neurônios, as células de Schwann começam a separar os axônios em pacotes sucessivamente menores, processo este conhecido como “triagem radial”. Por fim, o citoplasma da célula de Schwann separa os axônios de maneira individual [25] (Figura 1).



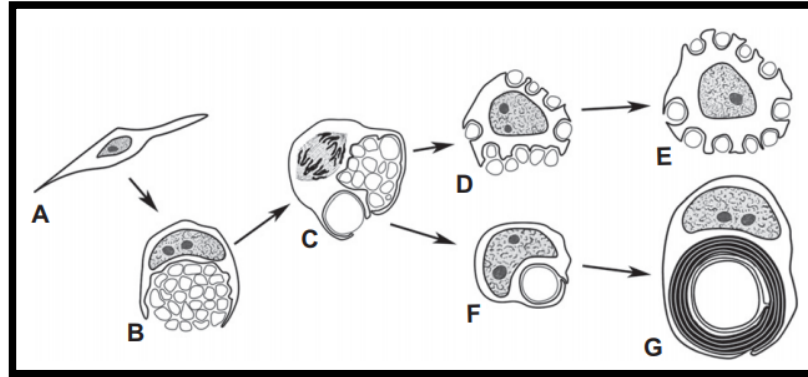


**Figura 1.** Durante o desenvolvimento, as células de Schwann migrantes (A) cercam feixes de axônios (B), separam um único axônio de grande calibre (C) e então passam por processo de divisão celular (C). Uma das células filhas mieliniza o axônio agora segregado (F-G) enquanto a outra célula proveniente da divisão celular permanece associada ao feixe de fibras (axônios) não mielinizados (D-E). Adaptado de *Trapp et al., 2004. Biology of Schwann cells.*

As células de Schwann podem se diferenciar em um fenótipo mielinizante ou não mielinizante [27]. Quando estas células são privadas de contato axonal, elas adotam um fenótipo molecular e morfológico que é similar, embora não idêntico, ao fenótipo de células de Schwann imaturas antes da mielinização [27]. Portanto, dependendo das circunstâncias, estas células podem fornecer suporte para os axônios por meio da elaboração da bainha de mielina ou fornecer um ambiente através do qual os axônios podem regredir após a lesão e subsequentemente remielinizar [27]. Os processos pelos quais as células de Schwann transitam entre estes dois fenótipos ainda é campo de intensa investigação.

Avanços importantes na compreensão dos mecanismos de sinalização axonal que controlam a mielinização ocorreu nos últimos anos [27]. Diversos trabalhos mostraram que a proteína de superfície axonal neuroregulina 1, atuando através de seus receptores ErbB2 e ErbB3, controla a espessura da bainha de mielina das células de Schwann, participa do mecanismo que controla a expressão dos genes da mielina e ainda induz o processo de mielinização [28-30]. Adicionalmente, o referido fator controla a sobrevivência dos precursores das células de Schwann [31, 32]. Entretanto, continua sendo um desafio entender o mecanismo pelo qual as células de Schwann muda sua resposta à neuroregulina de uma fase proliferativa não mielinizante para uma fase mielinizante não proliferativa [27].

Em relação ao comportamento das referidas células em ambiente hiperglicêmico, os estudos desenvolvidos até o presente momento não são suficientes para determinar se as células de Schwann sofrem danos estruturais independentes durante o diabetes ou se estão respondendo a sinais provenientes do processo de degeneração axonal [33]. No entanto, durante análises realizadas em amostras de biópsia do nervo sural tanto em modelo animal quanto em estudos envolvendo seres humanos diabéticos, foram relatadas mudanças morfológicas expressivas na bainha de mielina na presença de um axônio aparentemente normal, indicando que a “Schwannopatia” pode se desenvolver independentemente da “axoniopatia” [34].

Além disso, há descrito na literatura que as alterações degenerativas nas fibras nervosas periféricas são acompanhadas pela presença de mitocôndrias disfuncionais [35], observação esta consistente com evidências emergentes sobre a disfunção mitocondrial e o dano metabólico tanto em axônios quanto em células de Schwann em modelo animal de diabetes *mellitus* [35].

Recentemente, o estresse oxidativo e os distúrbios mitocondriais nas células de Schwann durante o diabetes são amplamente aceitos como fatores contribuintes para a disfunção neuronal [36]. A hiperglicemia crônica é amplamente reconhecida como um fator chave na produção excessiva de espécies reativas de oxigênio em todas as células, e exacerbadas por uma redução concomitante das defesas antioxidantes endógenas [37]. As células de Schwann são cada vez mais reconhecidas como um importante centro de produção de espécies reativas de oxigênio que, neste contexto, afeta sua própria função celular assim como, contribuem para as alterações metabólicas em outros tipos de células dentro do sistema nervoso periférico [38].

Outro mecanismo proposto para as consequências deletérias na neuropatia diabética periférica é a sinalização desregulada dos receptores para os produtos de glicação avançada (RAGE) nas células de Schwann [39]. A produção em excesso dos produtos de glicação avançada (AGEs) como resultado do excesso de glicose presente nas células de Schwann, ativa os receptores RAGE, contribuindo ativamente desta forma para a formação de espécies reativas de oxigênio [40]. Além disso, as modificações induzidas pelos AGEs em proteínas-chave como por exemplo, o colágeno, lipídios e ácidos nucleicos têm o potencial de alterar a estrutura e a função das células de Schwann, com efeitos prejudiciais aos axônios que estas células envolvem, levando à potencialização da neuropatia diabética [40].

A hiperglicemia é capaz de atuar na remodelação do proteoma mitocondrial das células de Schwann, conduzindo desta forma, ao aumento da expressão das subunidades  $\alpha$  e  $\beta$  da ATP sintase e, ainda, é capaz de conduzir a uma inefetiva capacidade respiratória mitocondrial [41]. Os altos níveis de glicose contribuem para a disfunção mitocondrial e diminuem a eficiência da fosforilação oxidativa em células de Schwann [41]. Em um estudo publicado em 2016, o dano mitocondrial caracterizado pela regulação de múltiplas subunidades dos complexos I, III, IV e V mitocondrial foi descrito em modelo animal de diabetes *mellitus* tipo 1 [42]. As alterações acima descritas foram observadas apenas nos nervos periféricos e não nos gânglios sensoriais ou trigeminais, refletindo-se desta maneira o papel crucial das células de Schwann no metabolismo das fibras nervosas periféricas [42].

O estado hiperglicêmico também participa ativamente da dinâmica mitocondrial. Estudos recentes apontam que o processo de fissão e/ou fusão mitocondrial podem estar envolvidos na neuropatia diabética [43]. A hiperglicemia pode influenciar nos processos de fusão e fissão mitocondrial pela modulação das proteínas mitocondriais mitofusina-2 e pela *dynamin related protein -1* (DRP1) [44]. Além disso, alterações nas proteínas relacionadas ao processo de fissão e de fusão mitocondrial que controlam a forma e o número de mitocôndrias nos tecidos podem prejudicar as funções celulares e podem levar ao processo degenerativo [43].

Ainda, em estado hiperglicêmico, as células de Schwann ativam cascatas intracelulares, incluindo aquelas reguladas pelo fator de transcrição nuclear NFkB que, uma vez ativado, regula a produção de uma vasta classe de citocinas e quimiocinas pró-inflamatórias [39]. Estes eventos contribuem de forma efetiva para a degeneração walleriana e enfatizam o potencial envolvimento das células de Schwann no processo inflamatório que é observado em pacientes com diabetes *mellitus* [45].

Outro fato que permite enfatizar a estreita associação entre as células de Schwann e os axônios é a capacidade destas células de influenciarem na excitabilidade das fibras nervosas periféricas assim como, na propagação do próprio potencial de ação, mesmo estas células não sendo excitáveis por si só [39]. A função mitocondrial prejudicada e o estresse oxidativo nas células de Schwann podem levar a mudanças no perfil de distribuição dos canais de sódio e potássio nos nódulos de Ranvier, contribuindo para os potenciais danos axonais [46].

Infelizmente, o dano decorrente do metabolismo em desequilíbrio das células de Schwann é em grande parte esquecido na NDP devido ao grande enfoque dado às doenças vasculares. Por outro lado, alguns estudos mostraram que células de Schwann lesadas afetam tanto a vasculatura quanto os axônios [39], trazendo as células de Schwann para o centro das atenções como as células grandemente responsáveis pela neuropatia diabética periférica.

#### ***1.4 Mitocôndrias – dinâmica mitocondrial e diabetes mellitus***

As mitocôndrias surgiram há cerca de dois bilhões de anos a partir do envolvimento (fagocitose) de proteobactérias por precursores da célula eucariótica moderna [47] e passaram a desempenhar papel crítico na geração de energia metabólica em células eucarióticas. A referida organela é responsável pela maior parte da energia útil derivada da decomposição de carboidratos e ácidos graxos, que é convertida em trifosfato de adenosina (ATP) pelo processo de fosforilação oxidativa [48]. Além disso, as mitocôndrias são únicas entre as organelas citoplasmáticas pelo fato de conterem o seu próprio ácido desoxirribonucléico (DNA), que codifica os ácidos ribonucleicos transportadores (tRNAs) e os ácidos ribonucleicos ribossômicos (rRNAs) [47]. A montagem das mitocôndrias envolve, desta forma, proteínas codificadas por seus próprios genomas e traduzidas dentro da organela, assim como proteínas codificadas pelo genoma nuclear e importadas do citosol [47].

As mitocôndrias são circundadas por um sistema duplo de membranas no qual consiste em uma membrana mitocondrial interna e outra externa separadas por um espaço intermembranoso (Figura 2). A membrana mitocondrial interna origina numerosas dobras conhecidas como cristas mitocondriais que se estendem para o interior (ou matriz) da organela [49]. Cada um dos componentes citados desempenha funções distintas, com a matriz e a membrana mitocondrial interna representando os principais compartimentos funcionais destas organelas [49]. A matriz contém o sistema genético mitocondrial, bem como as enzimas responsáveis pelas reações centrais do metabolismo oxidativo [49].

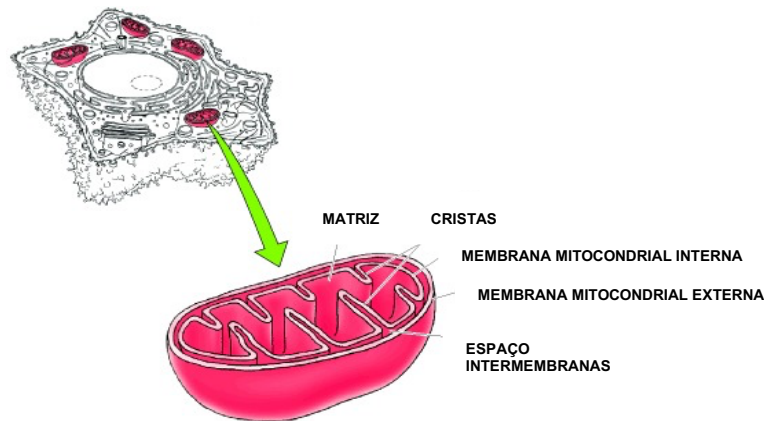


**Figura 2.** Morfologia mitocondrial. Adaptado de: *The Cell: A Molecular Approach*. Cooper, GM. 2nd Edition. Sinauer Associates, Sunderland (MA), 2000.

A glicólise - degradação oxidativa das moléculas de glicose - é a principal fonte de energia metabólica em células animais onde as moléculas de glicose são degradadas e então convertidas em piruvato [50]. O piruvato é então transportado para a mitocôndria, onde sua oxidação completa até o dióxido de carbono ( $\text{CO}_2$ ) produz a maior parte da energia utilizável (trifosfato de adenosina - ATP) obtida do metabolismo da glicose [50]. Isto envolve a oxidação inicial do piruvato em acetilcoenzima A (acetil-CoA), que é depois decomposto em dióxido de carbono ( $\text{CO}_2$ ) através do ciclo do ácido cítrico [50]. A oxidação de ácidos graxos também produz acetil-CoA [50], que é metabolizado de forma semelhante pelo ciclo do ácido cítrico na mitocôndria. As enzimas do ciclo do ácido cítrico (localizadas na matriz da mitocôndria) são, assim, componentes centrais na degradação oxidativa de carboidratos e ácidos graxos [50].

A oxidação da acetilcoenzima A (acetil-CoA) a dióxido de carbono ( $\text{CO}_2$ ) é acoplada à redução do dinucleotídeo de nicotinamida e adenina ( $\text{NAD}^+$ ) assim como a redução do dinucleotídeo de flavina e adenina (FAD) [51]. A maior parte da energia derivada do metabolismo oxidativo é então produzida pelo processo de fosforilação oxidativa, que ocorre na membrana mitocondrial interna. Os elétrons de alta energia do NADH e  $\text{FADH}_2$  são transferidos através de uma série de proteínas transportadoras, conhecidas por complexos I, II, III e IV na membrana mitocondrial interna para o oxigênio molecular [51] (Figura 3). A energia derivada dessas reações de transferência de elétrons é convertida em energia potencial armazenada em um gradiente de prótons através da membrana, que é então usada para conduzir a síntese de ATP [51]. A membrana

mitocondrial interna representa assim o principal local de geração de ATP, e esse papel crítico é refletido em sua estrutura.

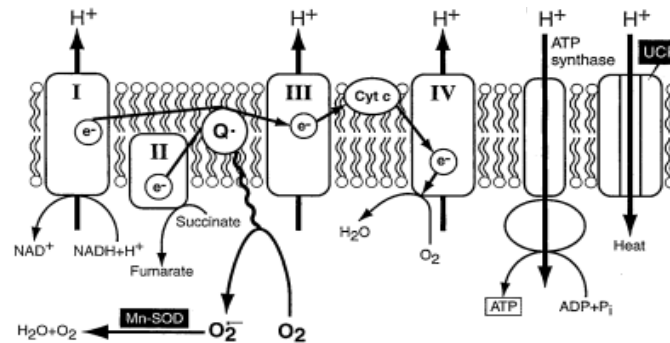


**Figura 3.** Cadeia transportadora de elétrons e ATP sintase. Adaptado de: The pathobiology of diabetic complications. Brownlee, American Diabetes Association, 2005.

Por muito tempo, as mitocôndrias foram consideradas organelas estáticas envolvidas apenas na produção de energia necessária para o metabolismo celular pela fosforilação oxidativa. Porém, é de grande conhecimento que as mitocôndrias também estão envolvidas em vários outros processos fisiológicos, como morte celular programada, imunidade inata, autofagia, sinalização redox, homeostase de cálcio e reprogramação de células-tronco [52-54]. Ainda, com o desenvolvimento de técnicas capazes de mostrar células funcionais em tempo real nos últimos 30 anos mudou drasticamente o conceito de mitocôndrias sendo estruturas estáticas e isoladas [55]. De fato, as mitocôndrias podem modular sua morfologia para criar uma rede tubular coordenada por eventos de fissão e fusão. O equilíbrio entre estes dois processos opostos regula o número mitocondrial, tamanho e posicionamento dentro do citoplasma e é referido como "dinâmica mitocondrial" [55].

A fissão mitocondrial é caracterizada pela divisão de uma mitocôndria em duas mitocôndrias filhas, enquanto a fusão mitocondrial é a união de duas mitocôndrias resultando em uma mitocôndria [55]. A desregulação desses eventos resulta em uma rede fragmentada caracterizada por um grande número de pequenas mitocôndrias redondas ou por uma rede hiperfusada com mitocôndrias alongadas e altamente conectadas [56]. Essas transições dinâmicas balanceadas não são necessárias apenas para garantir a função mitocondrial, mas também para responder às necessidades celulares, adaptando a rede à disponibilidade de nutrientes e ao estado metabólico da célula [56]. Além disso, diferentes estados morfológicos estão associados a múltiplas condições fisiológicas e fisiopatológicas

[57]. A fragmentação mitocondrial é frequentemente associada à disfunção mitocondrial, já que esse estado morfológico predomina durante níveis elevados de estresse e morte celular [56].

As principais proteínas que compõem o maquinário principal relacionado a dinâmica mitocondrial são as grandes proteínas GTPase, pertencentes à família das dinaminas [58]. Estas mecanoenzimas podem oligomerizar e alterar a conformação para conduzir a remodelação, constrição, cisão e / ou fusão das membranas mitocondriais [59]. A constrição e a cisão mitocondrial são realizadas pela proteína 1 (Drp1) e pela dinamina-2 (Dnm2) [60]. A fusão mitocondrial é assegurada pelas mitofusinas 1 e 2 (Mfn1 e Mfn2) que medeiam a fusão das membranas mitocondriais interna e externa [60]. Os processos de fusão e fissão mitocondrial são eventos cruciais para a regulação de numerosas funções fisiológicas celulares e a desregulação de tais processos está associada a uma diversidade de doenças, a citar o diabetes mellitus, o qual revela morfologia mitocondrial irregular [61].

Em cultura celular, altas concentrações de glicose induzem a fragmentação mitocondrial em linhagens celulares derivadas de fígado, coração, endotélio, ilhotas pancreáticas, bem como em culturas de células primárias do sistema nervoso e cardiovascular [62-65]. A fragmentação mitocondrial em condições de alta concentração de glicose requer maquinaria de fissão mitocondrial [62]. O tratamento de neurônios provenientes dos gânglios da raiz dorsal (DRG) com altas concentrações de glicose ocasiona fragmentação mitocondrial e aumenta a expressão e localização mitocondrial da proteína de fissão DRP1, indicando a ativação da fissão mitocondrial [62]. Aumentos de expressão, ativação e localização mitocondrial das proteínas pró-apoptóticas Bim e Bax também foram observadas no tratamento com concentração elevada de glicose, indicando que a fragmentação mitocondrial induzida por elevados níveis glicêmicos nos neurônios do DRG está associada à apoptose [61]. Adicionalmente, a expressão aumentada de DRP1 também foi observada nos gânglios da raiz dorsal de ratos diabéticos induzidos por estreptozotocina [62].

### **1.5 Fotobioestimulação e Sistema Nervoso**

Os lasers de baixa potência não emitem calor, som ou vibração. Eles atuam na faixa de 1 a 1000 mW e comprimento de onda entre 632 e 1064 nanômetros (nm). Ao contrário do efeito térmico, estes lasers induzem uma reação fotoquímica nas células, processo este conhecido como fotobioestimulação ou ainda como fotobiomodulação [66]. O princípio de funcionamento do laser é de que, quando a luz atinge algumas moléculas biológicas conhecidas por cromóforos, a energia do fóton faz com que os elétrons sejam excitados e saltem de órbitas de baixa energia para órbitas de alta energia [66]. Toda esta energia até então armazenada, pode ser usada pelo sistema biológico para a execução de uma ampla atividade celular, como por exemplo, a fotossíntese e a fotomorfogênese [67]. Outros exemplos de cromóforos existentes na natureza são a clorofila em plantas, bacterioclorofila em algas verdes, as flavoproteínas e a hemoglobina encontradas nos glóbulos vermelhos, além do citocromo c presente nas mitocôndrias [66].

As mitocôndrias são as organelas citoplasmáticas geradoras de energia representada pela síntese de trifosfato de adenosina (ATP) em células eucarióticas através da fosforilação oxidativa [68]. A ideia básica por trás da respiração celular é que os elétrons com alta energia são passados por transportadores de elétrons, como por exemplo, as formas reduzidas da nicotinamida adenina dinucleotídeo (NADH) e a forma reduzida de flavina adenina dinucleotídeo (FADH<sub>2</sub>), através de uma série de complexos transmembranares (incluindo o citocromo c oxidase) ao receptor final de elétrons, gerando um gradiente de prótons [69].

Vários experimentos *in vitro*, como os que usam mitocôndrias isoladas do fígado de ratos, mostraram que a respiração celular foi regulada positivamente quando as mitocôndrias foram expostas a um laser do tipo Hélio-Neônio (HeNe) [70]. A irradiação a laser causou um aumento nos produtos mitocondriais como ATP [71], NADH, ácido ribonucleico (RNA) [72] e ainda, conseqüentemente, um aumento recíproco no consumo de oxigênio [73]. A nível mitocondrial, o complexo IV também conhecido por citocromo c oxidase (CCO) atua como um importante cromóforo [74]. O CCO consiste em 2 centros de cobre e 2 centros de ferro-heme que são capazes de absorver a luz em uma ampla gama, incluindo aquele próximo ao infravermelho [75].

A irradiação de luz nessas organelas (mitocôndrias) pode ocasionar a fotodissociação de óxido nítrico (NO) do citocromo c oxidase (CCO) [70]. Em células estressadas, o óxido nítrico mitocondrial desloca oxigênio do complexo IV (CCO)



resultando em uma regulação negativa do processo de respiração celular e consequentemente uma diminuição na síntese de ATP [66]. Ao induzir o referido efeito de fotodissociação de óxido nítrico do complexo IV, a irradiação laser previne o deslocamento de oxigênio do citocromo c oxidase, permitindo desta forma uma regulação positiva no metabolismo mitocondrial [66]. Ainda, em relação aos efeitos do laser, a literatura expõe que o aumento na produção celular de ATP produzido por esse tipo de luz pode contribuir para os efeitos positivos deste, tanto pelo aumento dos níveis de energia celular quanto pela elevada síntese de monofosfato cíclico de adenosina (AMPc), formado bioquimicamente a partir de ATP e que participa ativamente de muitas vias de sinalização celular [66]. O laser também promove a síntese de ácido desoxirribonucleico (DNA) [76], aumenta a produção de proteínas [66], modula a atividade enzimática [66], afeta o pH intra/extracelular e além do mais acelera o metabolismo celular [66].

A terapia com FBE tem sido aplicada em estudos clínicos e na pesquisa básica. Rochkind *et al* mostraram que a fototerapia a laser no pós-operatório humano aumenta o processo regenerativo das fibras nervosas periféricas [77]. Morfologicamente, o grupo tratado com laser mostrou aumento no número de axônios mielinizados [78], apresentando ainda, melhora progressiva em relação à função motora [79].

Em ratos, uma única sessão de terapia transcraniana com FBE melhorou significativamente a recuperação de ratos que sofreram acidente vascular cerebral isquêmico induzido pela oclusão permanente da artéria cerebral média [80]. Efeito semelhante também ocorreu em modelo de isquemia cerebral em coelhos [81]. Em humanos, a terapia transcraniana com FBE mostrou melhora significativa em pacientes com acidente vascular cerebral agudo quando aplicado aproximadamente 18 horas após o acidente vascular cerebral ter ocorrido, independentemente de sua localização [82].

Em um outro modelo animal, com lesão cerebral traumática, concluiu-se que o tratamento com a FBE restabeleceu de forma expressiva as alterações observadas no quadro motor [83]. Estas observações sugerem que vários mecanismos podem estar envolvidos para estes resultados, incluindo o aumento na síntese de ATP, formação de antioxidantes, angiogênese, neurogênese, e ainda um efeito anti-apoptótico [84]. Moreira *et al* realizaram um estudo em 2009 utilizando FBE e observaram o efeito na imunomodulação local e sistêmica após lesão cerebral criogênica em ratos [85]. O estudo concluiu que a FBE poderia afetar positivamente o equilíbrio de citocinas e assim prevenir a morte celular após o traumatismo cerebral [85].

Em 2009, Moges *et al.* avaliaram a terapia com FBE sobre a esclerose lateral amiotrófica, doença neurodegenerativa caracterizada por perda progressiva de neurônios motores na qual a disfunção mitocondrial devido ao estresse oxidativo, tem importante papel na morte de tais neurônios [86]. O respectivo estudo salientou os efeitos da FBE na recuperação motora no estágio inicial da referida doença.

Annelise E. Barron *et., al* (2023) mostrou que a FBE, apresentou ação imunomoduladora em camundongos em modelo de inflamação sistêmica e central induzido por lipopolissacarídeo (LPS). Seu estudo mostrou ação anti-inflamatória da FBE através da modulação da interleucina anti-inflamatória IL-10 no hipocampo de camundongos expostos ao LPS. Annelise E. Barron *et., al* mostrou ainda, que camundongos pré tratados com a FBE apresentou diminuição de citocinas pro-inflamatórias (TNF-alfa, IL-6, IL-1 beta) no hipocampo de camundongos expostos ao LPS [87].

Com base nessas informações, destaca-se a escassez de pesquisa básica e clínica sobre o uso da fotobioestimulação (FBE) sobre a neuropatia diabética periférica (NDP), tema central deste projeto de pesquisa.

## **2. Justificativa**

As alterações metabólicas são fatores predominantes característicos em pacientes com NDP, contribuindo exacerbadamente com a deterioração da qualidade de vida. Entretanto, apesar de vivermos em uma sociedade consideravelmente desenvolvida em termos de tratamento para as mais diversas formas de doenças e suas complicações, o diabetes continua sendo aquela com maior impacto quanto à expressiva ineficácia observada em relação ao seu tratamento, salvo o uso da insulina. Por outro lado, os efeitos da FBE no tratamento do diabetes ainda é relativamente pouco conhecido. Ademais, há lacunas no conhecimento sobre os efeitos da FBE sobre as deletérias alterações metabólicas decorrentes da hiperglicemia, principalmente seus efeitos no metabolismo das células de Schwann, responsáveis em parte, pelas alterações metabólicas que contribuem de modo relevante para a geração das complicações crônicas observadas em quadro de hiperglicemia. Desta forma, o desafio científico desse projeto foi buscar o entendimento do envolvimento da FBE sobre alterações metabólicas no sistema nervoso periférico e adicionalmente no sistema nervoso central em modelo animal de NDP induzido por STZ. O presente estudo, avaliou também, os efeitos da FBE sobre o metabolismo (respiração celular) das células de Schwann.

### 3. Objetivos

#### 3.1 *Objetivo geral*

O objetivo geral deste projeto de pesquisa consistiu em compreender, experimentalmente, como a fotobioestimulação (FBE), pode atuar na reversão da hiperalgesia neuropática em modelo animal de neuropatia diabética periférica induzida por estreptozotocina.

#### 3.2 *Objetivo específicos*

- (i) Verificar o efeito da fotobioestimulação sobre a hiperalgesia mecânica decorrente da neuropatia diabética periférica induzida por estreptozotocina;
- (ii) Verificar se a fotobioestimulação modula proteínas relacionadas aos processos pró-inflamatórios (Carboximetilisina [CML], RAGE e NFkB) no nervo isquiático e gânglios da raiz dorsal de ratos diabéticos hiperalgésicos;
- (iii) Verificar se a fotobioestimulação modula citocinas pró e anti-inflamatórias (TNF-alfa, IL-6, IL-1Beta e IL-10) no nervo isquiático e gânglios da raiz dorsal de ratos diabéticos hiperalgésicos;
- (iv) Verificar se a fotobioestimulação modula os processos de fissão e fusão mitocondrial (Mitofusina-2 [MFN-2] e *Dynamin-related protein-1* [DRP-1]) no nervo isquiático e gânglios da raiz dorsal de ratos diabéticos hiperalgésicos;
- (v) Verificar se a fotobioestimulação atua no metabolismo energético mitocondrial (respiração celular) em cultura de células de Schwann;
- (vi) Verificar se a fotobioestimulação atua em áreas remotas a sua área de aplicação através de análises na medula espinal (segmento lombar) e córtex anterior cingular de ratos diabéticos hiperalgésicos.
- (vii) Verificar se a fotobioestimulação modula os receptores endocanabinóide CB<sub>1</sub> e CB<sub>2</sub> na medula espinal de ratos diabéticos hiperalgésicos.
- (viii) Verificar se a fotobioestimulação modula o receptor GLUR 1 e a enzima GAD65/67 no córtex anterior cingular de ratos diabéticos hiperalgésicos.
- (ix) Verificar se a fotobioestimulação modula a proteína fibrilar acídica glial (GFAP) no córtex anterior cingulado de ratos diabéticos hiperalgésicos.

- (x) Verificar se a fotobioestimulação modula o receptor opioide tipo  $\mu$  (MOR) no córtex anterior cingulado de ratos diabéticos hiperalgésicos.

## 4. Materiais e métodos

### 4.1 Animais

Foram utilizados o total de 135 ratos machos adultos da linhagem *Wistar*, pesando entre 120 e 220g. Os animais foram adquiridos do Biotério Central do Instituto de Ciências Biomédicas- ICB/ USP e mantidos no Biotério do Departamento de Anatomia, do mesmo Instituto. Todos os animais foram mantidos com água e ração *ad libitum* em uma sala apropriada, com isolamento acústico, temperatura controlada ( $22\text{ }^{\circ}\text{C} \pm 1$ ) e ciclo claro/escuro (12 h:12 h). Todos os procedimentos foram realizados de acordo com o protocolo da Comissão de Ética em Experimentação Animal (CEUA) do ICB (número de protocolo 123/2015). Os animais foram distribuídos nos seguintes grupos: Naive, Diabéticos (STZ) e Diabéticos Fotobioestimulados (STZ+FBE).

### 4.2 Indução do diabetes mellitus tipo 1

Para a indução do diabetes *mellitus* tipo 1 foi utilizado estreptozotocina (STZ) na dose de 85mg/kg de acordo com estudo prévio publicado pelo nosso grupo de pesquisa [88]. A administração da STZ foi realizada através de uma única injeção por via intraperitoneal na dose descrita acima (85mg/kg) diluída em 500 microlitros ( $\mu\text{L}$ ) de solução salina (0,9%) por animal.

**Verificação de glicemia:** Para controle glicêmico foi aplicado o uso de glicosímetro portátil da ULTRAMINI® | ONETOUCH®. A coleta de sangue para a verificação de glicemia foi realizada através de uma punção única na ponta da cauda do rato com agulha 0,30x13mm (30G). Foram considerados hiperglicêmicos (diabéticos) os animais que apresentaram glicemia igual ou maior a 200 mg/dl 48 horas após a administração da STZ. A verificação da glicemia foi realizada semanalmente.

**Teste de tolerância a glicose intraperitoneal.** Os animais de todos os grupos foram submetidos ao teste de tolerância a glicose intraperitoneal. Os ratos foram deixados em jejum alimentar por 12 horas, porém com livre acesso a água. A massa corporal dos animais submetidos ao teste foi medida anterior e posteriormente a aplicação do teste. No dia do ensaio, anterior a administração da solução de glicose foi inicialmente coletado sangue desses animais para a verificação de glicemia no “timepoint” zero (0) após as 12 horas de jejum. Após a verificação dos níveis glicêmicos, uma solução de glicose 5 g/kg foi

administrada por via intraperitoneal (i.p). Após a administração da referida solução, foi coletado sangue nos “timepoints” 30 min, 60 min e 120 min. As coletas de sangue inicial e em todos os respectivos “timepoint” (0, 30min, 60min e 120min) foram realizadas através de uma punção na ponta da cauda dos animais com agulha 0,30x13mm (30G). A concentração glicêmica foi medida com glicosímetro portátil.

### 4.3 Fotobioestimulação

Inicialmente os animais do grupo STZ+FBE foram anestesiados com Isoflurano com fluxo contínuo de oxigênio (5 L/ min). Após a anestesia, a caneta emissora de laser foi posicionada na pata posterior direita do rato ao longo do trajeto do nervo isquiático (Figura 4). O laser utilizado foi do tipo Arseneto de gálio (GaAs. IBRAMED-SP, Brasil) de modo pulsado com potência de saída de 45 mWpk e comprimento de onda de 904nm (Tabela 1). As dez sessões totais do tratamento apresentam uma exposição radiante total de 72.9 J/cm<sup>2</sup>. A primeira sessão da FBE foi iniciada no sexagésimo (60) dia após indução do diabetes *mellitus* tipo 1. No final do tratamento (décima sessão), todos os ratos foram eutanasiados e os tecidos (nervo isquiático, gânglio da raiz dorsal, medula espinal e encéfalo) coletados para posterior análise proteica por *Western blot* (Figura 5). A escolha do período do início da aplicação da FBE se deve aos bons resultados observados em estudo anterior, onde foi possível observar melhora do quadro nociceptivo dos animais e pela ação da FBE no processo de regeneração das fibras nervosas periféricas em modelo de neuropatia diabética periférica [88].

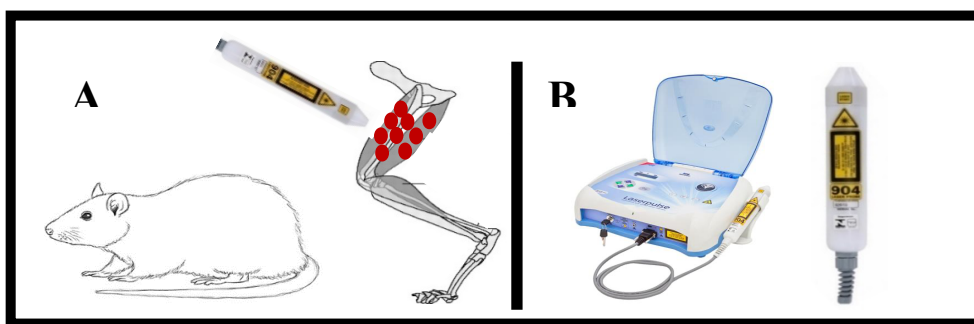


**Figura 4.** Esquema representativo da terapia com a FBE. **A)** Rato macho *Wistar* (*Rattus norvegicus*). Os círculos vermelhos representam os nove pontos superficiais de aplicação da FBE ao longo do trajeto do nervo isquiático. **B)** Aparelho de laser e caneta emissora de 904nm (infravermelho) – IBRAMED. São Paulo, Brasil.

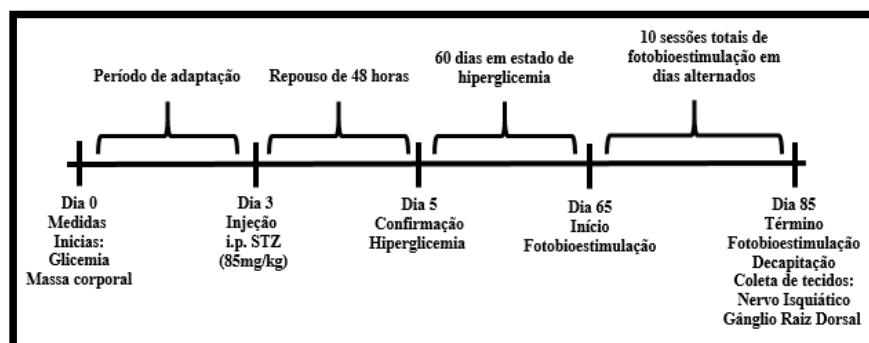


**Figura 5.** Delineamento experimental ao longo de oitenta e cinco (85) dias. Após um período de três (3) dias de adaptação ao biotério do Departamento de Anatomia, os ratos tiveram todas as medidas de peso e glicemia verificadas e posteriormente receberam dose única de STZ (85 mg/kg) por via i.p. Quarenta e oito (48) horas após a aplicação da STZ, os ratos apresentaram hiperglicemia (glicose >250 mg/dL). Uma vez confirmado o estabelecimento da hiperglicemia, os ratos foram mantidos e cuidados em condição de hiperglicemia por 60 dias. No sexagésimo dia após, teve início o tratamento com a FBE, realizado em dias alternados e com duração total de 10 sessões. Ao final da última sessão de FBE, todos os animais foram eutanasiados e os tecidos nervo isquiático, gânglio da raiz dorsal, medula espinal e córtex anterior cingular coletados e armazenados para posteriores análises.

**Tabela 1.** Parâmetros da FBE aplicada sobre a região do nervo isquiático.

<b>Parâmetros de irradiação</b>	
Comprimento de onda	904 nanômetros (nm)
Modo de operação	Pulsado
Frequência	9500 Hz
Duração do pulso em segundos	60 nano segundos
Formato do raio luminoso	Circular
<b>Parâmetros do tratamento</b>	
Circunferência do raio luminoso no alvo	0.13 cm <sup>2</sup>
Duração do tempo de exposição	18 segundos (s) por ponto de aplicação
Exposição radiante	6.23 J/cm <sup>2</sup>
Energia radiante	0.81 J por ponto
Área irradiada	1.17 cm <sup>2</sup>
Energia radiante total	7.29 J por sessão; 72.9 J total do tratamento (10 sessões)

#### **4.4 Teste comportamental de von Frey eletrônico**

Para a análise de hiperalgesia por meio do limiar mecânico de retirada da pata, utilizamos o teste comportamental de von Frey. Foi utilizado uma ponteira de polipropileno adaptada a um transdutor de força manual com pressão crescente na superfície da face plantar das patas traseiras direita e esquerda dos ratos de todos os grupos. O equipamento converte automaticamente a pressão aplicada na superfície da pata em grama – força (g) uma vez que a pata é retirada. Os ratos foram colocados individualmente em caixas plásticas com piso de malha metálica e aclimatados por 30 min anterior a aplicação do teste. O teste de von Frey eletrônico foi aplicado em todos os grupos (Naive, STZ,

STZ+FBE) para medida basal (dia 0) e nos dias 15, 30 e 60 após a aplicação da estreptozotocina. Após os 60 dias decorridos da cronificação da neuropatia diabética, foi iniciado o tratamento com a FBE e, em dias alternados a FBE, o teste de von Frey foi reaplicado para a verificação da eficácia da FBE na reversão da dor.

#### ***4.5 Cultura Celular - Células de Schwann linhagem RT4-D6P2T***

As células de Schwann de linhagem RT4-D6P2T originadas do ATCC e disponibilizadas pelo banco de células do Rio de Janeiro (BCRJ) foram semeadas a uma densidade de  $1 \times 10^6$  células em frasco de 75 cm<sup>2</sup>. As células foram semeadas em meio de cultura DMEN com concentração fisiológica e hiperglicêmica de glicose (5.5 e 55 mM) e mantidas da passagem zero (P0) a passagem P3 em estufa de CO<sub>2</sub> a 37C. O meio foi renovado a cada 48 horas.

#### ***4.6 Viabilidade celular por redução do MTT***

O ensaio de redução do brometo de 3-[4,5-Dimetil-2-il] -2,5-difenil-tetrazolium), conhecido como teste de viabilidade por redução do MTT, foi utilizado para a determinação da viabilidade celular das células de Schwann em meios fisiológico (5.5 mM) e hiperglicêmico (55.5 mM) referentes à concentração de glicose. O MTT é um sal o qual é convertido em formazam após clivagem do anel de tetrazólio por desidrogenases mitocondriais. O formazam foi então solubilizado com 200 uL de dimetil sulfóxido (DMSO), formando um composto colorido cuja densidade óptica foi medida em leitor de ELISA (540nm). A atividade mitocondrial (viabilidade celular) e diretamente proporcional à capacidade redutora do MTT e como consequente a produção do cromógeno.

As células de Schwann foram semeadas a uma densidade de  $1 \times 10^6$  células por poço e incubadas sob as mesmas condições de cultivo, porém com as diferentes concentrações de glicose (5.5 e 55 mM). A seguir, o MTT (5mg/ML) foi adicionado ao poço com as referidas células, permanecendo em estufa a 37C por 3 horas. Após este período, observou-se a redução do MTT, através de um precipitado colorido no fundo de cada poço. Esse precipitado foi então eluído com 200 uL de DMSO e imediatamente procedeu-se a leitura em leitor de ELISA. Para a aplicação da terapia, utilizamos os mesmos parâmetros mencionados anteriormente, no entanto, foi realizado apenas uma sessão da terapia. As placas foram irradiadas com um único ponto por poço, durante 18 segundos e 0.81 J-energia.

#### 4.7 Respiração mitocondrial e fotobioestimulação

Para as análises de como a hiperglicemia altera a funcionalidade mitocondrial,  $1.6 \times 10^6$  de células de Schwann (linhagem *RT4-D6P2T*) foram cultivadas em meio DEMEN com concentrações fisiológicas de glicose (5.5 mM) e incubadas nas câmaras do “Oroboros” a 37°C e submetidas a duas adições de solução de glicose a 27.5 e 55 mM para a indução da hiperglicemia (Figura 6). Foi medida sob as referidas condições, a respiração de rotina (respiração acoplada a oxidação fosforilativa em condições fisiológicas de ATP) seguida da respiração “vazada” (obtida após inibição da porção Fo da ATP sintase com oligomicina A (Oly)) para determinar a fração da respiração que não está acoplada a produção de ATP. Após todas essas análises serem observadas e determinadas, foi adicionado Cianeto de carbonila para-trifluoro-metil fenil hidrazina (FCCP) as câmaras. FCCP é um potente protonóforo que desacopla a oxidação fosforilativa através da dissipação do potencial de membrana mitocondrial interno. A adição deste composto nos permite acessar a capacidade funcional da cadeia transportadora de elétrons. O consumo de oxigênio foi medido utilizando células de Schwann intactas em um oxígrafo de alta resolução (OROBOROS, Oxygraph-2k, Innsbruck, AU). O tratamento com a FBE foi realizado com os mesmos parâmetros, porém uma única aplicação (904nm, 18sec, 0.81 J) feita diretamente câmaras do oxígrafo de alta resolução “Oroboros”, durante a mensuração mitocondrial.

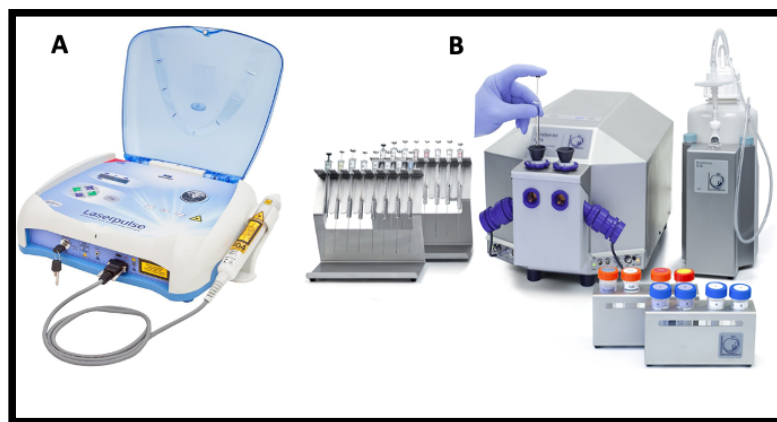


**Figura 6.** **A.** Aparelho emissor do laser de 940 nm utilizado para a irradiação das células de Schwann durante os ensaios de respiração mitocondrial em oxígrafo de alta resolução. Os mesmos parâmetros da FBE utilizados para os animais diabéticos foram utilizados para os ensaios de respiração celular. **B.** Oxígrafo de alta resolução “Oroboros”.



#### ***4.8 Coleta de tecidos: Nervo Isquiático, Gânglios da Raiz Dorsal (L4, L5, L6), Medula Espinal e Encéfalo para análise de expressão proteica por Western Blotting***

Após a última sessão (10ª sessão) de FBE, os animais dos diferentes grupos foram sedados com anestésico inalatório, e a seguir, eutanasiados com o uso de guilhotina (decapitação) para a retirada a fresco do nervo isquiático e gânglios da raiz dorsal (L4, L5, L6). Adicionalmente, foram coletados segmento lombar da medula espinal e córtex anterior cingular a fim de observar um possível efeito do tratamento em locais “distante” da aplicação. Imediatamente após a retirada dos referidos tecidos, estes foram colocados em *ependorfs* secos com identificação completa do tecido e submergidos em nitrogênio líquido, para posterior armazenamento em -80°C.

Foi realizado uma incisão longitudinal na pele e tecido subcutâneo, iniciada 0,5cm lateral em relação à linha média do animal e prolongada por 3cm em direção à articulação tíbio-femoral. Imediatamente à incisão, foram afastados os músculos bíceps femoral e glúteo, permitindo a exposição do nervo isquiático desde sua origem (incisura isquiática) até seu ponto de bifurcação (nervo tibial e fibular). Após a observação e identificação do nervo isquiático, este foi seccionado (2cm) entre seus pontos de origem/bifurcação e posteriormente armazenado conforme citado anteriormente.

Do mesmo animal foram retirados os gânglios da raiz dorsal (L4, L5, L6) – região lombar. Uma incisão com lâmina de bisturi foi realizada ao longo de toda linha média do animal, expondo toda musculatura e tecidos adjacentes à região dorsal. Os referidos tecidos foram removidos até a exposição distinta da coluna vertebral. Uma vez exposta, as vértebras da região lombar foram seccionadas lateralmente e removidas, revelando a medula espinal e conseqüentemente os gânglios da raiz dorsal. Estes foram seccionados entre as raízes dorsais e os feixes de fibras adjacentes e armazenados conforme descrito. Neste mesmo momento, após a coleta dos gânglios da raiz dorsal, o segmento lombar da medula espinal também foi coletado.

O crânio desses animais também passou por processo de dissecação com o objetivo de coletar seus respectivos encéfalos. Uma vez rebatidos os músculos da cabeça e pescoço, os ossos do crânio foram removidos e o encéfalo exposto. Este foi removido do crânio e seu lobo frontal dissecado para a coleta do córtex anterior cingulado.

#### 4.9 Análise de expressão proteica – Western Blotting

Para a extração de proteína total do referido tecido foi utilizado um tampão de lise (90 mM KCl, 10 mM Hepes, 3 mM MgCl<sup>2+</sup>, 5 mM EDTA, glicerol 1%, 1 mM DTT, 0,04% SDS, 20 mM Aprotinina, 20 mM Pepstatina, 20 mM Leupeptatina, 40 μM PMSF, 100 mM Ortovanadato). A concentração proteica total foi obtida pelo método de Bradford [89]. Em seguida, 40μg de proteína total foram submetidas à eletroforese em gel de poliacrilamida (gel de gradiente 4% e 20%) e transferidas para membrana de nitrocelulose (Bio-Rad). A referida membrana foi corada com solução *Ponceau* para avaliar se a concentração de proteínas é similar entre as amostras. Posteriormente a membrana foi incubada com os anticorpos primários descritos na tabela 2 em agitação constante a 4°C overnight. Após sua lavagem, com solução TBST (Trisma 1M, NaCl 5M, Tween20), a membrana foi incubada com os anticorpos secundários anti-rabbit (1:5000) conjugado à peroxidase por 45 minutos a temperatura ambiente. A membrana foi então lavada novamente com solução basal e em seguida submetida ao processo de revelação pelo detector de quimioluminescência (UviTec Gel Doc Systems). As bandas correspondentes à proteína de interesse foram quantificadas por densitometria utilizando o programa Image J, sendo os valores expressos em porcentagem. Beta actina e GAPDH foram utilizados para controle.

**Tabela 2** – Anticorpos primários para *Western Blotting*.

<b>Anticorpo</b>	<b>Origem</b>	<b>Diluição</b>	<b>Peso molecular</b>
Anti-Beta Tubulina	Abcam (ab6046)	1:5000	50KDa
Anti-CB1	Abcam (ab3558)	1:500	60KDa
Anti-CB2	Abcam (ab3561)	1:500	40KDa
Anti-CML	Abcam (ab27684)	1:500	10KDa
Anti-Drp-1	Cell Signalling (8570)	1:500	80KDa
Anti-GAPDH	Abcam (ab9483)	1:5000	37KDa
Anti-GFAP	Sigma (3893)	1:1000	50KDa
Anti-GAD65/67	Millipore (AB1511)	1:1000	65/67 KDa
Anti-GLUR1	Millipore (AB1504)	1:1000	106KDa
Anti-IL1β	Abcam (ab2105)	1:500	31KDa
Anti-IL6	Abcam (ab6672)	1:500	21KDa
Anti-IL10	Abcam (ab9969)	1:500	21KDa
Anti-Mitofusina-2	Cell Signalling (9482)	1:500	80KDa
Anti-MOR	Santa Cruz (15310)	1:1000	50KDa
Anti NFκB p65	Abcam (ab16502)	1:500	62KDa
Anti-RAGE	Abcam (ab3611)	1:500	42KDa
Anti-TNF alfa	Abcam (ab6671)	1:500	24KDa

#### ***4.10 Análise dos dados***

Os dados foram representados como média  $\pm$  e.p.m. e a análise estatística foi gerada utilizando o programa GraphPad Prism 5.01 (GraphPad Software Inc., CA, USA). A análise estatística foi realizada por meio de Análise de variância (ANOVA) com um e/ou dois fatores (grupos e tempo), associada ao teste de Bonferroni. Para comparar dois grupos independentes foi aplicado o teste t de Student ou teste não paramétrico de Mann-Whitney, caso a variável não apresente distribuição normal nos dois grupos. O índice de significância considerado foi de  $P < 0.05$  [90].

## 5. Resultados

Os resultados apresentados a seguir foram obtidos no Laboratório de Neuroanatomia Funcional da Dor localizado no Departamento de Anatomia do Instituto de Ciências Biomédicas.

### 5.1 Eficácia da indução do diabetes tipo 1 induzido por dose única de estreptozotocina (STZ)

O protocolo de indução do diabetes tipo 1 por dose única de STZ mostrou-se eficaz para o desenvolvimento da hiperglicemia (Fig. 7. A). Todos os ratos dos grupos experimentais STZ e STZ+FBE tornaram-se diabéticos (hiperglicemia >250 mg/dL) 72 horas após única administração de STZ (85 mg/kg) diluída em solução salina (0,9%) por via intraperitoneal (i.p). O grupo controle naive não apresentou alteração glicêmica. Ainda, não houve reversão do quadro hiperglicêmico ao longo de todo protocolo, índices hiperglicêmicos foram mantidos acima de 250 mg/dL para os animais diabéticos (Fig. 7. A). Outros sinais clínicos do diabetes foram observados ao longo do tempo, como, por exemplo, interrupção no ganho de peso (Fig. 7. B), além de poliúria, polifagia e polidipsia.

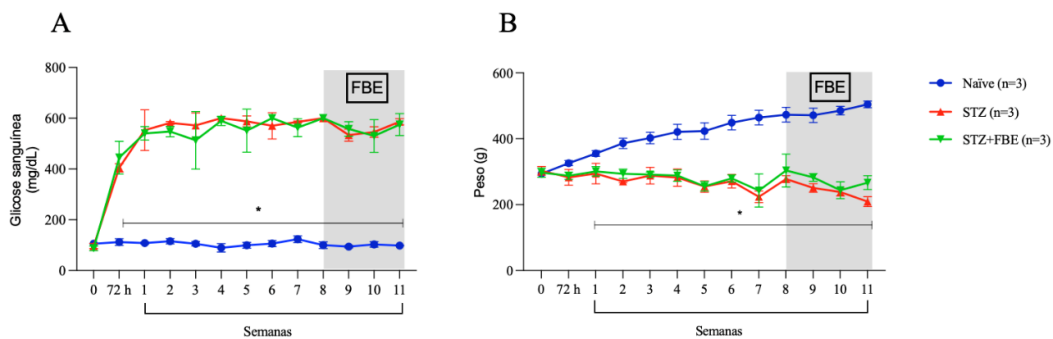


**Figura 7. A.** Glicemia de rotina ao longo de todo período experimental. \* $p < 0.0001$  STZ, STZ+FEB comparados com o grupo controle naive. **B.** Peso corporal ao longo de todo período experimental \* $p < 0.0001$  STZ, STZ+FBE comparados com o grupo controle naive. A coluna em cinza representa o período de tratamento com a terapia de fotobioestimulação (FBE).

### 5.2 Efeitos da estreptozotocina sobre o teste de tolerância à glicose intraperitoneal

Como descrito anteriormente, o protocolo de indução do diabetes tipo 1 por dose única de STZ mostrou-se eficaz para o desenvolvimento da hiperglicemia. Adicionalmente, realizamos o teste de tolerância a glicose intraperitoneal (ipGTT) como ferramenta indispensável para a comprovação do desenvolvimento do diabetes tipo 1 neste trabalho. O teste (ipGTT) foi realizado no sexagésimo (60<sup>o</sup>) dia após a indução do diabetes e anteriormente ao início do tratamento com a FBE. Observamos que os ratos diabéticos (STZ e STZ+FBE) não foram capazes de regular os níveis glicêmicos ao longo das 2 horas do teste (Fig. 8) quando comparados com os ratos do grupo controle naive. O resultado observado indica inadequada produção de insulina pelo pâncreas desses ratos, resultando assim na ineficácia desses ratos em regular seus níveis glicêmicos.

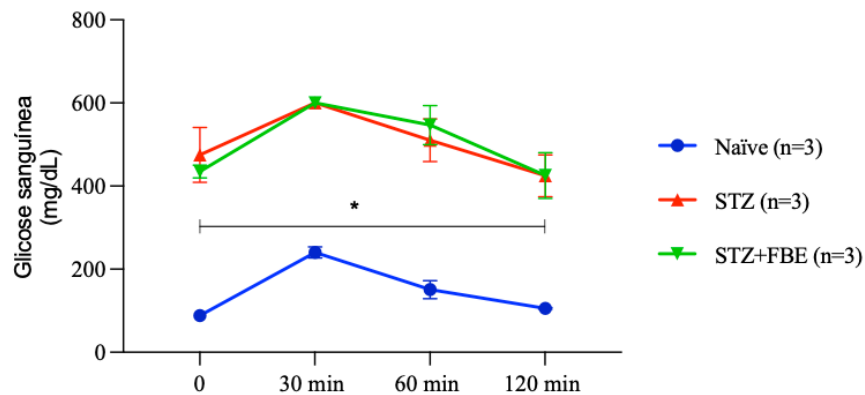


**Figura 8.** Teste de tolerância a glicose intraperitoneal. \* $p < 0.0001$  comparados os grupos controle (Naive e Salina) com os grupos diabéticos STZ e STZ+FBE. Os ratos diabéticos são incapazes de regular os níveis hiperglicêmicos ao longo das 2 horas do teste. Evidenciando a produção insuficiente de insulina pelo pâncreas desses animais.

### 5.3 Efeitos da fotobioestimulação sobre o limiar e intensidade de dor em ratos diabéticos hiperalgésicos

O uso da fotobioestimulação foi capaz de reverter o limiar de dor assim como diminuir a sua intensidade (Fig. 9. A). Os ratos diabéticos (STZ) não tratados com a FBE apresentaram diminuição significativa do limiar de dor e aumento de sua intensidade quando comparados com os grupos controles ( $*p<0.005$ , Naive e Salina). Por outro lado, os ratos diabéticos do grupo tratado com a FBE (STZ+FBE) apresentaram reversão do quadro de dor (Fig. 9. A. & $p<0.005$ ) assim como diminuição de sua intensidade a partir do 2º dia de tratamento com a FBE quando comparados com o grupo STZ (Fig. 9. B & $p<0.005$ ). A figura 9. A e B evidencia os efeitos analgésicos da FBE nos ratos diabéticos.

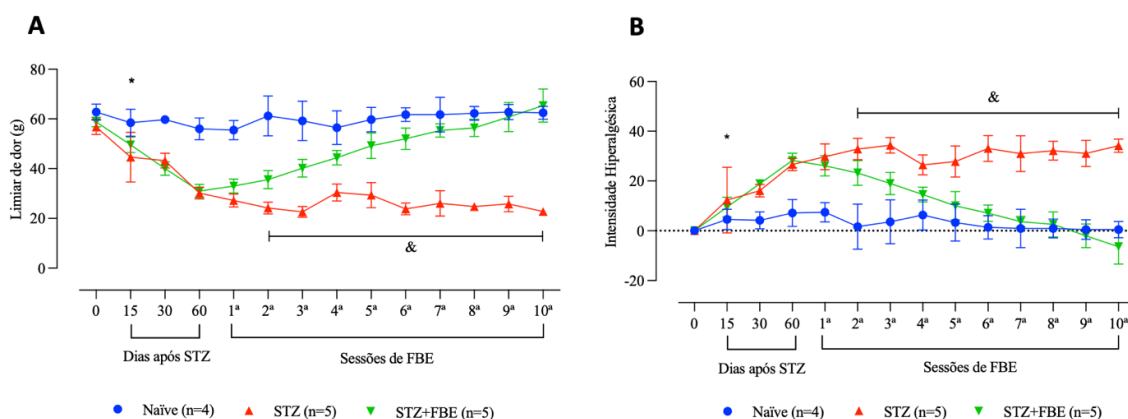
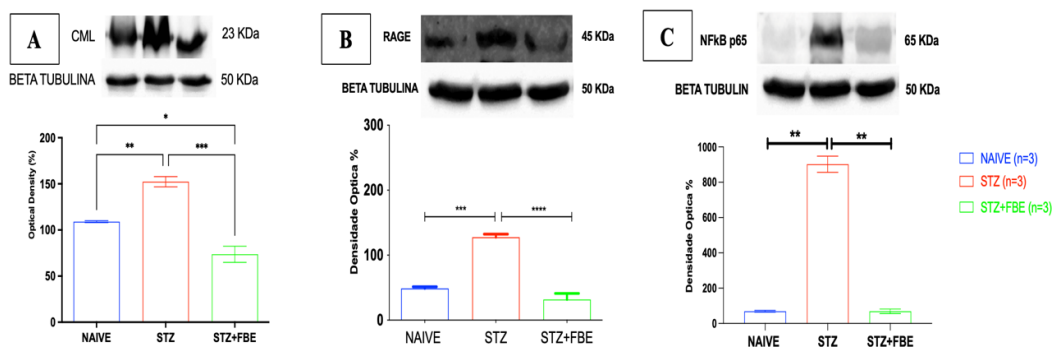


Figura. 9. A. Limiar de retirada da pata pelo estímulo de filamento de von Frey eletrônico.  $*p<0.005$  STZ, STZ+FBE comparado com o controle Naive após 15 dias decorridos da aplicação da STZ. & $p<0.005$  STZ+FBE comparados com STZ. B. Intensidade de dor.  $*p<0.005$  STZ, STZ+FBE comparado com o controle Naive. & $p<0.0005$  STZ+FBE comparado com STZ. A coluna em cinza representa o período de tratamento com a terapia de fotobioestimulação (FBE).

**Os resultados apresentados a seguir foram obtidos do sistema nervoso periférico:  
nervo isquiático**

***5.4 Efeitos da fotobioestimulação sobre proteínas envolvidas nos processos pró-inflamatórios no nervo isquiático de ratos diabéticos hiperalgésicos***

Com base nos resultados da fotobioestimulação sobre a reversão do quadro de dor, analisamos por meio da técnica de Western Blot, o provável envolvimento da fotobioestimulação sobre a modulação de proteínas que participam ativamente dos processos pró-inflamatórios. Representado na Fig. 10, podemos observar um aumento da expressão do produto de glicação avançada carboximetilisina (CML), produtos finais de glicação avançada (RAGE) e o fator de transcrição nuclear kappa B (NFkB) no grupo diabético (STZ). Por outro lado, após o tratamento com a terapia, observamos uma diminuição da expressão em todas as proteínas analisadas. Observamos que a FBE (STZ + FBE) diminuiu a expressão de CML (Fig. 10. A,  $***p<0.001$ ); RAGE (Fig. 10. B,  $***p<0.001$ ) e NFkB (Fig. 10. C,  $**p<0.0001$ ) no nervo isquiático de ratos diabéticos quando comparado com o grupo sem tratamento (STZ).



**Figura 10.** Efeitos da fotobioestimulação sobre proteínas envolvidas nos processos pró-inflamatórios no nervo isquiático. **A.** Carboximetil lisina (CML)  $***p<0.001$  STZ+FBE comparado com STZ. **B.** Receptor para os produtos finais de glicação avançada (RAGE).  $***P<0.001$  STZ+FBE comparado com STZ. **C.** Fator de transcrição nuclear Kappa B p65.  $**p<0.0001$  STZ+FBE comparado com STZ.

### 5.5 Efeitos da fotobioestimulação sobre citocinas pró e anti-inflamatórias no nervo isquiático de ratos diabéticos hiperalgésicos

Com base nos resultados apresentados anteriormente, analisamos ainda os efeitos da FBE sobre as citocinas pró e anti-inflamatórias (TNF-alfa, IL-6, IL1-Beta e IL-10) no nervo isquiáticos dos diferentes grupos. Observamos um aumento estatístico na densidade óptica do TNF-alfa no grupo diabético (STZ) comparado com o grupo controle naive (Fig. 11. A,  $*p < 0.001$ ). No entanto, após o tratamento, não foi possível observar alteração estatística entre os grupos diabéticos (STZ) e o grupo diabético fotobioestimulado (STZ+FBE) (Fig. 11. A). Com relação a expressão da citocina IL-6 não observamos diferença estatística entre os grupos analisados (Fig. 11. B). Resultado similar ao TNF-alfa foi observado para a citocina IL1-Beta (Fig. 11. C). Não houve diferença estatística entre os grupos STZ e STZ+FBE, porém houve aumento significativo na densidade óptica dessa citocina no grupo diabético (STZ) em comparação com o grupo controle naive (Fig. 11. C,  $***p < 0.005$ ). Por outro lado, quando avaliamos a expressão da interleucina anti-inflamatória IL-10, observamos que o tratamento com a fotobioestimulação foi capaz de aumentar a expressão dessa citocina no grupo STZ+FBE comparado com o grupo STZ (Fig. 11. D,  $**p < 0.001$ ), chegando a níveis basais.

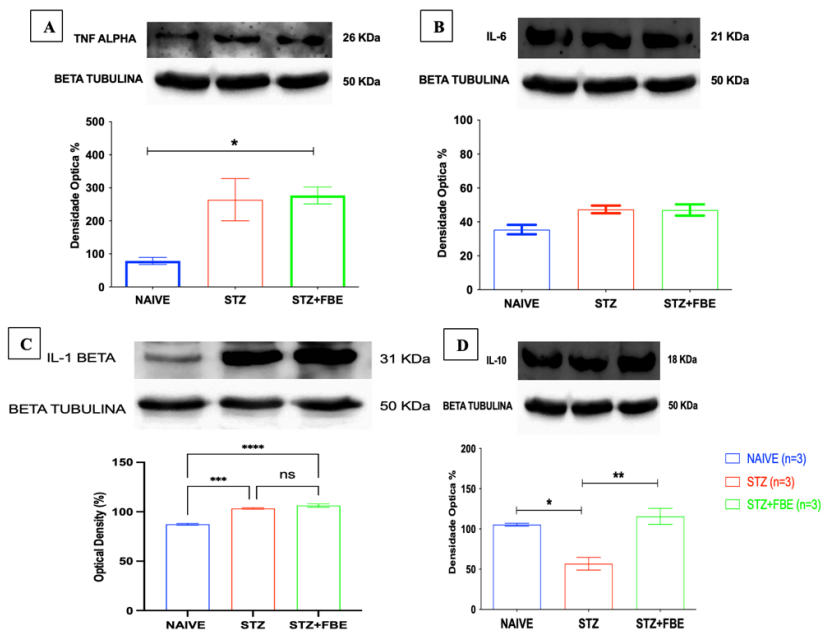


**Figura 11.** Efeitos da fotobioestimulação sobre citocinas pró e anti-inflamatórias no nervo isquiático. **A.** TNF-alfa,  $*p < 0.001$  STZ comparado com o grupo controle naive. **B.** IL-6, não houve diferença estatística entre os grupos analisados. **C.** IL-1 Beta,  $***p < 0.005$  STZ comprado com o grupo controle naive. **D.** IL-10,  $**p < 0.001$  STZ+FBE comparado com o grupo diabético (STZ).



### 5.6 Efeitos da fotobioestimulação sobre a dinâmica mitocondrial no nervo isquiático de ratos diabéticos hiperalgésicos

Como mencionado nos capítulos introdutórios, um dos objetivos do presente estudo, foi a avaliação da FBE sobre a dinâmica mitocondrial. A FBE foi capaz de modular os processos de fissão e fusão mitocondrial no nervo isquiático dos ratos diabéticos (STZ+FBE). A Figura 12. A e B destaca as proteínas mitocondriais DRP-1 (fissão) e MFN-2 (fusão), respectivamente. Observamos que a FBE pode estar protegendo as fibras nervosas periféricas dos processos de fissão mitocondrial (Fig. 12. A,  $**p<0.001$  STZ+FBE comparado com STZ) e paralelamente aumentando os processos de fusão mitocondrial nessas mesmas fibras nos ratos diabéticos (Fig. 12. B,  $*p<0.001$  STZ+FBE comparado com STZ).

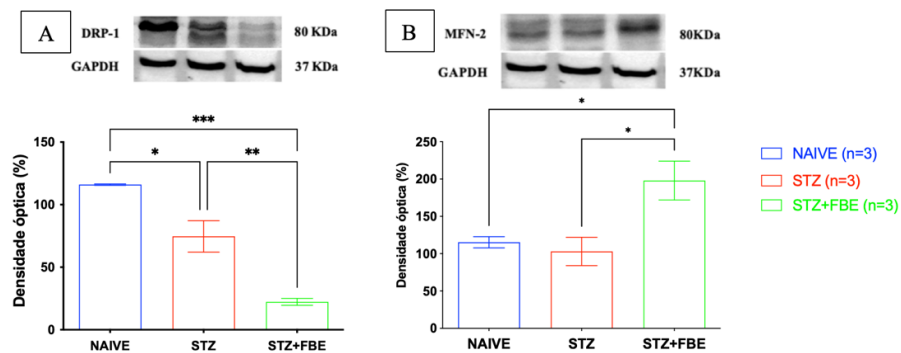


**Figura 12.** Efeitos da fotobioestimulação sobre os processos de fissão e fusão mitocondrial no nervo isquiático. **A.** DRP-1 (fissão)  $**p<0.001$  STZ+FBE comparado com STZ. **B.** MFN-2 (fusão)  $*p<0.001$  STZ+FBE comparado com STZ.

Os resultados apresentados a seguir foram obtidos do sistema nervoso periférico:  
gânglio da raiz dorsal

*5.7 Efeitos da fotobioestimulação sobre proteínas envolvidas nos processos pró-inflamatórios no gânglio da raiz dorsal de ratos diabéticos hiperalgésicos*

Diferentemente do resultado observado no nervo isquiático para o produto final de glicação avançada carboximetilisina (CML), não foi observado diferença estatística entre os grupos analisados para essa proteína no GRD (Fig. 13. A). Porém, foram observados resultados similares aqueles do nervo isquiático, para o receptor RAGE e o fator de transcrição nuclear kappa B (NFkB) no gânglio da raiz dorsal. A FBE diminuiu estatisticamente a densidade óptica do receptor RAGE no GRD de ratos diabéticos (Fig. 13. B, \*\*\*\* $p < 0.0001$  STZ+FBE comparado com STZ). Neste mesmo tecido, a FBE também modulou o fator de transcrição nuclear kappa B (Fig. 13. C, \*\*\* $p < 0.005$  STZ+FBE comparado com STZ).

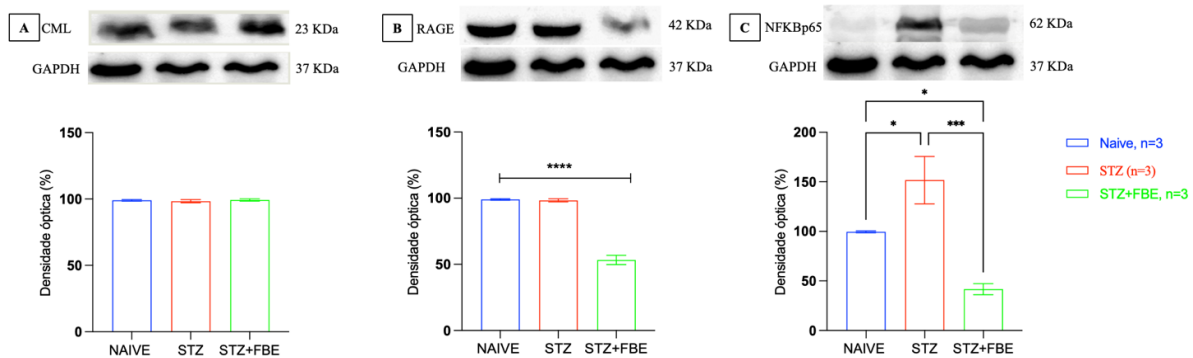


**Figura 13.** Efeitos da fotobioestimulação sobre proteínas envolvidas nos processos pró e anti-inflamatórios no gânglio da raiz dorsal. **A.** Carboximetil lisina (CML). Não houve diferença estatística entre os grupos analisados. **B.** Receptor para os produtos de glicação avançado RAGE. \*\*\*\* $p < 0.0001$  STZ+FBE comparado com STZ. **C.** Fator de transcrição nuclear Kappa B (NFkB). \*\*\* $p < 0.005$  STZ+FBE comparado com STZ.

### 5.8 Efeitos da fotobioestimulação sobre citocinas pró e anti-inflamatórias no gânglio da raiz dorsal de ratos diabéticos hiperalgésicos

Resultados opostos àqueles mostrados no nervo isquiático foram observados para o GRD em relação as citocinas pro-inflamatórias. A FBE diminuiu estatisticamente a expressão da citocina TNF-alfa no GRD dos ratos diabéticos (Fig. 14. A,  $***p < 0.001$  STZ+FBE comparado com STZ). Em contrapartida, não foi observado diferença estatística para a interleucina IL-6 entre os grupos avaliados (Fig. 14. B). A FBE também diminuiu estatisticamente a densidade óptica da interleucina IL-1beta no GRD dos ratos diabéticos (Fig. 14. C,  $***p < 0.005$  STZ+FBE comparado com STZ). Foi observado ainda, de modo similar ao apresentado para o nervo isquiático, que a FBE aumentou os níveis da interleucina anti-inflamatória IL-10 no GRD dos ratos diabéticos (Fig. 14. D,  $***p < 0.0001$  STZ+FBE comparado com STZ).

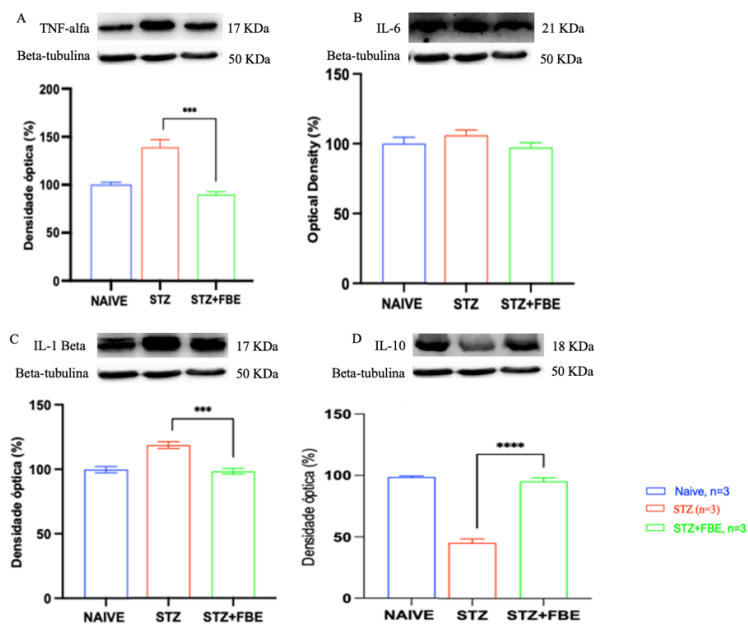


**Figura 14.** Efeitos da fotobioestimulação sobre as citocinas pró e anti-inflamatórias. **A.** TNF-alfa,  $***p < 0.001$  STZ+FBE comparado com STZ. **B.** IL-6, não foi observado diferença estatística para os grupos analisados. **C.** IL-1 Beta,  $***p < 0.005$  STZ+FBE comparado com STZ. **D.** IL-10,  $***p < 0.0001$  STZ+FBE comparado com STZ.

### 5.9 Efeitos da fotobioestimulação sobre a dinâmica mitocondrial no gânglio da raiz dorsal de ratos diabéticos hiperalgésicos

A FBE foi também capaz de modular os processos de fissão e fusão mitocondrial no GRD dos ratos diabéticos (STZ+FBE) conforme observado para o nervo isquiático. A Figura 15. A e B destaca as proteínas mitocondriais DRP-1 (fissão) e MFN-2 (fusão). Foi observado que a FBE pode estar de alguma maneira protegendo os corpos celulares das fibras periféricas do processo de fissão mitocondrial (Fig. 15. A, \*\*\*\* $p < 0.0001$  STZ+FBE comparado com STZ). Em contrapartida, a FBE aumentou os níveis da proteína de fusão mitocondrial mitofusina-2 (MFN-2) no GRD dos ratos diabéticos (Fig. 15. B, \*\*\*\* $p < 0.0001$  STZ+FBE comparado com STZ).

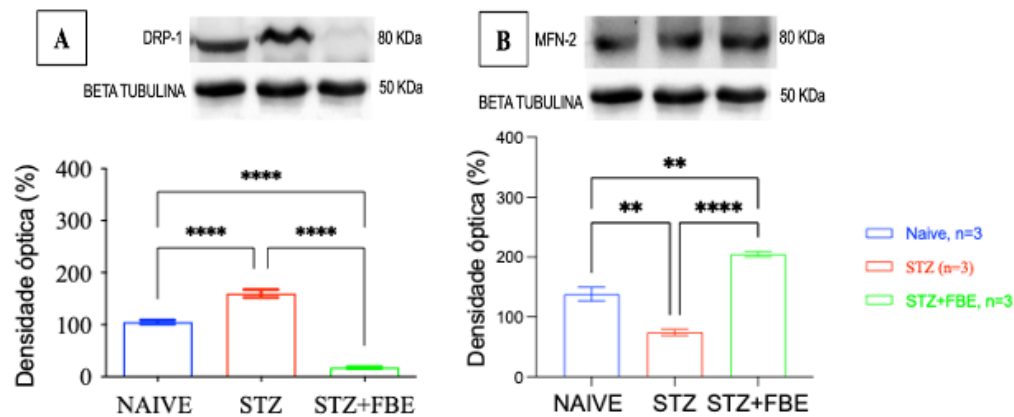


**Figura 15.** Efeitos da fotobioestimulação sobre as proteínas de fissão e fusão mitocondrial. **A**, proteína DRP-1 (fissão mitocondrial), \*\*\*\* $p < 0.0001$  STZ+FBE comparado com STZ. **B**, proteína MFN-2 (fusão mitocondrial), \*\*\*\* $p < 0.0001$  STZ+FBE comparado com STZ.

### 5.10 Ensaios de viabilidade celular por redução do MTT – Células de Schwann (Linhagem RT4-D6P2T)

O ensaio de viabilidade celular por redução do MTT indicou que a FBE aumentou a viabilidade das células de Schwann cultivadas em meio fisiológico de concentração de glicose (Fig. 16, \*\*\*\* $p < 0.0001$  5.5 mM + FBE comparado com 5.5 mM). De modo interessante, a concentração hiperglicêmica do meio de cultura (55 mM) não foi tóxica para a linhagem das células de Schwann estudadas.

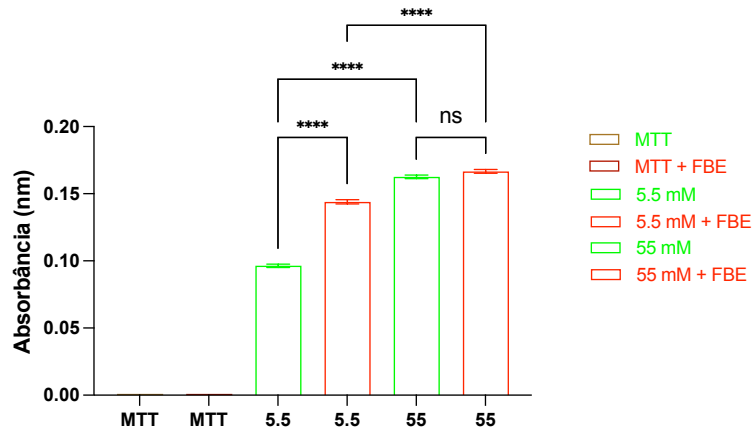


**Figura 16.** Ensaio de viabilidade celular por redução do MTT. \*\*\*\* $p < 0.0001$  5.5 mM + FBE comparado com 5.5 mM. Não houve diferença estatística para a concentração hiperglicêmica (55mM) para as células tratadas e não tratada com a FBE.

### 5.11 Efeitos da fotobioestimulação sobre o metabolismo mitocondrial das células de Schwann

Em relação aos ensaios de respiração celular, foi observado que o meio hiperglicêmico (55 mM) afeta de maneira rigorosamente negativa a produção de ATP mitocondrial (Fig. 17). Em contrapartida, a aplicação da FBE sobre as células de Schwann em meio hiperglicêmico, recupera de maneira parcial e similar a concentração fisiológica de glicose (5.5 mM) a produção de ATP mitocondrial. Esse resultado sugere que a FBE reverte a produção ineficaz de ATP nas células de Schwann hiperglicêmicas.

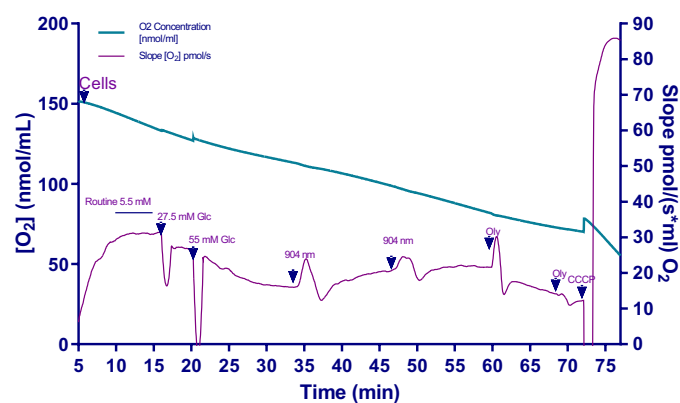


**Figura 17.** Efeitos da fotobioestimulação sobre a respiração mitocondrial. A FBE reverte a produção ineficaz de ATP nas células de Schwann em meio hiperglicêmico. Os mesmos parâmetros da FBE utilizados para o tratamento dos animais diabéticos foram utilizados para a irradiação das células de Schwann nas câmaras do oxígrafo de alta resolução “Oroboros”. Durante os ensaios de respiração celular, foram utilizados duas aplicações da FBE, mostrada no gráfico como 904 nm.

### Os resultados apresentados a seguir foram obtidos do sistema nervoso central: medula espinal e córtex anterior cingulado

Adicionalmente aos estudos da FBE sobre a NDP, verificamos também os possíveis efeitos da FBE em áreas remotas a sua aplicação de origem (nervo isquiático). Para tanto, coletamos o segmento lombar da medula espinal e córtex anterior cingulado de todos os grupos experimentais. No segmento lombar da medula espinal foi analisado o sistema endocanabinoide, representado pelos receptores CB<sub>1</sub> e CB<sub>2</sub>. Para o córtex anterior cingulado, foi verificada as proteínas GAD65/67, GLUR1, GFAP e o receptor opioide tipo  $\mu$  (MOR).

#### 5.12 Efeitos da fotobioestimulação sobre os receptores endocanabinoide CB<sub>1</sub> e CB<sub>2</sub> na medula espinal de ratos diabéticos hiperalgésicos

Nossos resultados mostraram que a FBE aumentou os níveis do receptor CB<sub>1</sub> (Fig. 18 A) no segmento lombar de ratos diabéticos (Fig. 18. A, \* $p < 0.005$  STZ+FBE comparado com STZ). Em contrapartida, não houve diferença estatística para o receptor CB<sub>2</sub> nos grupos avaliados (Fig. 18. B).

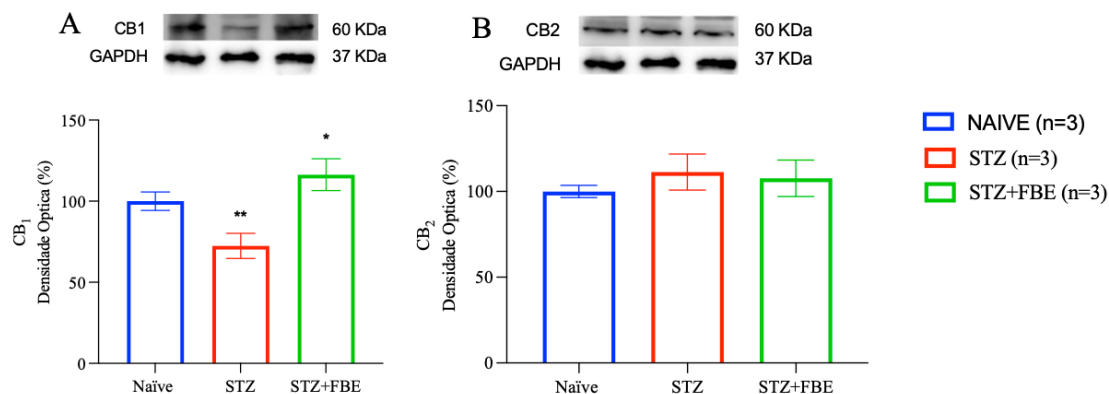


**Figura 18.** Efeitos da fotobioestimulação sobre o sistema endocanabinoide na medula espinal (segmento lombar) de ratos diabéticos hiperalgésicos. A \* $p < 0.005$  STZ+FBE comparado com STZ. B Não houve diferença estatística entre os grupos observados para o receptor endocanabinoide CB<sub>2</sub>.

### 5.13 Efeitos da fotobioestimulação sobre o córtex anterior cingulado de ratos diabéticos hiperalgésicos

Não houve diferença estatística para a proteína GAD65/67 (presente em neurônios inibitórios) entre os grupos diabéticos e diabéticos fotobioestimulados. Porém, ambos os grupos (STZ e STZ+FBE) apresentaram diminuição significativa para o GAD65/67 em comparação com o grupo controle naive (Fig. 19. A, \*\*\*\* $p < 0.001$  STZ+FBE comparado com Naive). Em contrapartida, a FBE diminuiu a expressão do receptor excitatório GLUR1 no ACC dos ratos diabéticos (Fig. 19. B, \*\*\*\* $p < 0.005$  STZ+FBE comparado com STZ). Quando avaliamos a expressão de células gliais, aqui representado pela proteína GFAP (marcador de astrócitos), observamos aumento na expressão dessa proteína em ratos diabéticos (STZ) (Fig. 19 C). Por outro lado, a FBE reduziu de maneira significativa os níveis da proteína marcadora de astrócitos (GFAP) nos ratos diabéticos (Fig. 19. C, \*\*\*\* $p < 0.0001$  STZ+FBE comparado com STZ). O inverso foi observado quando avaliamos o receptor opioide tipo  $\mu$  (MOR). A FBE aumentou os níveis do receptor opioide MOR nos ratos diabéticos (Fig. 19 D \*\* $p < 0.005$  STZ+FBE comparado com STZ).

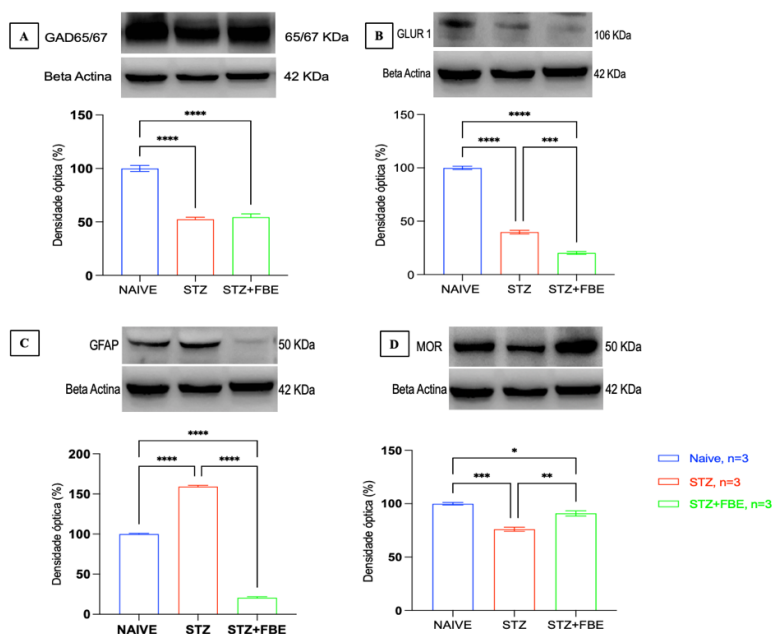


**Figura 19.** Efeitos da fotobioestimulação sobre o córtex anterior cingulado. A. GAD65/67, \*\*\*\* $p < 0.001$  STZ+FBE comparado com Naive. B. GLUR1, \*\*\* $p < 0.005$  STZ+FBE comparado com STZ. C. GFAP, \*\*\*\* $p < 0.0001$  STZ+FBE comparado com STZ. D. MOR, (\*\* $p < 0.005$  STZ+FBE comparado com STZ).



## 6. Discussão

A proposta deste estudo mostrou alguns dos promissores efeitos da FBE sobre a ND em modelo animal de diabetes *mellitus* tipo 1 induzido por STZ. Os efeitos benéficos da FBE apresentados aqui corroboram a literatura atual, a qual evidencia o uso da FBE em diversas doenças como ferramenta terapêutica para o tratamento do componente inflamatório [91-93] tanto quanto o seu uso com a finalidade de modulação mitocondrial [94-96].

Foi padronizado com sucesso o uso da STZ como modelo eficaz para o desenvolvimento da hiperglicemia crônica em ratos. A literatura indica para o desenvolvimento do diabetes o uso de múltiplas e baixas doses de estreptozotocina [97, 98] porém, durante estudos prévios realizados por nosso grupo de pesquisa, observamos que das 4 concentrações diferentes de STZ utilizadas (50mg/kg – 65mg/kg – 75mg/kg – 85mg/kg), a única que se mostrou eficaz para responder os nossos objetivos foi a concentração de 85mg/kg. Esta dose foi capaz de alterar de maneira expressiva e contínua os níveis glicêmicos de ratos logo após 72 horas de sua administração por via i.p. Os animais submetidos à indução do diabetes *mellitus* apresentaram características essenciais do quadro das complicações crônicas do modelo experimental ao longo do período experimental (80 dias totais). Estes apresentaram relevante perda de massa corporal, sede e urina em excesso (polidipsia e poliúria), quadro severo de desidratação e debilidade, além do desenvolvimento de catarata em ambos os olhos no período mais tardio da doença, aproximadamente 60 dias após a aplicação da estreptozotocina.

O tempo de escolha para o início do tratamento com a FBE também está de acordo com estudos prévios desenvolvidos pelo nosso grupo de pesquisa [99]. Fizemos a análise temporal – 30, 60, 90 e 120 dias – de ratos em condição de hiperglicemia e observamos que a ND (periférica) estava instalada a partir do sexagésimo dia (60º dia), tempo no qual foi observado expressivo dano as fibras nervosas periféricas, caracterizado por significativo processo degenerativo observado por microscopia eletrônica de transmissão (MET). Adicionalmente ao processo degenerativo, os animais diabéticos apresentaram relevante quadro nociceptivo caracterizado por alodínia e hiperalgesia mecânica, “dor” em resposta à estímulos não nocivos. Condição esta característica da neuropatia diabética periférica [100].

Cabe ressaltar que o objetivo do trabalho foi observar se a terapia com a FBE seria capaz de interferir em características como: processo degenerativo; nocicepção (dor), ambos em condição de hiperglicemia e sem o uso de insulina. A finalidade de análise foi observar a participação da FBE como agente anti-inflamatório e indutor de regeneração das fibras nervosas periféricas assim como ferramenta para a reversão do quadro nociceptivo em modelo animal de diabetes. Descartando desta forma o uso de insulina.

Uma vez observado em estudos prévios que a FBE foi capaz de reverter o quadro nociceptivo e ainda de induzir de maneira expressiva a regeneração de fibras nervosas periféricas na ND (periférica) em modelo animal de diabetes *mellitus* tipo 1 induzido por STZ [88], os objetivos aqui foram o de avaliar se esta mesma terapia poderia ser ferramenta útil na modulação de proteínas relacionadas ao processo inflamatório – CML, RAGE, NF $\kappa$ B – assim como na modulação de citocinas com atividade pró e anti-inflamatórias (TNF- $\alpha$ , IL-6, IL1- $\beta$  / IL-10) respectivamente.

Outro ponto de relevante, foi a análise da dinâmica mitocondrial em condição de hiperglicemia e ainda a observação da terapia proposta como agente modulador das proteínas relacionadas à dinâmica mitocondrial – DRP-1 / MFN-2, ponto de grande interesse na literatura atual sobre o diabetes e suas complicações [61]. Estudos recentes têm apontado a dinâmica mitocondrial como alvo de investigação para a geração das complicações crônicas decorrentes da hiperglicemia e ainda como alvo terapêutico para a reversão ou inibição das complicações anteriormente citadas [44, 101].

Os resultados aqui obtidos mostraram o efetivo envolvimento do modelo de diabetes *mellitus* tipo 1 por STZ em induzir de forma expressiva a glicação de proteínas nas fibras nervosas periféricas dos animais diabéticos. O processo de glicação das fibras nervosas periféricas nos ratos diabéticos foi nitidamente constatado pelo aumento expressivo da densidade óptica do produto de glicação avançada carboximetil lisina (CML) no nervo isquiático dos referidos animais. Por outro lado, não foi observado aqui diferença significativa deste mesmo fator (CML) no gânglio da raiz dorsal.

No que se refere aos receptores dos produtos finais de glicação avançada (RAGE), foi apresentado relevante expressão proteica do referido receptor no nervo isquiático dos animais diabéticos. Por outro lado, a FBE diminuiu estatisticamente a expressão proteica deste receptor nos animais submetidos ao protocolo de tratamento proposto. De modo interessante, apesar de não ter sido observado diferença nos níveis de CML no DRG, observou-se aqui que a FBE modulou os receptores RAGE no gânglio da raiz dorsal (DRG) no grupo diabético tratado (STZ+FBE).

Já em relação ao fator de transcrição nuclear NF $\kappa$ B, responsável pela geração do processo inflamatório juntamente com envolvimento da carboximetil lisina (CML) e de seu receptor RAGE, foi apresentado aqui que a FBE modulou de forma significativa as referidas proteínas. No que se refere as citocinas pró-inflamatórias, o modelo de neuropatia diabética periférica em estudo mostrou elevado aumento do fator de necrose tumoral alfa (TNF- $\alpha$ ), assim como expressivo aumento dos níveis da citocina pró-inflamatória IL-6 no nervo isquiático dos animais do grupo diabético. Em contrapartida, a FBE não revelou efeito modulatório sobre as citocinas citadas. Por outro lado, a FBE modulou de forma expressiva os níveis da citocina anti-inflamatória IL-10 no nervo isquiático e no GRD dos animais do grupo diabético submetidos ao tratamento (STZ+FEB).

Em paralelo a toda essa cascata de dano acometida ao sistema nervoso em situação de hiperglicemia, outro fator tem ganhado destaque no que se refere ao diabetes e suas complicações crônicas. As mitocôndrias estão no centro do metabolismo energético celular e são as organelas celulares que regulam a vida e a morte das células que as acolhem [61]. O aspecto morfológico celular das mitocôndrias, especialmente a dinâmica mitocondrial, desperta a atenção através de implicações em diversas doenças humana, incluindo distúrbios neurológicos e doenças metabólicas [61].

Ainda, foi demonstrado que a fotobioestimulação também foi capaz de atuar no processo de dinâmica mitocondrial através da modulação de proteínas chaves para o processo de fissão e fusão mitocondrial. Os resultados aqui apresentados indicaram que o tratamento proposto reverteu de modo expressivo a fissão mitocondrial no nervo periférico dos ratos diabéticos submetidos a fotobioestimulação observado pela diminuição dos níveis proteicos da DRP-1. Por outro lado, a fotobioestimulação elevou significativamente os níveis de MFN-2 no sistema nervoso periférico dos ratos submetidos ao tratamento.

Atualmente, estudos tem demonstrado efeito “remoto” da FBE, ou seja, alguns grupos de pesquisa demonstram um possível efeito dessa terapia em locais longe de sua aplicação de origem [102]. Com esse intuito, tanto a porção lombar da medula espinal e o córtex cingulado anterior foi coletado. No presente trabalho demonstramos o envolvimento da FBE na modulação do receptor endocanabinóide CB<sub>1</sub> na medula espinal dos ratos diabéticos. É sabido que os receptores endocanabinóide são componentes essenciais para a regulação da dor em todas as suas etapas de processamento, incluído o processamento da dor por neuropatia diabética [103]. Aqui corroboramos a literatura

apresentando os efeitos da FBE sobre o receptor endocanabinóide CB<sub>1</sub> [104]. Mostramos que a FBE reverte o quadro de dor dos ratos diabéticos assim como diminui sua intensidade. Tais efeitos podem estar relacionados com o aumento da densidade do receptor CB<sub>1</sub> na medula espinal destes ratos.

Ainda em relação aos efeitos remotos da FBE, mostramos que houve significativo envolvimento da FBE na modulação de proteínas presentes em neurônios e/ou células gliais (não especificado no presente estudo) no córtex anterior cingulado dos ratos diabéticos. O córtex anterior cingulado tem participação ativa no processamento e modulação de dor crônica, inclusive na dor de origem diabética [105]. A FBE aumentou no ACC de ratos diabéticos hiperalgésicos, o receptor opioide do tipo  $\mu$  (MOR), assim como, reduziu a hiper-reatividade de astrócitos neste mesmo tecido.

Uma vez exposto uma sucessão de fatores que cooperam mutuamente para a geração dos danos que acometem o sistema nervoso no diabetes mellitus, deve-se ressaltar a inexistência de uma forma terapêutica que impossibilite o surgimento das complicações crônicas que afetam a vida cotidiana dos indivíduos portadores do diabetes. Salvo o uso da insulina que apenas retarda a aparecimento de tais complicações, não há descrito na literatura nenhuma forma de terapia que seja eficaz para impedir ou reverter os danos decorrentes do metabolismo totalmente desregulado em meio hiperglicêmico.

A presente proposta de estudo mostrou resultados similares aos encontrados na literatura, reforçando a ideia de que a FBE pode ser sem dúvida uma nova forma terapêutica a ser utilizada de maneira favorável no que se refere ao tratamento da NDP. Diante do que foi exposto podemos nos referir a FBE como uma ferramenta coadjuvante eficaz para o tratamento da NDP. A fotobioestimulação pode oferecer aqueles que sofrem com o diabetes uma melhor qualidade de vida.

## **7. Conclusão**

Foi apresentado ao longo do desenvolvimento do presente projeto de pesquisa, os efeitos promissores da FBE sobre o sistema nervoso periférico e central em modelo animal de NDP induzida por estreptozotocina. A FBE foi capaz de atuar de maneira eficaz na reversão de dor neuropática crônica apresentado pelos animais diabéticos e atuou de maneira expressiva na modulação de proteínas envolvidas nos processos pró e anti-inflamatórios. Apresentamos ainda, sua participação na melhora da respiração mitocondrial em cultura celular de células de Schwann. Para além dos seus efeitos benéficos no local de aplicação, observamos também que a FBE foi capaz de atingir por meios não elucidados, áreas distantes do seu local de aplicação.

Baseado no trabalho apresentado, podemos sugerir e afirmar, que a fotobioestimulação pode ser, seguramente, uma ferramenta promissora e indispensável para o tratamento da neuropatia diabética periférica.

## 8. Referências bibliográficas

1. Zhou, B., *Worldwide trends in diabetes since 1980: a pooled analysis of 751 population-based studies with 4.4 million participants*. Lancet, 2016. **387**(10027): p. 1513-30.
2. Federation, I.D. *Diabetes Atlas*. 2015.
3. Katsarou, A., et al., *Type 1 diabetes mellitus*. Nat Rev Dis Primers, 2017. **3**: p. 17016.
4. Judyta Juranek, R.R., Marta Banach, Vivek Rai., *Receptor for advanced glycation end products in neurodegenerative diseases*. Rev. Neurosci., 2015.
5. Varun Parkash Singh, A.B., Nirmal Singh, Amteshwar Singh Jaggi., *Advanced glycation end products and diabetic complications*. Korean J Physiol Pharmacol, 2014. **Vol. 18: 1-14**.
6. Jennifer Zenker, D.Z., Roman Chrast. *Novel pathogenic pathways in diabetic neuropathy., Novel pathogenic pathways in diabetic neuropathy*. Trends in Neuroscience., 2013. **Vol. 36, Nº 8**.
7. Brownlee, M., *Biochemistry and molecular cell biology of diabetic complications*. Nature, 2001. **414**(6865): p. 813-20.
8. Lin, Q., et al., *Oxidative Stress in Diabetic Peripheral Neuropathy: Pathway and Mechanism-Based Treatment*. Molecular Neurobiology, 2023.
9. Braswell, K., C.A. Dickey, and U.K. Jinwal, *A commentary on: Modulating molecular chaperones improves sensory fiber recovery and mitochondrial function in diabetic peripheral neuropathy*. Exp Neurol, 2013. **241**: p. 122-4.
10. Román-Pintos, L.M., et al., *Diabetic Polyneuropathy in Type 2 Diabetes Mellitus: Inflammation, Oxidative Stress, and Mitochondrial Function*. J Diabetes Res, 2016. **2016**: p. 3425617.
11. Farias, V.X., et al., *Chronic treatment with D-chiro-inositol prevents autonomic and somatic neuropathy in STZ-induced diabetic mice*. Diabetes Obes Metab, 2011. **13**(3): p. 243-50.
12. Gerald, P. and G.L. King, *Activation of protein kinase C isoforms and its impact on diabetic complications*. Circ Res, 2010. **106**(8): p. 1319-31.
13. Newton, A.C., *Regulation of the ABC kinases by phosphorylation: protein kinase C as a paradigm*. Biochem J, 2003. **370**(Pt 2): p. 361-71.
14. Cameron, N.E., et al., *Protein kinase C effects on nerve function, perfusion, Na(+), K(+)-ATPase activity and glutathione content in diabetic rats*. Diabetologia, 1999. **42**(9): p. 1120-30.
15. Lehning, E.J., et al., *Changes in Na-K ATPase and protein kinase C activities in peripheral nerve of acrylamide-treated rats*. J Toxicol Environ Health, 1994. **42**(3): p. 331-42.
16. Pang, L., et al., *Understanding Diabetic Neuropathy: Focus on Oxidative Stress*. Oxidative Medicine and Cellular Longevity, 2020. **2020**: p. 9524635.
17. Marshall, S., V. Bacote, and R.R. Traxinger, *Discovery of a metabolic pathway mediating glucose-induced desensitization of the glucose transport system. Role of hexosamine biosynthesis in the induction of insulin resistance*. J Biol Chem, 1991. **266**(8): p. 4706-12.
18. Sugimoto, K., M. Yasujima, and S. Yagihashi, *Role of advanced glycation end products in diabetic neuropathy*. Curr Pharm Des, 2008. **14**(10): p. 953-61.
19. Kumari, S., et al., *Hyperglycemia alters mitochondrial fission and fusion proteins in mice subjected to cerebral ischemia and reperfusion*. Transl Stroke Res, 2012. **3**(2): p. 296-304.
20. Yagihashi, S., Mizukami, H. and Sugimoto, K., *Mechanism of diabetic neuropathy: Where are we now and where to go?* Journal of Diabetes Investigation., 2011.
21. Roy Chowdhury, S.K., et al., *Impaired adenosine monophosphate-activated protein kinase signalling in dorsal root ganglia neurons is linked to mitochondrial dysfunction and peripheral neuropathy in diabetes*. Brain, 2012. **135**(Pt 6): p. 1751-66.

22. Furlan, A. and I. Adameyko, *Schwann cell precursor: a neural crest cell in disguise?* Dev Biol, 2018. **444 Suppl 1**: p. S25-s35.
23. Adameyko, I., et al., *Schwann cell precursors from nerve innervation are a cellular origin of melanocytes in skin.* Cell, 2009. **139**(2): p. 366-79.
24. Bremer, M., et al., *Sox10 is required for Schwann-cell homeostasis and myelin maintenance in the adult peripheral nerve.* Glia, 2011. **59**(7): p. 1022-32.
25. Monk, K.R., M.L. Feltri, and C. Taveggia, *New insights on Schwann cell development.* Glia, 2015. **63**(8): p. 1376-93.
26. Feng, S., M. Zhuang, and R. Wu, *Secretion of nerve growth factor, brain-derived neurotrophic factor, and glial cell-line derived neurotrophic factor in co-culture of four cell types in cerebrospinal fluid-containing medium.* Neural Regen Res, 2012. **7**(36): p. 2907-14.
27. Jessen, K.R. and R. Mirsky, *Control of Schwann cell myelination.* F1000 Biol Rep, 2010. **2**.
28. Garratt, A.N., et al., *A dual role of erbB2 in myelination and in expansion of the schwann cell precursor pool.* J Cell Biol, 2000. **148**(5): p. 1035-46.
29. Michailov, G.V., et al., *Axonal neuregulin-1 regulates myelin sheath thickness.* Science, 2004. **304**(5671): p. 700-3.
30. Taveggia, C., et al., *Neuregulin-1 type III determines the ensheathment fate of axons.* Neuron, 2005. **47**(5): p. 681-94.
31. Chen, S., et al., *Neuregulin 1-erbB signaling is necessary for normal myelination and sensory function.* J Neurosci, 2006. **26**(12): p. 3079-86.
32. Lyons, D.A., et al., *erbB3 and erbB2 are essential for schwann cell migration and myelination in zebrafish.* Curr Biol, 2005. **15**(6): p. 513-24.
33. Behse, F., F. Buchthal, and F. Carlsen, *Nerve biopsy and conduction studies in diabetic neuropathy.* J Neurol Neurosurg Psychiatry, 1977. **40**(11): p. 1072-82.
34. Malik, R.A., et al., *Sural nerve pathology in diabetic patients with minimal but progressive neuropathy.* Diabetologia, 2005. **48**(3): p. 578-85.
35. Chowdhury, S.K., D.R. Smith, and P. Fernyhough, *The role of aberrant mitochondrial bioenergetics in diabetic neuropathy.* Neurobiol Dis, 2013. **51**: p. 56-65.
36. Vincent, A.M., et al., *Oxidative stress in the pathogenesis of diabetic neuropathy.* Endocr Rev, 2004. **25**(4): p. 612-28.
37. Babizhayev, M.A., et al., *The Role of Oxidative Stress in Diabetic Neuropathy: Generation of Free Radical Species in the Glycation Reaction and Gene Polymorphisms Encoding Antioxidant Enzymes to Genetic Susceptibility to Diabetic Neuropathy in Population of Type I Diabetic Patients.* Cell Biochem Biophys, 2015. **71**(3): p. 1425-43.
38. Uttara, B., et al., *Oxidative stress and neurodegenerative diseases: a review of upstream and downstream antioxidant therapeutic options.* Curr Neuropharmacol, 2009. **7**(1): p. 65-74.
39. Goncalves, N.P., et al., *Schwann cell interactions with axons and microvessels in diabetic neuropathy.* Nat Rev Neurol, 2017. **13**(3): p. 135-147.
40. Yagihashi, S., et al., *Effect of aminoguanidine on functional and structural abnormalities in peripheral nerve of STZ-induced diabetic rats.* Diabetes, 1992. **41**(1): p. 47-52.
41. Zhang, L., et al., *Hyperglycemia alters the schwann cell mitochondrial proteome and decreases coupled respiration in the absence of superoxide production.* J Proteome Res, 2010. **9**(1): p. 458-71.
42. Freeman, O.J., et al., *Metabolic Dysfunction Is Restricted to the Sciatic Nerve in Experimental Diabetic Neuropathy.* Diabetes, 2016. **65**(1): p. 228-38.
43. Leininger, G.M., et al., *Mechanisms of disease: mitochondria as new therapeutic targets in diabetic neuropathy.* Nat Clin Pract Neurol, 2006. **2**(11): p. 620-8.
44. Rovira-Llopis, S., et al., *Mitochondrial dynamics in type 2 diabetes: Pathophysiological implications.* Redox Biol, 2017. **11**: p. 637-645.

45. Herder, C., et al., *Subclinical inflammation and diabetic polyneuropathy: MONICA/KORA Survey F3 (Augsburg, Germany)*. Diabetes Care, 2009. **32**(4): p. 680-2.
46. Fernyhough, P. and N.A. Calcutt, *Abnormal calcium homeostasis in peripheral neuropathies*. Cell Calcium, 2010. **47**(2): p. 130-9.
47. Friedman, J.R. and J. Nunnari, *Mitochondrial form and function*. Nature, 2014. **505**(7483): p. 335-43.
48. Hroudova, J. and Z. Fisar, *Control mechanisms in mitochondrial oxidative phosphorylation*. Neural Regen Res, 2013. **8**(4): p. 363-75.
49. Cooper, *The Cell: A Molecular Approach*, in *Mitochondria*. 2000, Sinauer Associates.
50. Alberts, *Molecular Biology of the Cell*, G. Science, Editor. 2000: New York.
51. Guo, R., et al., *Structure and mechanism of mitochondrial electron transport chain*. Biomed J, 2018. **41**(1): p. 9-20.
52. Kamer, K.J. and V.K. Mootha, *The molecular era of the mitochondrial calcium uniporter*. Nat Rev Mol Cell Biol, 2015. **16**(9): p. 545-53.
53. Nikolettou, V., et al., *Crosstalk between apoptosis, necrosis and autophagy*. Biochim Biophys Acta, 2013. **1833**(12): p. 3448-3459.
54. Rambold, A.S. and E.L. Pearce, *Mitochondrial Dynamics at the Interface of Immune Cell Metabolism and Function*. Trends Immunol, 2018. **39**(1): p. 6-18.
55. Tilokani, L., et al., *Mitochondrial dynamics: overview of molecular mechanisms*. Essays Biochem, 2018. **62**(3): p. 341-360.
56. Zemirli, N., E. Morel, and D. Molino, *Mitochondrial Dynamics in Basal and Stressful Conditions*. Int J Mol Sci, 2018. **19**(2).
57. Nunnari, J. and A. Suomalainen, *Mitochondria: in sickness and in health*. Cell, 2012. **148**(6): p. 1145-59.
58. Ferguson, S.M. and P. De Camilli, *Dynamin, a membrane-remodelling GTPase*. Nature Reviews Molecular Cell Biology, 2012. **13**: p. 75.
59. Kraus, F. and M.T. Ryan, *The constriction and scission machineries involved in mitochondrial fission*. J Cell Sci, 2017. **130**(18): p. 2953-2960.
60. Pernas, L. and L. Scorrano, *Mito-Morphosis: Mitochondrial Fusion, Fission, and Cristae Remodeling as Key Mediators of Cellular Function*. Annu Rev Physiol, 2016. **78**: p. 505-31.
61. Yoon, Y., et al., *Mitochondrial dynamics in diabetes*. Antioxid Redox Signal, 2011. **14**(3): p. 439-57.
62. Leininger, G.M., et al., *Mitochondria in DRG neurons undergo hyperglycemic mediated injury through Bim, Bax and the fission protein Drp1*. Neurobiol Dis, 2006. **23**(1): p. 11-22.
63. Men, X., et al., *Dynamin-related protein 1 mediates high glucose induced pancreatic beta cell apoptosis*. Int J Biochem Cell Biol, 2009. **41**(4): p. 879-90.
64. Paltauf-Doburzynska, J., R. Malli, and W.F. Graier, *Hyperglycemic conditions affect shape and Ca<sup>2+</sup> homeostasis of mitochondria in endothelial cells*. J Cardiovasc Pharmacol, 2004. **44**(4): p. 423-36.
65. Yu, T., et al., *Mitochondrial fission mediates high glucose-induced cell death through elevated production of reactive oxygen species*. Cardiovasc Res, 2008. **79**(2): p. 341-51.
66. Hashmi, J.T., et al., *Role of low-level laser therapy in neurorehabilitation*. PM R, 2010. **2**(12 Suppl 2): p. S292-305.
67. Arsovski, A.A., et al., *Photomorphogenesis*. Arabidopsis Book, 2012. **10**: p. e0147.
68. GM, C., *The Cell: A Molecular Approach*, S. Associates, Editor. 2000: Sunderland (MA).
69. Osellame, L.D., T.S. Blacker, and M.R. Duchen, *Cellular and molecular mechanisms of mitochondrial function*. Best Pract Res Clin Endocrinol Metab, 2012. **26**(6): p. 711-23.
70. Greco, *Helium-neon laser irradiation of rat liver mitochondria gives rise to a new subpopulation of mitochondria: isolation and first biochemical characterization*



- . Journal of Photochemistry and Photobiology, 1991. **10**: p. 71-78
71. Karu, T., *Primary and secondary mechanisms of action of visible to near-IR radiation on cells*. J Photochem Photobiol B, 1999. **49**(1): p. 1-17.
  72. Passarella, S., et al., *Increase of proton electrochemical potential and ATP synthesis in rat liver mitochondria irradiated in vitro by helium-neon laser*. FEBS Lett, 1984. **175**(1): p. 95-9.
  73. Osipov, A.N., et al., *Effects of Laser Radiation on Mitochondria and Mitochondrial Proteins Subjected to Nitric Oxide*. Front Med (Lausanne), 2018. **5**: p. 112.
  74. Karu, T., *Photobiology of low-power laser effects*. Health Phys, 1989. **56**(5): p. 691-704.
  75. de Freitas, L.F. and M.R. Hamblin, *Proposed Mechanisms of Photobiomodulation or Low-Level Light Therapy*. IEEE J Sel Top Quantum Electron, 2016. **22**(3).
  76. Karu, T.J., et al., *Biostimulation of Hela cells by low-intensity visible light*. Il Nuovo Cimento D, 1984. **3**(2): p. 309-318.
  77. Rochkind, S., et al., *New methods of treatment of severely injured sciatic nerve and spinal cord. An experimental study*. Acta Neurochir Suppl (Wien), 1988. **43**: p. 91-3.
  78. Rochkind, S., et al., *Efficacy of 780-nm laser phototherapy on peripheral nerve regeneration after neurotube reconstruction procedure (double-blind randomized study)*. Photomed Laser Surg, 2007. **25**(3): p. 137-43.
  79. Rochkind, S., et al., *Laser phototherapy (780 nm), a new modality in treatment of long-term incomplete peripheral nerve injury: a randomized double-blind placebo-controlled study*. Photomed Laser Surg, 2007. **25**(5): p. 436-42.
  80. Lampl, Y., *Laser treatment for stroke*. Expert Rev Neurother, 2007. **7**(8): p. 961-5.
  81. Lapchak, P.A., et al., *Transcranial near-infrared light therapy improves motor function following embolic strokes in rabbits: an extended therapeutic window study using continuous and pulse frequency delivery modes*. Neuroscience, 2007. **148**(4): p. 907-14.
  82. Lampl, Y., et al., *Infrared laser therapy for ischemic stroke: a new treatment strategy: results of the NeuroThera Effectiveness and Safety Trial-1 (NEST-1)*. Stroke, 2007. **38**(6): p. 1843-9.
  83. Oron, A., et al., *low-level laser therapy applied transcranially to mice following traumatic brain injury significantly reduces long-term neurological deficits*. J Neurotrauma, 2007. **24**(4): p. 651-6.
  84. Shefer, G., et al., *Low-energy laser irradiation promotes the survival and cell cycle entry of skeletal muscle satellite cells*. J Cell Sci, 2002. **115**(Pt 7): p. 1461-9.
  85. Moreira, M.S., et al., *Effect of phototherapy with low intensity laser on local and systemic immunomodulation following focal brain damage in rat*. J Photochem Photobiol B, 2009. **97**(3): p. 145-51.
  86. Moges, H., et al., *Light therapy and supplementary Riboflavin in the SOD1 transgenic mouse model of familial amyotrophic lateral sclerosis (FALS)*. Lasers Surg Med, 2009. **41**(1): p. 52-9.
  87. Shamloo, S., et al., *The anti-inflammatory effects of photobiomodulation are mediated by cytokines: Evidence from a mouse model of inflammation*. Frontiers in Neuroscience, 2023. **17**.
  88. Rocha, I.R., et al., *Photobiostimulation reverses allodynia and peripheral nerve damage in streptozotocin-induced type 1 diabetes*. Lasers Med Sci, 2017. **32**(3): p. 495-501.
  89. Bradford, M.M., *A rapid and sensitive method for the quantitation of microgram quantities of protein utilizing the principle of protein-dye binding*. Anal Biochem, 1976. **72**: p. 248-54.
  90. Sokal, R.R. and F.J. Rohlf, *Biometry*, ed. W.H.F. Co. 1981, New York. 859.
  91. Alves, A.C., et al., *Effect of low-level laser therapy on the expression of inflammatory mediators and on neutrophils and macrophages in acute joint inflammation*. Arthritis Res Ther, 2013. **15**(5): p. R116.

92. Lee, J.H., et al., *Anti-inflammatory effects of low-level laser therapy on human periodontal ligament cells: in vitro study*. *Lasers Med Sci*, 2018. **33**(3): p. 469-477.
93. da Cunha Moraes, G., et al., *Low-Level Laser Therapy Reduces Lung Inflammation in an Experimental Model of Chronic Obstructive Pulmonary Disease Involving P2X7 Receptor*. *Oxid Med Cell Longev*, 2018. **2018**: p. 6798238.
94. Ferraresi, C., et al., *Low-level laser (light) therapy increases mitochondrial membrane potential and ATP synthesis in C2C12 myotubes with a peak response at 3-6 h*. *Photochem Photobiol*, 2015. **91**(2): p. 411-6.
95. Farivar, S., T. Malekshahi, and R. Shiari, *Biological effects of low level laser therapy*. *J Lasers Med Sci*, 2014. **5**(2): p. 58-62.
96. Yadav, A., et al., *Photobiomodulatory effects of superpulsed 904nm laser therapy on bioenergetics status in burn wound healing*. *J Photochem Photobiol B*, 2016. **162**: p. 77-85.
97. McEvoy, R.C., et al., *Multiple low-dose streptozotocin-induced diabetes in the mouse. Evidence for stimulation of a cytotoxic cellular immune response against an insulin-producing beta cell line*. *J Clin Invest*, 1984. **74**(3): p. 715-22.
98. Khurana, A., S. Tekula, and C. Godugu, *Nanoceria suppresses multiple low doses of streptozotocin-induced Type 1 diabetes by inhibition of Nrf2/NF-kappaB pathway and reduction of apoptosis*. *Nanomedicine (Lond)*, 2018. **13**(15): p. 1905-1922.
99. Correia Rocha, I.R., et al., *Photobiostimulation reverses allodynia and peripheral nerve damage in streptozotocin-induced type 1 diabetes*. *Lasers in Medical Science*, 2017. **32**(3): p. 495-501.
100. Ziegler, D., *Painful diabetic neuropathy: advantage of novel drugs over old drugs?* *Diabetes Care*, 2009. **32 Suppl 2**: p. S414-9.
101. Kaikini, A.A., et al., *Targeting Mitochondrial Dysfunction for the Treatment of Diabetic Complications: Pharmacological Interventions through Natural Products*. *Pharmacogn Rev*, 2017. **11**(22): p. 128-135.
102. Gordon, L.C., et al., *Remote photobiomodulation targeted at the abdomen or legs provides effective neuroprotection against parkinsonian MPTP insult*. *Eur J Neurosci*, 2023.
103. Gonçalves, M.R., et al., *Spinal cannabinoid CB1 or CB2 receptors activation attenuates mechanical allodynia in streptozotocin-induced diabetic rats*. *Behav Pharmacol*, 2022. **33**(2&3): p. 158-164.
104. Neves, L.M.S., et al., *Photobiomodulation Therapy Improves Acute Inflammatory Response in Mice: the Role of Cannabinoid Receptors/ATP-Sensitive K(+) Channel/p38-MAPK Signalling Pathway*. *Mol Neurobiol*, 2018. **55**(7): p. 5580-5593.
105. Song, Z.H., et al., *Up-regulation of microglial chemokine CXCL12 in anterior cingulate cortex mediates neuropathic pain in diabetic mice*. *Acta Pharmacol Sin*, 2023.

## **9. Trajetória no Departamento de Anatomia, Instituto de Ciências Biomédicas. Universidade de São Paulo.**

Eu apresento aqui, com imensurável felicidade, um breve resumo da minha história no Departamento de Anatomia num período de 10 anos!

Ingressei na graduação (Ciências Biológicas, bacharelado e licenciatura) na Universidade Paulista (UNIP) em fevereiro de 2012. No mesmo ano, mês de julho, ingressei no laboratório da Profa. Dra. Marucia Chacur (Departamento de Anatomia, do Instituto de Ciências Biomédicas da Universidade de São Paulo. ICB-USP) como aluno de Iniciação Científica (IC). Em 2013, fui contemplado com minha primeira bolsa FAPESP (nível IC), *e essa foi só o começo de muitas e muitas outras!* Desenvolvi por 5 felizes anos ao longo da minha graduação os estágios de IC sob a orientação da Profa. Marucia. Em 2014, fui contemplado com bolsa BEPE-FAPESP (categoria IC) para estágio no exterior durante a graduação. Este estágio foi desenvolvido na universidade de Oxford, Reino Unido sob a orientação da Profa Dra Annina Schmid. Em 2017 logo após concluir meus estudos de graduação, ingressei de imediato no Programa de Pós-graduação em Ciências Morfofuncionais (ICB-USP), hoje Biologia de Sistemas.

Do período de 2017 a 2018 contemplado com bolsa FAPESP, desenvolvi meus estudos de mestrado ainda sob a orientação da Profa. Marucia. Durante este período, participei ativamente das reuniões da pós-graduação e através de votação, fui selecionado por 2 anos, representante discente dos alunos do departamento de anatomia. Junto com a Profa. Dra. Maria Inês, participei dos programas de cultura e extensão (modalidade neurociências) com a produção de vídeos e textos sobre meu projeto de pesquisa.

Princípio de 2019, logo após conclusão do mestrado e contemplado com bolsa FAPESP, iniciei meus estudos de doutorado ainda sob a orientação da Profa. Marucia. Ao longo dos estudos de doutorado, tive a grande felicidade de ter mais duas experiências de estágio de pesquisa no exterior. A primeira, desenvolvida na Universidade de Virginia, esta com financiamento internacional. E a segunda, desenvolvida com o financiamento da FAPESP (BEPE, categoria doutorado), na Universidade do Colorado, ambas as experiências desenvolvidas nos Estados Unidos da América. Ao longo do desenvolvimento do meu projeto de pesquisa (doutorado) aqui no departamento, participei da organização e produção de algumas Jornadas de Anatomia (evento nacional, ofertado pelo departamento de anatomia). Fui vice coordenador geral, coordenador geral e ainda

coordenador pedagógico desse evento de extraordinária importância para os estudos de anatomia humana. Adicionalmente, participei como coordenador (organização) geral de alguns Simpósios ofertados pelo departamento de Anatomia. Ainda, fui avaliador de trabalhos científicos apresentados por alunos de IC e Mestrado dentro dos referidos simpósios. Além da organização dos simpósios, recebi menção honrosa nas categorias IC e Doutorado pelos posters que apresentei. Junto com a Profa. Marucia e equipe, participei da organização do SIBBAS (Semana de Inovações Biológicas e Biotecnológicas Aplicadas a Saúde).

Tive a grande honra de ter sido selecionado pela Profa. Dra. Patrícia Castelucci para compor o grupo daqueles seletos alunos do departamento de anatomia, na organização das aulas práticas de anatomia assim como auxiliar os professores nas aulas teóricas do curso de especialização em anatomia humana e comparada, curso este, ofertado pelo departamento de anatomia junto com a escola de veterinária e zootecnia da USP. Após a conclusão do curso de especialização, fui contemplado com o título de especialista em anatomia humana e comparada.

Com relação aos estudos teóricos e práticos de anatomia humana, participei de inúmeros PAE (Programa de Aperfeiçoamento de Ensino). Auxiliei com a organização das aulas práticas de anatomia humana os Professores (as) Marucia Chacur, Maria Luiza, Maria Inês, Júlio Ferreira, Katiucia Batista e Cecilia Gouveia. Adicionalmente, organizei e liderei plantões de dúvidas com as aulas teóricas de anatomia humana. E muito mais ...

**MUITO GRATO!**

## 10. Artigos publicados ao longo da pós-graduação

Relação por ordem crescente dos anos, dos artigos publicados (em anexo) ao longo de todo o período da pós-graduação.

- 2017 Photobiostimulation reverses allodynia and peripheral nerve damage in streptozotocin-induced type 1 diabetes. Rocha IRC, Ciena AP, Rosa AS, Martins DO, Chacur M. *Lasers Med Sci.* 2017 Apr;32(3):495-501. doi: 10.1007/s10103-016-2140-3. Epub 2017 Jan 30. PMID: 28138810
- 2018 Non-Pharmacological treatment affects neuropeptide expression in neuropathic pain model. Santos FM, Silva JT, **Rocha IRC**, Martins DO, Chacur M. *Brain Res.* 2018 May 15;1687:60-65. doi: 10.1016/j.brainres.2018.02.034. Epub 2018 Feb 26. PMID: 29496478
- 2021 Effect of photobiomodulation on mitochondrial dynamics in peripheral nervous system in streptozotocin-induced type 1 diabetes in rats. Rocha IRC, Perez-Reyes E, Chacur M. *Photochem Photobiol Sci.* 2021 Feb;20(2):293-301. doi: 10.1007/s43630-021-00018-w. Epub 2021 Feb 18. PMID: 33721255
- 2021 Modulatory effects of photobiomodulation in the anterior cingulate cortex of diabetic rats. Correia Rocha IR, Chacur M. *Photochem Photobiol Sci.* 2021 Jun;20(6):781-790. doi: 10.1007/s43630-021-00059-1. Epub 2021 May 30. PMID: 34053000



## Photobiostimulation reverses allodynia and peripheral nerve damage in streptozotocin-induced type 1 diabetes

Igor Rafael Correia Rocha<sup>1</sup> · Adriano Polican Ciena<sup>2</sup> · Alyne Santana Rosa<sup>1</sup> · Daniel Oliveira Martins<sup>1</sup> · Marucia Chacur<sup>1</sup>

Received: 1 November 2016 / Accepted: 26 December 2016 / Published online: 30 January 2017  
© Springer-Verlag London 2017

**Abstract** For better evaluation of the efficacy of low-level laser therapy in treating painful diabetic neuropathy and in protecting nerve fiber damage, we conducted a study with type 1 diabetic rats induced by streptozotocin. It is well known that diabetic peripheral neuropathy is the leading cause of pain in those individuals who suffer from diabetes. Despite the efficacy of insulin in controlling glucose level in blood, there is no effective treatment to prevent or reverse neuropathic damage for total pain relief. Male Wistar rats were divided into saline, vehicle, and treatment groups. A single intraperitoneal (i.p.) injection of streptozotocin (STZ) (85 mg/kg) was administered for the induction of diabetes. The von Frey filaments were used to assess nociceptive thresholds (allodynia). Behavioral measurements were accessed 14, 28, 48, and 56 days after STZ administration. Rats were irradiated with GaAs Laser (Gallium Arsenide, Laserpulse, Ibramed Brazil)

emitting a wavelength of 904 nm, an output power of 45 mWpk, beam spot size at target 0.13 cm<sup>2</sup>, a frequency of 9500 Hz, a pulse time 60 ns, and an energy density of 6,23 J/cm<sup>2</sup>. The application of four sessions of low-level laser therapy was sufficient to reverse allodynia and protect peripheral nerve damage in diabetic rats. The results of this study indicate that low-level laser therapy is feasible to treat painful diabetic condition in rats using this protocol. Although its efficacy in reversing painful stimuli and protecting nerve fibers from damage was demonstrated, this treatment protocol must be further evaluated in biochemical levels to confirm its biological effects.

**Keywords** Diabetes mellitus · Sciatic nerve · Nociception · Myelin sheath · Rat · Streptozotocin

### Abbreviations

i.p. Intraperitoneal  
STZ Streptozotocin

### Introduction

Diabetes is a chronic condition that occurs when the body cannot produce or use enough insulin, and it is diagnosed by increased levels of glucose in the blood. Insulin is a hormone produced by  $\beta$  cells in the pancreas; it is required to transport glucose from the bloodstream into the cells where it is used as energy. The lack or ineffectiveness of insulin in a person with diabetes results in high glucose concentration in the blood. Over time, the resulting high levels of glucose in the blood (hyperglycemia) cause damage to several tissues in the body, especially in the nervous system, leading to the development of disabilities and life-threatening health complications [1].

✉ Marucia Chacur  
chacurm@icb.usp.br

Igor Rafael Correia Rocha  
irrocha@usp.br

Adriano Polican Ciena  
apciena@rc.unesp.br

Alyne Santana Rosa  
alynesrosa@usp.br

Daniel Oliveira Martins  
martinsd@usp.br

<sup>1</sup> Department of Anatomy, Biomedical Sciences Institute, University of São Paulo, Av. Prof. Lineu Prestes, 2415, 05508-900 São Paulo, Brazil

<sup>2</sup> Institute of Biosciences, University Estadual Paulista Júlio de Mesquita Filho, Rio Claro, 13506900 São Paulo, Brazil

Diabetic peripheral neuropathy (DPN) is a group of heterogeneous disorders caused by neuronal dysfunction, and it affects approximately 50% of patients with diabetes *mellitus*. These disorders show different clinical courses, distributions, fiber involvement (large and small), and pathophysiological [2]. DPN is thought to occur as a result of two situations: (1) Hyperglycemia-induced damage to nerve cells; (2) Neuronal ischemia caused by the decrease in neurovascular flow due to hyperglycemia [3]. Both axonal loss and sensory nerve fiber dysfunction [4] occur in diabetes mellitus but the exact pathomechanism underlying nerve damage in diabetes remains unknown.

Diabetic peripheral neuropathy is a complication of diabetes that comprises functional and structural changes in peripheral nerves, such as a reduction of velocity in nerve conduction, axonal degeneration, paranodal demyelination, and loss of myelinated and unmyelinated fibers. Some of the morphological alterations in peripheral nerve fibers associated with hyperglycemia are also seen in rat models of STZ-induced diabetic neuropathy [5].

Alterations in myelin damage include invaginations in the axoplasm (infoldings) and myelin evaginations in the Schwann cell cytoplasm (outfoldings). These changes also include myelin compaction such as abnormal wide incisures and aberrant separation of myelin lamellae, similar to those seen in aged rodents [6]. The predominant myelin abnormalities found in STZ-treated rats are myelin infoldings [7].

The myelin sheath is a multilayered membrane produced in the peripheral nervous system by differentiation of the plasma membrane of Schwann cells. The main role of this membrane is to allow efficient transmission of nerve impulses along the axons that it surrounds [5].

Over time, people with diabetes mellitus may or may not develop symptoms such as severe pain, tingling, numbness, and loss of sensation in the hands and feet [8]. Painful diabetic neuropathy is the most common manifestation of diabetes [9], and it appears as a burning, excruciating, and stabbing intractable type of pain [10].

Treatment for painful diabetic neuropathy is based on intensive glycemic control and symptomatic pain management [2]. This includes antidepressants like tricyclic antidepressants (TCAs), selective norepinephrine reuptake inhibitors (SNRIs), anticonvulsants including pregabalin, gabapentin and lamotrigine, and also topical agents such as capsaicin [10].

Despite all these pharmacological agents available for pain relief, their efficacy is limited due to several side effects. There are no therapeutic approaches available for preventing peripheral nerve damage that reverse degeneration or that prevent peripheral unmyelinated nerve fibers loss in patients with diabetes mellitus. The use of alternative approaches for improving pain, preventing peripheral nerve fibers loss, and restoring

the quality of life for those suffering from DPN is strongly recommended in all fields of diabetic research.

One of these alternatives is the use of low-level laser therapy, first described in Europe and Russia in the 1960s [11]. Low-level laser therapy is well known for treating chronic pain by increasing nociceptive threshold after its application [12] although its mechanisms of action are not well understood.

The mechanisms by which low-level laser therapy improve neuropathic pain are possibly related to the increase in mitochondrial ATP production [13] and in the release of endorphins [14] as well as a higher release in local anti-inflammatory cytokines, such as interleukin-10 [15].

In the present study, we observed myelin sheath structural alterations in a rat model of streptozotocin-induced type 1 diabetes and also a possible correlation between these morphological alterations and behavioral changes.

## Methods and materials

### Animals

Male Wistar rats, weighing between 200 and 220 g (2 months old), were used in all experiments. They were housed in cages (five per cage) and maintained on a 12:12-h light/dark cycle. The rats were adapted to the experimental environment 15 min prior to the experiments. All animals were tested during the light cycle at the same time of the day (9:00 am–14:00 pm). Due to polyuria, animal bedding was changed twice a day, early in the morning at 8 am and in the night at 8 pm. All procedures were approved by the Institutional Animal Care Committee of the University of São Paulo (protocol number 123/2015) and performed in accordance with the guidelines for the ethical use of conscious animals in pain study published by the international association for the study of pain (IASP). Efforts were made to minimize the number of animals used and their suffering [16].

### Methods

#### *Induction of diabetes mellitus*

Diabetes was induced by a single dose (85 mg/kg) of streptozotocin (STZ, Sigma-Aldrich, St. Louis, MO, USA) diluted in saline 0, 9% and administered via intraperitoneal. Blood glucose levels (glycemic control) were assessed from the second day until the end of the experiment using an ULTRAMINI® | ONETOUCH® blood glucose monitoring system (Table 2). A single administration of streptozotocin induced insulin-dependent diabetes mellitus within 24–48 h by destruction of pancreatic islet cells [17]. Plasma glucose levels higher than 300 mg/dl were considered indicative of

diabetes [18]. Normal control rats received the same volume of saline 0, 9% (streptozotocin vehicle).

#### Transmission electron microscopy

The animals were intraperitoneally anesthetized with urethane (3 g/kg) and perfused with a modified Karnovsky fixative solution (containing 2.5% glutaraldehyde and 2% paraformaldehyde in 0.1 M sodium phosphate buffer, pH 7.4) [19]. After dissecting the affected sciatic nerve, samples (3 mm) were post fixed in a 1% osmium tetroxide solution at 4 °C and subsequently immersed in a 5% uranyl acetate aqueous solution at room temperature. Next, the samples were dehydrated in an increasing alcohol series, immersed in propylene oxide, and embedded in Spur resin. Semi-thin sections were cut with a Reichert Ultra Cut ultra-microtome and stained with a 1% toluidine blue solution to test the region to be analyzed. Ultrathin 60-nm sections were then cut, collected on 200 “mesh” copper grids (Sigma), and contrasted with a 4% uranyl acetate solution and 0.4% lead citrate solution [20]. The grids were observed with a Jeol 1010 transmission electron microscope (Peabody, MA, USA) [21].

#### Assessment of tactile allodynia

Rats were transferred to a testing cage with a wire mesh bottom that allowed full access to the paws. Behavioral adaptation was allowed for approximately 15 min, until the cage exploration and major grooming activities had ceased. The area tested was the plantar surface of the animal's hind paw. The von Frey test was used to assess nociceptive thresholds. Briefly, a logarithmic series of 7 calibrated Semmes-Weinstein monofilaments (Von Frey hair test, Stoelting, USA) were applied to the middle of the plantar surface of the right hindpaw, for a maximum of 10 s to determine the threshold intensity of the stiffness stimulus required to elicit a paw withdrawal response. Log stiffness of the hairs is determined by ranges starting at 4.56 N (3.630 g); 3.61 (0.407 g.); 3.84 (0.692 g.); 4.17 (1.479 g.); 4.93 (8.511 g.); 5.18 (15.136 g.); and 5.46 (28.840 g). During each testing trial, the series of filaments were presented following an up-down procedure as described and previously validated by Chaplan [22] and the 50% response threshold was calculated for each rat. The allodynic measurements were accessed on days 14, 28, 48, and 56 after streptozotocin intraperitoneal administration.

#### Laser therapy

The laser treatment was performed every other day, totaling 4 sessions, starting on day 45 after the induction of diabetes mellitus type 1. After sterilization, the laser was placed on the skin surface on the right thigh directly above the course of the sciatic nerve. Animals were irradiated with laser GaAs

(Gallium Arsenide, Laserpulse-Laser, Ibramed Brazil) emitting a wavelength of 904 nm, an output power of 45 mWpk, a spot area of 0.13 cm<sup>2</sup>, a frequency of 9500 Hz, a pulse time of 60 ns, and an energy density of 6.23 J/cm<sup>2</sup> (Table 1). Each session included the stimulation of nine points along the sciatic nerve, lasting 18 s on each point, and 7.29 J of energy per session [23].

#### Statistical analysis

Results are presented as the mean ± SEM. Statistical analyses of data were generated using GraphPAD Prism, version 5 (Graph-Pad Software Inc., San Diego, CA). Statistical comparison of the groups was performed using one-way analysis of variance; differences between means were tested by Bonferroni's multiple comparison test. In all cases,  $p < 0.05$  was considered statistically significant [24].

#### Results

We performed allodynia tests during the time course of 56 days of the development of streptozotocin-induced type 1 diabetes mellitus as described in materials and methods. We also assessed the blood glucose levels during the first 30 days after intraperitoneal administration of streptozotocin to confirm the hyperglycemic state. In addition, we also observed that diabetic rats showed significant loss of body weight and increase

**Table 1** Specifications for laser parameters

Device information	
Manufacturer	IBRAMED
Model identifier	LASERPULSE Diamond
Emitter type	GaAs
Irradiation parameters	
Wavelength (nm)	904 nm
Operating mode	Pulsed
Frequency (Hz)	9500
Pulse on duration (sec)	60 ns
Beam shape	Circular
Treatment parameters	
Beam spot size at target (cm <sup>2</sup> )	0.13 cm <sup>2</sup>
Exposure duration (sec)	18 s per point, 162 s per session
Radiant exposure (J/cm <sup>2</sup> )	6.23 J/cm <sup>2</sup>
Radiant energy (J)	0.81 J
Number of points irradiated	9 points
Area irradiated (cm <sup>2</sup> )	1.17 cm <sup>2</sup>
Application technique	Skin contact
Number and frequency of treatment sessions	5 sessions, performed every other day
Total radiant energy (J)	7,291 J per session; 29,16 J over all sessions



in food and water intake (polyphagia and polydipsia) and also increase in urination (polyuria) (data not shown).

#### Effect of streptozotocin on blood glucose

From 24 h until 30 day after streptozotocin administration, diabetic rats ( $n = 5$ ) exhibited significantly increase in blood glucose levels as compared to the levels of the control group (saline) (Fig. 1). In Table 2, we can observe the effect of streptozotocin administration from each animal compared with control animals.

#### Effect of streptozotocin-induced diabetes mellitus on nociceptive threshold

When analyzing the allodynic response of the animals with diabetes mellitus, it was possible to observe a significant decrease in nociceptive threshold starting at day 14 after streptozotocin administration and maintained until the end of 56 days when compared with saline animals, used as control (Fig. 2).

#### Effect of photobiostimulation on nociceptive threshold

Low-level laser therapy started 45 days after STZ injection. Figure 3 shows a decrease in pain sensitivity initiating after the first session of laser treatment. After four sessions of low level laser therapy on diabetic rats, our data showed significant statistical difference ( $p < 0.05$ ) between diabetic rats before and after the laser application. Furthermore, there were no statistical differences between rats treated with laser and baseline (Fig. 3).

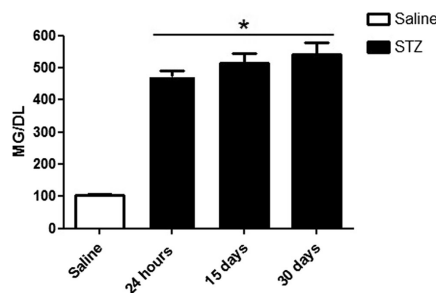


**Fig. 1** Blood glucose measurement in saline (control group) and in diabetic rats. Animals were measured with 24 h, 15 days, and 30 days after streptozotocin injection. Results represent the mean  $\text{SEM} \pm 5$  animals per group  $*P < 0.05$  compared with saline

**Table 2** Glycemic control were assessed using an ULTRAMINI® | ONETOUCH® blood glucose monitoring system

Basal blood glucose levels (mg/dl)	24 h after STZ injection (mg/dl)	14 days after STZ injection (mg/dl)	1 month after STZ injection (mg/dl)
106	494	509	543
115	511	425	400
99	453	600	591
100	440	515	600
95	485	533	573

STZ streptozotocin

#### Effect of streptozotocin-induced type 1 diabetes mellitus on myelin sheath abnormalities in the sciatic nerve

Electron microscopy analysis showed that sciatic nerve fibers from the control group (saline) exhibited a normal morphology of axons and Schwann cells (Fig. 4). No difference was observed within saline group before and 30 days after the injections (data not shown).

During a time course of 53 days in a model of streptozotocin-induced type 1 diabetes mellitus, morphological changes appear in the rat sciatic nerve. Some abnormalities include myelin infoldings, derangement in myelin compaction, and also a reduction in unmyelinated fibers starting 30 days after diabetes induction. These alterations worsen within 60 days after STZ injection (Fig. 4). Regarding the myelin organization, after laser treatment, we observed an improvement in STZ animals after four sessions of treatment (in Fig. 4d).

In Fig. 5, we can observe the quantification of myelin sheath obtained from transmission electron microscopy (8 animals per group). Note that the group of diabetic rats after laser

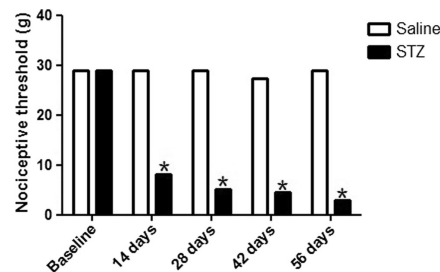


**Fig. 2** Allodynia response in rats with streptozotocin. Nociceptive threshold measured by Von Frey hair (expressed in grams) was determined in saline (used as control group) and streptozotocin (STZ) groups, before (baseline) and on days 14, 28, 42, and on 56 days after both injections (saline and STZ). Results represent the mean  $\text{SEM} \pm 8$ –10 animals per group.  $*P < 0.0001$  compared with saline

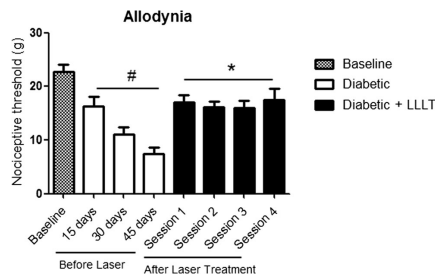


**Fig. 3** Effect of laser therapy on nociceptive threshold measured by Von Frey hair (expressed in grams). Allodynic test was measured before (baseline) and after 15, 30, and 45 days after STZ injections. First session of laser therapy was applied after 45 days from STZ and measured every 2 days (STZ + LLLT). Results represent the mean SEM  $\pm$  8 animals per group \* $P$  < 0.05 compared with STZ animals; # $P$  < 0.05 compared with baseline

treatment does not show statistical differences in the thickness of myelinated nerve fibers when compared with saline group, used as control. Still, there were no statistical differences between naive and saline group (data not shown).

## Discussion

High levels of glucose in the blood (hyperglycemia) induce abnormal structural changes in peripheral nerve fibers both myelinated and unmyelinated, which is a common characteristic of diabetic peripheral neuropathy. In association with other symptoms, chronic pain is the most prevalent symptom of those who suffer from diabetes, leading to a disabling life and affecting every aspect of a patient's life.

Here, we demonstrated that diabetic animals induced by a single dose of streptozotocin showed a decrease in their nociceptive thresholds. According to the results obtained in the present study, type 1 diabetes mellitus induced by streptozotocin has significantly effects on developing allodynia.

It was demonstrated that after four sessions of low level laser therapy, there is an increase in pain sensitivity. This effect was shown from the first session onwards, suggesting that low-level laser therapy could be a useful tool for patients with severe pain.

As mentioned in the "Introduction," the use of low-level laser therapy was first described in Europe and Russia in the 1960s [11], but its analgesic mechanisms are not yet well understood. In addition, previous studies have shown relevant data involving laser therapy and pain. Bingol et al. showed the effectiveness of low-level laser in patients with shoulder pain [25]. In a double blind study, Venancio et al. were able to show an improvement in patients with temporomandibular joint pain and also in mandibular dysfunction [26]. Previous studies from our group have also demonstrated the beneficial effects of laser therapy in animals with trigeminal nerve injury [23].

Moreover, the streptozotocin-induced type 1 diabetes mellitus model is able to cause significant nerve damage in myelinated as well as unmyelinated fibers. These findings are in accordance with previous data published about streptozotocin-induced diabetes mellitus and its chronic complications [27, 28].

In order to further evaluate the progression of demyelination and other possible alterations after streptozotocin-induced type 1 diabetes mellitus, we designed a temporal analysis of sciatic nerve by electron transmission microscopy. The sciatic nerve of diabetic rats was collected after 30 and 60 days of the disease for morphometric analysis of myelin sheath. Morphological changes in myelin sheath and fiber loss were clearly observed from the thirtieth day that worsened in the sixtieth after streptozotocin administration.

So according to these results, we decided to add a group of animals treated with low-level laser beginning 45 days after streptozotocin intraperitoneal administration. The choice of this timepoint was based on the behavioral tests where we noted that 45 days after streptozotocin administration there was a great decrease in pain sensitivity. At the end of the treatment, an improvement in myelin sheath structural organization as well as the reduction of fiber loss was observed when compared with

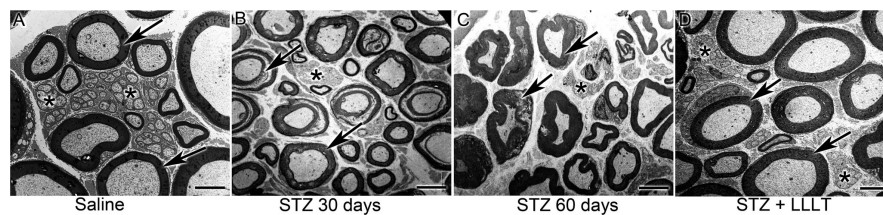


**Fig. 4** Electron microscopic transverse section of the sciatic nerve. Myelinated nerve fibers are in normal morphology and structure in saline a control group (30 days). The photographs showed structural abnormality in myelin sheath in streptozotocin diabetic groups (b STZ 30 days, c STZ 60 days), d fibers from sciatic nerve after the last session of laser treatment (STZ + LLLT). Myelin Sheath (arrow), Schwann cell nucleus (arrow head), unmyelinated fibers (asterisk). Scale Bar 10  $\mu$ m

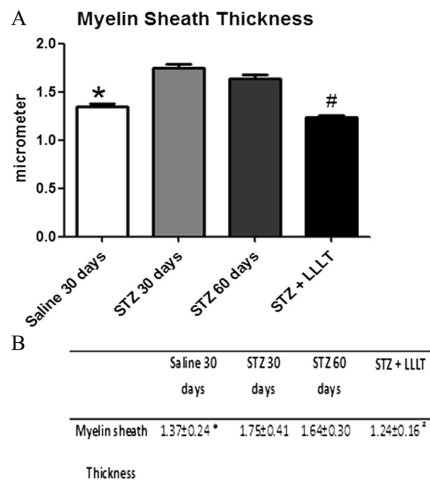


**Fig. 5** Morphometric analysis of myelin sheath thickness of sciatic nerve. **a** the quantification of the images from myelin sheath. **b** the mean of the same animals during the days. Results represent the mean SEM  $\pm$  8 animals per group. \* $p \leq 0.01$  indicates a significant difference between STZ 30 and STZ 60 days and saline; <sup>#</sup> $p \leq 0.05$  indicates a significant difference between the STZ + LLLT and diabetic animals (STZ 30 and STZ 60 days)

untreated groups. It is worth mentioning that despite the importance of the g-ratio for assessing axonal myelination, firstly described by Rushton [29], in this first approach, we intended to make some initial observations of low-level laser therapy in a 904-nm wavelength on nociceptive thresholds (allodynia) and if this treatment would probably have beneficial effects on sciatic nerve fibers in diabetic rats. In addition, this study is not intended to evaluate nerve conduction.

## Conclusion

These findings may contribute to previous studies that showed other event may be in relation with pain symptoms in diabetes mellitus not only the degeneration itself.

We can attribute methylglyoxal, an alpha-carbonyl, with a possible role in the activation of sodium channels in peripheral nerves, contributing to the pain sensitivity observed in diabetic rats [30]. It should be mentioned that more research needs to be done to improve our knowledge about how hyperglycemia induces peripheral nerve damage and chronic pain.

Despite the lack of biochemical and molecular studies to confirm our results, we can suggest and ensure that low-level laser therapy is a useful tool for treating pain in diabetic

animals. Moreover, this same therapy was able to prevent morphological changes and loss of peripheral unmyelinated and myelinated fibers.

**Acknowledgments** FAPESP 2014/24533-0.

**Authors' contributions** All authors made substantial contributions to the following tasks of research: initial conception (Rocha, I.R.C; Martins, D.O. Chacur, M.); design (Rocha, I.R.C; Martins D.O., Chacur M); provision of resources (Chacur M); collection of data (Rocha, I.R.C; Rosa, S. Ciena A.P); analysis and interpretation of data (Rocha, I.R.C; Chacur M.); writing the first draft of the paper or important intellectual content (Rocha, I.R.C; Martins D.O., Chacur M.); and revision of the paper (Rocha, I.R.C; Martins D.O., Chacur M).

**Compliance with ethical standards**

**Ethics approval and consent to participate** All procedures were approved by the Institutional Animal Care Committee of the University of São Paulo (protocol number 123/2015) and performed in accordance with the guidelines for the ethical use of conscious animals in pain study published by the International Association for the Study of Pain.

**Consent for publication** Not applicable.

**Availability of data and materials** Not applicable.

**Competing interests** The authors declare that they have no competing interests.

**Funding** FAPESP 2014/24533-0.

## References

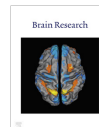
1. Federation ID (2013) Diabetes Atlas; Available from: <http://www.idf.org/diabetesatlas>
2. Javed S, Petropoulos IN, Alam U, Malik RA (2015) Treatment of painful diabetic neuropathy. *Ther Adv Chronic Dis* 6:15–28
3. Jin HY, Lee KA, Song SK, Liu WJ, Choi JH, Song CH, Baek HS, Park TS (2012) Sulodexide prevents peripheral nerve damage in streptozotocin induced diabetic rats. *Eur J Pharmacol* 674:217–26
4. Yagihashi S, Mizukami H, Sugimoto K (2011) Mechanism of diabetic neuropathy: where are we now and where to go? *J Diabetes Investig* 2:18–32
5. Cermenati G, Abbiati F, Cermenati S, Brioschi E, Volonterio A, Cavaletti G, Saez E, De Fabiani E, Crestani M, Garcia-Segura LM, Melcangi RC, Caruso D, Mitro N (2012) Diabetes-induced myelin abnormalities are associated with an altered lipid pattern: protective effects of LXR activation. *J Lipid Res* 53:300–10
6. Azcoitia I, Leonelli E, Magnaghi V, Veiga S, Garcia-Segura LM, Melcangi RC (2003) Progesterone and its derivatives dihydroprogesterone and tetrahydroprogesterone reduce myelin fiber morphological abnormalities and myelin fiber loss in the sciatic nerve of aged rats. *Neurobiol Aging* 24:853–60
7. Veiga S, Leonelli E, Beelke M, Garcia-Segura LM, Melcangi RC (2006) Neuroactive steroids prevent peripheral myelin alterations induced by diabetes. *Neurosci Lett* 402:150–3
8. Services USDoHaH (2009) Diabetic neuropathies: the nerve damage of diabetes
9. Javed S, Alam U, Malik RA (2015) Treating diabetic neuropathy: present strategies and emerging solutions. *Rev Diabet Stud* 12:63–83

10. Kaur S, Pandhi P, Dutta P (2011) Painful diabetic neuropathy: an update. *Ann Neurosci* 18:168–75
11. Ribas ES, Paiva WS, Pinto NC, Yeng LT, Okada M, Fonoff ET, Chavantes MC, Teixeira MJ (2012) Use of low intensity laser treatment in neuropathic pain refractory to clinical treatment in amputation stumps. *Int J Gen Med* 5:739–42
12. Kingsley JD, Demchak T, Mathis R (2014) Low-level laser therapy as a treatment for chronic pain. *Front Physiol* 5:306
13. Passarella S (1989) He-Ne laser irradiation of isolated mitochondria. *J Photochem Photobiol B* 3:642–3
14. Yamamoto H, Oka H, Kinoshita S (1988) Antinociceptive effects of laser irradiation of Hoku point in rats. *Pain Clin*
15. L-AL AC (1999) Beneficial effects of laser therapy in the early stages of rheumatoid arthritis onset. *Laser Ther*
16. Zimmermann M (1983) Ethical guidelines for investigations of experimental pain in conscious animals. *Pain* 16:109–10
17. Cheng Y, Kang H, Shen J, Hao H, Liu J, Guo Y, Mu Y, Han W (2015) Beta-cell regeneration from vimentin+/MafB+ cells after STZ-induced extreme beta-cell ablation. *Sci Rep* 5:11703
18. Araiza-Saldana CI, Pedraza-Priego EF, Torres-Lopez JE, Rocha-Gonzalez HI, Castaneda-Corral G, Hong-Chong E, Granados-Soto V (2015) Fosinopril prevents the development of tactile allodynia in a streptozotocin-induced diabetic rat model. *Drug Dev Res* 76:442–9
19. Ciena AP, de Almeida SR, Dias FJ, Bolina Cde S, Issa JP, Iyomasa MM, Ogawa K, Watanabe IS (2012) Fine structure of myotendinous junction between the anterior belly of the digastric muscle and intermediate tendon in adults rats. *Micron* 43:258–62
20. Watanabe I, Yamada E (1983) The fine structure of lamellated nerve endings found in the rat gingiva. *Arch Histol Jpn* 46:173–82
21. da Silva JT, Santos FM, Giardini AC, Martins Dde O, de Oliveira ME, Ciena AP, Gutierrez VP, Watanabe IS, Britto LR, Chacur M (2015) Neural mobilization promotes nerve regeneration by nerve growth factor and myelin protein zero increased after sciatic nerve injury. *Growth Factors* 33:8–13
22. Chaplan SR, Bach FW, Pogrel JW, Chung JM, Yaksh TL (1994) Quantitative assessment of tactile allodynia in the rat paw. *J Neurosci Methods* 53:55–63
23. de Oliveira MD, Martinez dos Santos F, Evany de Oliveira M, de Britto LR, Benedito Dias Lemos J, Chacur M (2013) Laser therapy and pain-related behavior after injury of the inferior alveolar nerve: possible involvement of neurotrophins. *J Neurotrauma* 30:480–6
24. Snedecor GW, R.S. FJ Rohlf (1946) *Statistical methods biometry*. Freeman & Co
25. Bingol U, Altan L, Yurtkuran M (2005) Low-power laser treatment for shoulder pain. *Photomed Laser Surg* 23:459–64
26. Venancio Rde A, Camparis CM, Lizarelli Rde F (2005) Low intensity laser therapy in the treatment of temporomandibular disorders: a double-blind study. *J Oral Rehabil* 32:800–7
27. Hanani M, Blum E, Liu S, Peng L, Liang S (2014) Satellite glial cells in dorsal root ganglia are activated in streptozotocin-treated rodents. *J Cell Mol Med* 18:2367–71
28. Hoybergs YM, Meert TF (2007) The effect of low-dose insulin on mechanical sensitivity and allodynia in type I diabetes neuropathy. *Neurosci Lett* 417:149–54
29. Rushton WA (1951) A theory of the effects of fibre size in medullated nerve. *J Physiol* 115:101–22
30. Huang Q, Chen Y, Gong N, Wang YX (2016) Methylglyoxal mediates streptozotocin-induced diabetic neuropathic pain via activation of the peripheral TRPA1 and Nav1.8 channels. *Metabolism* 65:463–74



Contents lists available at ScienceDirect

Brain Research

journal homepage: [www.elsevier.com/locate/bres](http://www.elsevier.com/locate/bres)

Research report

## Non-pharmacological treatment affects neuropeptide expression in neuropathic pain model

Fabio Martinez Santos<sup>a,b,1</sup>, Joyce Teixeira Silva<sup>c,2</sup>, Igor Rafael Correia Rocha<sup>a,1</sup>, Daniel Oliveira Martins<sup>a,\*</sup>, Marucia Chacur<sup>a,3</sup>

<sup>a</sup> Department of Anatomy, Laboratory of Functional Neuroanatomy of Pain, Institute of Biomedical Sciences, University of São Paulo, SP, Brazil

<sup>b</sup> Department of Health Sciences, University Nove de Julho, SP, Brazil

<sup>c</sup> Department of Neural and Pain Sciences, University of Maryland, School of Dentistry, Baltimore, MD, USA



### ARTICLE INFO

#### Article history:

Received 17 October 2017  
Received in revised form 2 January 2018  
Accepted 21 February 2018  
Available online 26 February 2018

#### Keywords:

Sciatic nerve  
TRPV1  
Substance P  
Manual therapy, DRG  
Neuropathic pain

### ABSTRACT

Chronic constriction injury (CCI) of the sciatic nerve elicits changes in neuropeptide expression on the dorsal root ganglia (DRG). The neural mobilization (NM) technique is a noninvasive method that has been proven clinically effective in reducing pain. The aim of this study was to analyze the expression of substance P, transient receptor potential vanilloid 1 (TRPV1) and opioid receptors in the DRG of rats with chronic constriction injury and to compare it to animals that received NM treatment. CCI was performed on adult male rats. Each animal was submitted to 10 sessions of neural mobilization every other day, starting 14 days after the CCI injury. At the end of the sessions, the DRG (L4–L6) were analyzed using Western blot assays for substance P, TRPV1 and opioid receptors ( $\mu$ -opioid receptor,  $\delta$ -opioid receptor and  $\kappa$ -opioid receptor). We observed a decreased substance P and TRPV1 expression (48% and 35%, respectively) and an important increase of  $\mu$ -opioid receptor expression (200%) in the DRG after NM treatment compared to control animals. The data provide evidence that NM promotes substantial changes in neuropeptide expression in the DRG; these results may provide new options for treating neuropathic pain.

© 2018 Elsevier B.V. All rights reserved.

### 1. Introduction

Many studies have shown that changes in the molecules or receptors expressed in the DRG are responsible for pain-related behaviors, and that the DRG spinal neurons are responsible for transmission of nociceptive information (Kuo et al., 2011;

LaCroix-Fralish et al., 2011; Sapunar et al., 2012). Nerve injury results in molecular changes, which are involved in the mechanism of neuropathic pain, and DRG neurons may become an important source of increased nociceptive signaling through increased neuronal excitability and generation of ectopic discharges (Sapunar et al., 2005; Xie et al., 2006). Many investigations have focused on the functional changes of receptors, proteins, peptides in both the spinal cord and DRG neurons following nerve injury (Narita et al., 2004; Obara et al., 2009; Svensson et al., 2006). It has been shown that inflammation and tissue injury increase expression of the TRPV1 in myelinated neurons, contributing to hyperalgesia (Ueda, 2006). TRPV1 upregulation contributes to mechanical allodynia and thermal hyperalgesia, while the administration of its antagonists can reverse the allodynia and hyperalgesia in a spinal nerve ligation model (Vilceanu et al., 2010). The activation of TRPV1 triggers the propagation of pain sensation and affects the release of some neurotransmitters, including substance P, that are released from activated nerve endings, resulting in a neurogenic inflammation (Pailleux et al., 2012).

Substance P is an 11-amino-acid peptide of the tachykinin family which is produced in the central and peripheral terminals of

**Abbreviations:** CCI, chronic constriction injury; DOR,  $\delta$ -opioid receptor; DRG, dorsal root ganglion; KOR,  $\kappa$ -opioid receptor; MOR,  $\mu$ -opioid receptor; NM, neural mobilization; TRPV1, transient receptor potential vanilloid 1.

\* Corresponding author at: Laboratory of Functional Neuroanatomy of Pain, Department of Anatomy, Institute of Biomedical Sciences, University of São Paulo, Av. Prof. Lineu Prestes, 2415, 05508-000, SP, Brazil.

E-mail addresses: [fabiomartinez@usp.br](mailto:fabiomartinez@usp.br) (F.M. Santos), [jteixeira@umaryland.edu](mailto:jteixeira@umaryland.edu) (J.T. Silva), [ircrocha@usp.br](mailto:ircrocha@usp.br) (I.R.C. Rocha), [martinsd@usp.br](mailto:martinsd@usp.br) (D.O. Martins), [chacur-m@icb.usp.br](mailto:chacur-m@icb.usp.br) (M. Chacur).

<sup>1</sup> Laboratory of Functional Neuroanatomy of Pain, Department of Anatomy, Institute of Biomedical Sciences, University of São Paulo, Av. Prof. Lineu Prestes, 2415, 05508-000, SP, Brazil.

<sup>2</sup> Department of Neural and Pain Sciences, University of Maryland, Dental School, 650 W. Baltimore Street, 8 South, Room 8404, Baltimore, MD 21201, USA.

<sup>3</sup> Laboratory of Functional Neuroanatomy of Pain, Department of Anatomy, Institute of Biomedical Sciences, University of São Paulo, Av. Prof. Lineu Prestes, 2415, 05508-900, SP, Brazil.

<https://doi.org/10.1016/j.brainres.2018.02.034>  
0006-8993/© 2018 Elsevier B.V. All rights reserved.

primary sensory neurons and released following noxious stimuli in the periphery (Chen et al., 2006). Substance P also plays an important role in the development of chronic pain (Gao et al., 2003; Steinhoff et al., 2003), acting on a G protein-coupled receptor known as a tachykinin receptor (NK1). Studies have demonstrated the involvement of the NK1 receptor in neuropathic pain induced by sciatic nerve constriction, showing that substance P is responsible for the development of hyperalgesia in rats (Hoot et al., 2011; Jang et al., 2004). In clinical practice, it has been extensively reported that neuropathic pain is difficult to treat, due to inadequate understanding of the cellular and molecular mechanisms involved in the development and maintenance of this type of pain (Sapunar et al., 2005; Xie et al., 2006). Opioid drugs are the most widely used to treat pain ranging from moderate to severe. More recently, studies showed that endomorphin-2, one of the endogenous ligands for the  $\mu$ -opioid receptor (MOR) is co-localized with substance P in DRG neurons and in the spinal cord (Luo et al., 2014; Sanderson Nydahl et al., 2004; Wu et al., 2015). Opioid receptors are heterogeneously distributed in the neuronal nociceptive system, and all three types of opioid receptors are synthesized and expressed in the cell bodies of DRG neurons. Studies that evaluate the effects of opioids in different models of neuropathic and inflammatory pain have obtained different results in relation to different types of opioid receptors. There is no pattern of opioid receptor expression for inflammatory pain models or for neuropathic pain models (Porreca et al., 1998; Truong et al., 2003; Zhang et al., 2016).

The NM technique is a manual therapy method used by physiotherapists to treat patients with neural origin pain, such as the compression of the sciatic nerve. The technique aims to restore mobility and elasticity of the peripheral nervous system by strains that are imposed on the nerve trunks, roots, nerves, spinal cord and their epineurium and to decrease sensitivity (Santos et al., 2012). We have shown that NM treatment reverses pain symptoms in rats submitted to CCI and induces changes in glial cells and neurotrophins, besides improving the nerve regeneration after treatment (da Silva et al., 2015; Santos et al., 2012; Santos et al., 2014). Additionally, in this work we focused on evaluating whether the NM can influence TRPV1, substance P and opioid receptor expression on DRG neurons in animals under a neuropathic pain condition. This issue was evaluated by Western blotting assays in the DRG of adult neuropathic rats after treatment with NM.

## 2. Results

### 2.1. Effects of NM on substance P expression

Fig. 1 shows an increase of substance P protein levels (48%) after CCI in comparison to naive rats ( $p \leq 0.05$ ), taken as a control. After NM treatment (CCI-NM), we observed a decrease of substance P expression of approximately 65% when compared to CCI animals ( $p \leq 0.001$ ) (Fig. 1). No significant differences in substance P expression were observed between sham and naive rats or between sham and sham-NM animals (data not shown).

### 2.2. Effects of NM on TRPV1 expression

We have evaluated the protein expression of TRPV1 in the DRG to assess the possible effects of CCI and NM treatment. Our results showed an increase of 35% in TRPV1 levels after CCI injury when compared to naive animals ( $p \leq 0.05$ ), (Fig. 2). After NM treatment, we observed a decrease of 80% above the control in TRPV1 expression and a decrease of 110% when comparing the CCI-NM group to the CCI group ( $p \leq 0.001$ ). No differences were observed between naive and sham rats or between sham and sham-NM rats (data not shown).

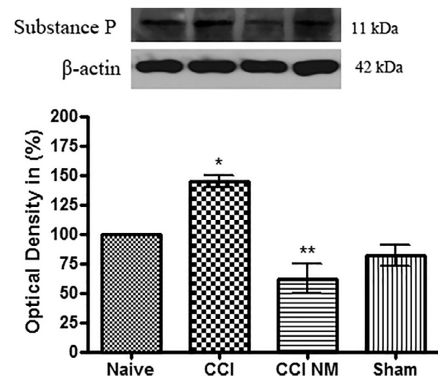


Fig. 1. Densitometric analysis of Substance P levels in the DRG. The normalized average between sham and experimental groups (CCI and CCI-NM) is reported. Data for naive animals were taken as 100% and mean  $\pm$  SEM of 6 animals per group.  $p \leq 0.05$  compared CCI and naive groups.

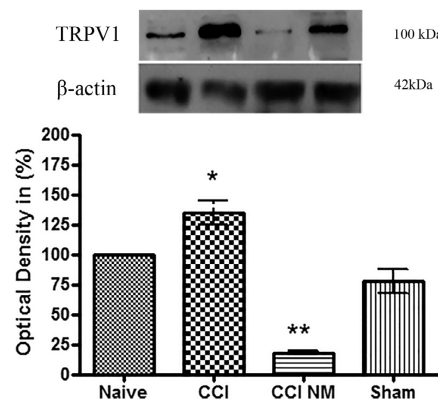
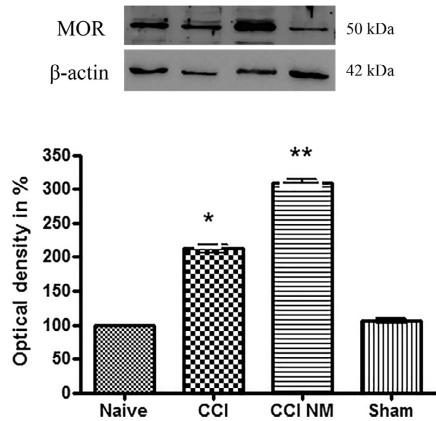


Fig. 2. Densitometric analysis of TRPV1 levels in the DRG. The normalized average between sham and experimental groups (CCI and CCI-NM) is reported. Data for naive animals were taken as 100% and mean  $\pm$  SEM of 6 animals per group.  $p \leq 0.05$  compared CCI and naive groups.

### 2.3. Effects of NM on opioid receptor expression

To evaluate how NM treatment can interfere with opioid receptors, we also analyzed MOR, DOR and KOR protein expression. Our results showed an increase of 110% ( $p \leq 0.001$ ) in MOR levels after CCI injury when compared to naive animals (Fig. 3). After NM treatment, we observed an enhancement of MOR expression when compared to the control group (200% naive  $p \leq 0.001$ ) and when compared with CCI injury animals (43% CCI  $p \leq 0.01$ ). No difference was observed between naive and sham rats or between sham and sham-NM rats (data not shown). Regarding the evaluation of DOR and KOR opioid receptors, it was not possible to observe any immunoreactivity of these receptors in our model (data not shown).



**Fig. 3.** Densitometric analysis of MOR levels in the DRG. The normalized average between sham and experimental groups (CCI and CCI-NM) is reported. Data for naive animals were taken as 100% and mean  $\pm$  SEM of 6 animals per group.  $p \leq 0.001$  compared CCI with naive groups.  $**p \leq 0.01$  compared CCI NM with other groups.

No differences were observed for  $\beta$ -actin between control and experimental sides at any of the time points analyzed (Figs. 1–3).

### 3. Discussion

A large body of evidence has shown that peripheral nerve injury usually induces neuropathic pain. Numerous patients with diagnoses of chronic pain have not been successfully treated with the use of conventional analgesics. Furthermore, many of these drugs induce dependence and side effects. In this regard, alternative tools to combat neuropathic pain have become necessary. Physical therapy, especially neural mobilization, which is non-invasive and does not have any side effects, has heavily contributed as an analgesic tool for neuropathic pain (Marcioli et al., 2013; Martins et al., 2013a; Martins et al., 2013b). In our previous studies, we showed that treatment with NM reverses pain-related behavior due to the CCI (Santos et al., 2012). The decrease of pain sensitivity could be because of the cellular changes observed after NM treatment, such as a decrease of the neural growth factor (NGF) and the glial fibrillary acidic protein (GFAP) in the DRG and spinal cord (da Silva et al., 2015), and changes in the expression of opioid receptors in the periaqueductal gray (PAG). In addition, we demonstrated an improvement in locomotion and muscle force after NM (Santos et al., 2014).

Substance P and opioids acts in different ways on pain behavior, substance P release plays an important role in the development of chronic pain whereas opioids acts inhibiting the release of excitatory neurotransmitters. Studies suggest that the inhibition of substance P release is one of the most important presynaptic mechanisms for opioid analgesia (Chen et al., 2014; Kondo et al., 2005; Marvizon et al., 2003). Opioid resistance is a common phenomenon in the treatment of neuropathic pain and this may due to the activity of substance P within the DRG. Here we show that NM decreased the substance P expression and increased MOR expression in the DRG, which was probably the reason for the improvement of pain behavior in the animals treated with NM, once was already reported that the MOR activation may inhibit substance P release (Yaksh et al., 1980).

The major finding of the present study is that NM was able to alter the expression of substance P and TRPV1 in the DRG of animals treated with neural mobilization (CCI-NM) when compared to control animals and increase the expression of the MOR. This finding, combined with the results of previous behavioral tests [for more detail see (Santos et al., 2014)], suggests that NM contributes to reducing cellular and molecular changes induced by nerve injury. This effect, which is probably due to NM, may cause a nerve decompression that restores the mobility and elasticity of the peripheral nervous system. The dysfunctional signaling mechanisms induced by compressive syndromes, clinically, leads to nerve degeneration, failure of nerve conduction and pain. In addition, the interval between nerve injury and nerve decompression affect the degree of nerve dysfunction and damage. Neural mobilization is said to induce the movement between neural structures and its connective tissue (Coppeters et al., 2009; Nee and Butler, 2006) by alteration of the pressure in the nervous system and dispersion of intraneural edema (Schmid et al., 2012) restoring the mechanical and neurophysiological function of the nerve (Shacklock, 1995). Ours previous studies reveled that NM reduces thermal and mechanical hyperalgesia, improves muscle strength and promotes nerve regeneration in rats (da Silva et al., 2015; Santos et al., 2012; Santos et al., 2014). Therefore, the correlation between our molecular and previous behavioral results provides evidence that NM is reliable as a clinical method and could have an impact on clinical routines regarding treatment of compression injuries.

Clinically, surgery decompression remains an essential procedure for the resolution of cases of pain due to compressive syndromes affecting peripheral nerves (Ducic et al., 2006; Padua et al., 2016; Thomson, 2017). Andreu et al. shows that decompressive surgery is clinically more effective in reducing symptoms of carpal tunnel syndrome when compared with local corticosteroid injection (Andreu et al., 2014). Our findings corroborate previous data showing that ankle joint mobilization can decrease hypersensitivity in the mouse plantar incision model of postoperative pain. The results indicated that joint mobilization reduces postoperative pain by the activation of the peripheral opioid pathway (Gebhart, 2004).

Recent studies conducted by our group demonstrated that NM improves neuropathic pain behaviors; however, the potential effect of NM in the model of chronic pain by CCI of the sciatic nerve used for pain relief has not been fully explored. In this work, the NM technique causes a decrease of substance P and TRPV1 and an increase of MOR expression. Several studies have shown that substance P is a neuropeptide that mediates nociception and is used as a marker for pain in animal models (Hutchinson et al., 2004; Munro et al., 2012). Studies have demonstrated the involvement of the NK1 receptor in the model of neuropathic pain by CCI, suggesting that substance P is responsible for the development of hyperalgesia in rats (Hoot et al., 2011; Jang et al., 2004). In our study, we observed an increase of 48% in substance P after CCI injury and a reduction to baseline levels after treatment with NM, reinforcing the involvement of substance P in pain conditions.

Heat pain is in part mediated by TRPV1 expressed by C-fiber nociceptors in the DRG and trigeminal ganglion (Caterina et al., 1997; Tominaga et al., 1998). TRPV1 is upregulated in DRG neurons after persistent inflammation (Ji et al., 2002) and is essential for the development of inflammatory heat hyperalgesia (Caterina et al., 2000; Davis et al., 2000). Our results showed an important modulation of TRPV1 levels in the CCI model and after manual therapy (NM). It is currently known that TRPV1 also responds to other stimuli, such as endogenous pro-inflammatory agents, pH changes (pH 5.2), and changes in body temperature ( $>43^{\circ}\text{C}$ ). These stimuli activate signaling cascades, which are responsible for the reduction of pain threshold (Coggeshall et al., 1997; Paxinos and Watson, 2006).



Studies involving the TRPV1 receptor support the possibility of the involvement of this receptor as a therapeutic target for pain (van Sloten et al., 2011). As observed for substance P, TRPV1, when present, sensitizes the primary afferent neuron, which in turn depolarizes the existing second-order neurons in laminae I and II of the spinal cord, favoring the establishment of LTP. Moreover, the destruction of TRPV1-expressing afferent neurons eliminates presynaptic MOR present on TRPV1-expressing afferent neurons, which paradoxically potentiates the antinociceptive effect produced by intrathecal and systemic MOR agonists (Chen and Pan, 2006). MOR receptors have an important function in modulation of mechanical nociception transmitted by non-TRPV1 afferent neurons, which extend our current knowledge of the pain pathways and mechanisms underlying opioid analgesia (Chen and Pan, 2006).

Animals treated with NM showed an increase of 200% in the expression of MORs. We also analyzed the other opioid receptors, but we did not detect any immunoreactivity of these receptors in any group analyzed. Opioids are potent analgesics that exert pharmacological and physiological effects due to interaction with receptors distributed in various regions associated with decreased neural excitability, as well as those associated with the release of neuropeptides, such as substance P, corroborating our data (Sicuteri et al., 1983; Stein et al., 1988; Yaksh, 1988). There is a decrease of hyperalgesia when opioid agonists are applied, suggesting a decrease of spontaneous discharges in C-type fibers (Basbaum and Fields, 1984; Mayer et al., 1971; Paxinos and Watson, 2006). The lack of involvement of DOR and KOR in our model is not clear. However, some studies using different pain models showed controversial results about the involvement of opioid receptors. There is no definite pattern of expression for inflammatory or neuropathic pain models, but it seems that DOR expression increases in neuropathic and postoperative pain and MOR increases in inflammation (de Oliveira Junior et al., 2016). The participation of KOR was seen in the anti-nociceptive effect induced by prostaglandin E2, carrageenan, and crocophaline (Ji et al., 1995; Konno et al., 2008). Additionally, the involvement of KOR and DOR in a cancer pain model was shown, with the increase of its expression (Brigatte et al., 2007). However, the lack of opioid receptor expression (DOR and KOR) has not affected the NM antinociception during treatment.

Noxious stimulus information is project to neurons within the DRG of the spinal cord. This information is transmitted to the somatosensory cortex via the thalamus, giving the location and intensity of the painful stimulus. Other cerebral areas, such the cingulate and insular cortices via connections in the brainstem (parabrachial nucleus) and amygdala, contribute to the affective component of the pain experience. This ascending information also connects with neurons of the rostral ventral medulla and midbrain periaqueductal gray to engage descending feedback systems that regulate the output from the spinal cord (Basbaum et al., 2009). We already showed in a previous study that the same treatment with NM increased the expression of opioid receptors, in the periaqueductal gray (Santos et al., 2014). Those results added with the data of current study, provides an insight into the correlation between endogenous opioid system and analgesic efficacy of NM. These observations may contribute to increasing the knowledge of neurobiological mechanisms underlying the therapeutic action of NM, which are only partially understood.

#### 4. Conclusion

In summary, our data reveal a decrease of substance P and TRPV1 in the DRG induced by NM treatment in CCI animals. We also demonstrated that NM sessions are able to increase opioid receptor levels in the DRG. Thus, we believe that the neural mobilization technique, through basic research, appears to be effective

in the nociceptive process, probably causing a nerve decompression, which can improve the synaptic plasticity in DRG neurons. Accordingly, we can contribute to an understanding of the mechanisms involved in the rehabilitation process. Current treatment options for neuropathic pain are limited and the first and second line pharmacological approaches to treat neuropathic pain have limited effectiveness. We are exploring the potential application of such therapy as an alternative choice for treating neuropathic pain.

## 5. Methods and materials

### 5.1. Animals

Fifty male Wistar rats, weighing between 200 and 220 g, were used in all experiments. They were maintained on a 12:12 h light/dark cycle. All procedures were approved by the Institutional Animal Care Committee of the University of São Paulo (protocol number 091 – book number 02/2012) and performed in accordance with the guidelines for the ethical use of conscious animals in pain research published by the International Association for the Study of Pain (Zimmermann, 1983). Efforts were made to minimize the number of animals used and their suffering. All animals were submitted to behavioral tests to evaluate sensibility in a previous study (Santos et al., 2012).

### 5.2. Surgical procedure

#### 5.2.1. Chronic constriction injury – (CCI)

For the induction of neuropathic pain, chronic constriction of the sciatic nerve was performed as previously described by Bennett and Xie (1988). In short, rats were anesthetized with isoflurane (Cristalia, Brazil), and the right sciatic nerve was exposed. Proximal to the sciatic trifurcation, the nerve was freed of adhering tissue and 4 ligatures (4.0 chromic gut) were tied loosely around it with approximately 1 mm spacing. The incision was closed in layers. In sham-operated rats, the right sciatic nerve was exposed but left unaffected and served as a control. Each rat was closely observed during the recovery from anesthesia and then returned to the home cage and was observed carefully during the following 24 h. During the 5 day-period after CCI, the walking and cage exploration, degree of limping, and conditions of the hind paw, including signs of excessive grooming or autotomy, were all observed.

#### 5.2.2. Neural mobilization technique – (NM)

The NM technique used here has been described by Butler (1989) and adapted by our laboratory (da Silva et al., 2015; Santos et al., 2012; Santos et al., 2014). Briefly, rats were anesthetized with isoflurane and received a continuous flow of medicinal oxygen throughout the procedure (5 mL/L). After anesthesia, the animals were positioned in the left lateral position to mobilize the right side. The right knee joint was positioned in full extension (at 0 degrees) and remained so throughout the session. The right hip joint was bent between 70 and 80 degrees with the knee in extension until obtaining a small resistance induced by stretching the muscles from the posterior compartment of the thigh (biceps femoris, semimembranosus and semitendinosus). Then, the ankle joint was angled between 30 and 45 degrees, and oscillatory movements were initiated. The right ankle joint was manipulated in dorsiflexion (30–45 degrees) by approximately 20 oscillations per minute for 2 min, followed by a 25-s pause for rest. The treatment occurred for ten minutes, and in the last minute, the cervical spine was fully flexed, with the purpose of tensioning the entire neuraxis (Lew and Briggs, 1997). Treatment with the NM technique started



14 days after injury or sham procedure, and the NM sessions were applied every other day, similar to clinical practice, for a total of 10 sessions.

The animals were initially divided into five groups with 10 animals per group. Group 1 consisted of animals that suffered nerve damage and had neural mobilization treatment (CCI + NM); Group 2 consisted of sham animals with neural mobilization (SHAM + NM); Group 3 consisted of sham animals without NM treatment (SHAM); Group 4 consisted of operated animals, but without any treatment (CCI); and Group 5 comprised a NAIVE group used as a control (without neural treatment or surgery).

### 5.3. Immunoblotting

Western blotting analyses were performed on samples from individual animals sacrificed at the end of the NM session (34 days after baseline). Neuropathic (CCI), sham and naive rats were sacrificed by decapitation under isoflurane anesthesia, and the DRG (L4-L6) was quickly removed and transferred to a tube containing 100  $\mu$ L extraction buffer (100 mM of Tris, pH 7.4, 1% SDS, 10 mM of EDTA, 2 mM of PMSF, and 10  $\mu$ g/mL of aprotinin) in ice-cold (4 °C) during 30 min. Then they were homogenized using an ultrasonic processor (Sonic & Materials, Newtown, PA). After extraction, the homogenates were centrifuged at 12,000 rpm at 4 °C for 20 min, and the protein concentration of the supernatant was determined using the Bradford protein assay with albumin as a standard (Bio-Rad, USA) (Bradford, 1976). Samples containing 75  $\mu$ g of protein were loaded on acrylamide gradient gel (Miller et al., 2016) and transferred by electrophoresis to nitrocellulose membranes using a Bio-Rad miniature transfer apparatus for 1.5 h at 120 V. After transfer, the membranes were treated for 2 h at room temperature with a blocking solution containing 5% powdered milk, washed and incubated overnight at 4 °C with rat polyclonal antibodies against goat substance P (1:1000; Santa Cruz Biotechnology, INC, USA), TRPV1 (1:1000 Chemicon, Canada) and against MOR, DOR and KOR (1:250; Santa Cruz Biotechnology, INC, USA). The membranes were then washed and incubated for 2 h at room temperature with a peroxidase-conjugated, anti-rabbit, anti-goat secondary antibody, diluted 1:5000 (ZIMED Laboratories Inc, USA), and an anti-mouse secondary antibody, diluted 1:5000 (GE Healthcare, USA). In every immunoblotting experiment,  $\beta$ -actin (mouse, 1:10,000; Sigma, USA) was used as an internal control. The specifically bound antibody was visualized using a chemiluminescence kit (Amersham Biosciences, USA). The blot was analyzed densitometrically using the NIH-Scion Image 4.0.2, quantified by optical densitometry of the developed autoradiographs (Scion Corporation, USA) and corrected by the optical density for  $\beta$ -actin, whereas samples from control animals were used as the standard for normalization of the results (assuming 100% for naive animals).

### 5.4. Statistical analysis

Results are presented as the mean  $\pm$  SEM. Statistical analyses of data were generated using GraphPAD Prism, version 5.01 (Graph-Pad Software Inc., San Diego, CA). Statistical comparison was performed using analysis of variance (ANOVA); differences between means were tested by Tukey's test. In all cases,  $p \leq 0.05$  was considered statistically significant (Snedecor et al., 1946).

### Author's contributions

All authors made substantial contributions to the following aspects of this research: initial conception (Santos F.M., Martins D.O., Silva J.T., Chacur M.); design (Santos F.M., Martins D.O., Chacur M.); provision of resources (Chacur M); collection of data

(Martins D.O., Santos F.M., Silva J.T., Rocha, IRC); analysis and interpretation of data (Santos F.M., Martins D.O., Chacur M., Silva J.T., Rocha, IRC); writing the first draft of the paper or important intellectual content (Santos F.M., Martins D.O., Silva J.T., Rocha, IRC); revision of the paper (Santos F.M., Martins D.O., Chacur M.). All authors read and approved the final manuscript.

### Ethics approval and consent to participate

All experimental procedures carried out in this study have been approved by the Institutional Animal Care and Use Committee of the University of São Paulo (protocol number 091 – book number 02/2012) and were in compliance with the guidelines for animal care and use set forth by that committee.

### Acknowledgements

Santos, F.M., was the recipient of a FAPESP Ph.D's scholarship.

### Disclosure

This study was supported by the FAPESP (2012/05840-4; 2014/24533-0), CNPq (Brazil). The funding bodies play no role in the design of the study, data collection, analysis, interpretation of the data, or in writing the manuscript.

### Conflicts of interest

None of the authors have any potential or actual conflicts of interest to declare.

### References

- Andreu, J.L., Ly-Pen, D., Millan, I., de Blas, G., Sanchez-Olaso, A., 2014. Local injection versus surgery in carpal tunnel syndrome: neurophysiologic outcomes of a randomized clinical trial. *Clin. Neurophysiol.* 125, 1479–1484.
- Basbaum, A.I., Fields, H.L., 1984. Endogenous pain control systems: brainstem spinal pathways and endorphin circuitry. *Annu. Rev. Neurosci.* 7, 309–338.
- Basbaum, A.I., Bautista, D.M., Scherrer, G., Julius, D., 2009. Cellular and molecular mechanisms of pain. *Cell* 139, 267–284.
- Bennett, G.J., Xie, Y.K., 1988. A peripheral mononeuropathy in rat that produces disorders of pain sensation like those seen in man. *Pain* 33, 87–107.
- Bradford, M.M., 1976. A rapid and sensitive method for the quantitation of microgram quantities of protein utilizing the principle of protein-dye binding. *Anal. Biochem.* 72, 248–254.
- Brigatte, P., Sampaio, S.C., Gutierrez, V.P., Guerra, J.L., Sinhorini, L.L., Curi, R., Cury, Y., 2007. Walker 256 tumor-bearing rats as a model to study cancer pain. *J. Pain* 8, 412–421.
- Caterina, M.J., Schumacher, M.A., Tominaga, M., Rosen, T.A., Levine, J.D., Julius, D., 1997. The capsaicin receptor: a heat-activated ion channel in the pain pathway. *Nature* 389, 816–824.
- Caterina, M.J., Leffler, A., Malmberg, A., Martin, W., Trafton, J., Petersen-Zeit, K., Koltzenburg, M., Basbaum, A., Julius, D., 2000. Impaired nociception and pain sensation in mice lacking the capsaicin receptor. *Sci. Signal.* 288, 306.
- Chen, S.-R., Pan, H.-L., 2006. Loss of TRPV1-expressing sensory neurons reduces spinal  $\mu$  opioid receptors but paradoxically potentiates opioid analgesia. *J. Neurophysiol.* 95, 3086–3096.
- Chen, W., McRoberts, J.A., Marvizon, J.C., 2014.  $\mu$ -Opioid receptor inhibition of substance P release from primary afferents disappears in neuropathic pain but not inflammatory pain. *Neuroscience* 267, 67–82.
- Chen, W.L., Zhang, Y.Q., Zhao, Z.Q., 2006. Neurokinin-1 receptor in peripheral nerve terminals mediates thermal hyperalgesia. *Biochem. Biophys. Res. Commun.* 339, 132–136.
- Coggeshall, R.E., Zhou, S., Carlton, S.M., 1997. Opioid receptors on peripheral sensory axons. *Brain Res.* 764, 126–132.
- Coppieters, M.W., Hough, A.D., Dilley, A., 2009. Different nerve-gliding exercises induce different magnitudes of median nerve longitudinal excursion: an in vivo study using dynamic ultrasound imaging. *J. Orthop. Sports Phys. Ther.* 39, 164–171.
- da Silva, J.T., Santos, F.M., Giardini, A.C., Martins Dde, O., de Oliveira, M.E., Ciena, A. P., Gutierrez, V.P., Watanabe, I.S., Britto, L.R., Chacur, M., 2015. Neural mobilization promotes nerve regeneration by nerve growth factor and myelin protein zero increased after sciatic nerve injury. *Growth Factors* 33, 8–13.

- Davis, J.B., Gray, J., Gunthorpe, M.J., Hatcher, J.P., Davey, P.T., Overend, P., Harries, M. H., Latcham, J., Clapham, C., Atkinson, K., 2000. Vanilloid receptor-1 is essential for inflammatory thermal hyperalgesia. *Nature* 405, 183–187.
- de Oliveira Junior, J.O., de Freitas, M.F., Bullara, de Andrade, C., Chacur, M., Ashmawi, H.A., 2016. Local analgesic effect of tramadol is mediated by opioid receptors in late postoperative pain after plantar incision in rats. *J. Pain Res.* 9, 797–802.
- Ducic, I., Taylor, N.S., Dellon, A.L., 2006. Relationship between peripheral nerve decompression and gain of pedal sensibility and balance in patients with peripheral neuropathy. *Ann. Plast. Surg.* 56, 145–150.
- Gao, Y.J., Zhang, Y.Q., Zhao, Z.Q., 2003. Involvement of spinal neurokinin-1 receptors in the maintenance but not induction of carrageenan-induced thermal hyperalgesia in the rat. *Brain Res. Bull.* 61, 587–593.
- Gebhart, G., 2004. Descending modulation of pain. *Neurosci. Biobehav. Rev.* 27, 729–737.
- Hoot, M.R., Sim-Selley, L.J., Selley, D.E., Scoggins, K.L., Dewey, W.L., 2011. Chronic neuropathic pain in mice reduces  $\mu$ -opioid receptor-mediated G-protein activity in the thalamus. *Brain Res.* 1406, 1–7.
- Hutchinson, K.J., Gómez-Pinilla, F., Crowe, M.J., Ying, Z., Basso, D.M., 2004. Three exercise paradigms differentially improve sensory recovery after spinal cord contusion in rats. *Brain* 127, 1403–1414.
- Jang, J.H., Nam, T.S., Paik, K.S., Leem, J.W., 2004. Involvement of peripherally released substance P and calcitonin gene-related peptide in mediating mechanical hyperalgesia in a traumatic neuropathy model of the rat. *Neurosci. Lett.* 360, 129–132.
- Ji, R.-R., Samad, T.A., Jin, S.-X., Schmolz, R., Woolf, C.J., 2002. p38 MAPK activation by NGF in primary sensory neurons after inflammation increases TRPV1 levels and maintains heat hyperalgesia. *Neuron* 36, 57–68.
- Ji, R.R., Zhang, Q., Law, P.Y., Low, H.H., Elde, R., Hökfelt, T., 1995. Expression of  $\mu$ ,  $\delta$ , and  $\kappa$ -opioid receptor-like immunoreactivities in rat dorsal root ganglia after carrageenan-induced inflammation. *J. Neurosci.* 15, 8156–8166.
- Kondo, I., Marvizon, J.C., Song, B., Salgado, F., Codeluppi, S., Hua, X.Y., Yaksh, T.L., 2005. Inhibition by spinal  $\mu$ - and  $\delta$ -opioid agonists of afferent-evoked substance P release. *J. Neurosci.* 25, 3651–3660.
- Konno, K., Picolo, G., Gutierrez, V.P., Brigatte, P., Zambelli, V.O., Camargo, A.C., Cury, Y., 2008. Crotalaphine, a novel potent analgesic peptide from the venom of the South American rattlesnake *Crotalus durissus terrificus*. *Peptides* 29, 1293–1304.
- Kuo, P.Y., Yen, J.T., Parker, G.M., Chapman, S., Kandikattu, S., Sohanpal, I., Barbachano, Y., Williams, J.E., 2011. The prevalence of pain in patients attending sarcoma outpatient clinics. *Sarcoma* 2011, 813483.
- LaCroix-Fralish, M.L., Austin, J.S., Zheng, F.Y., Levitin, D.J., Mogil, J.S., 2011. Patterns of pain: meta-analysis of microarray studies of pain. *Pain* 152, 1888–1898.
- Lew, P.C., Briggs, C.A., 1997. Relationship between the cervical component of the slump test and change in hamstring muscle tension. *Man Ther.* 2, 98–105.
- Luo, D.S., Huang, J., Dong, Y.L., Wu, Z.Y., Wei, Y.Y., Lu, Y.C., Wang, Y.Y., Yanagawa, Y., Wu, S.X., Wang, W., Li, Y.Q., 2014. Connections between EM2- and SP-containing terminals and GABAergic neurons in the mouse spinal dorsal horn. *Neurosci. Lett.* 35, 1421–1427.
- Marcioli, M.A., Coradini, J.G., Kunz, R.I., Ribeiro Lde, F., Brancalho, R.M., Bertolini, G. R., 2013. Nociceptive and histomorphometric evaluation of neural mobilization in experimental injury of the median nerve. *Sci. World J.* 2013, 476890.
- Martins, D.F., Mazzardo-Martins, L., Cidral-Filho, F.J., Gadotti, V.M., Santos, A.R., 2013a. Peripheral and spinal activation of cannabinoid receptors by joint mobilization alleviates postoperative pain in mice. *Neuroscience* 255, 110–121.
- Martins, D.F., Mazzardo-Martins, L., Cidral-Filho, F.J., Stramoski, J., Santos, A.R., 2013b. Ankle joint mobilization affects postoperative pain through peripheral and central adenosine A1 receptors. *Phys. Ther.* 93, 401–412.
- Marvizon, J.C., Wang, X., Matsuka, Y., Neubert, J.K., Spiegelman, I., 2003. Relationship between capsaicin-evoked substance P release and neurokinin 1 receptor internalization in the rat spinal cord. *Neuroscience* 118, 535–545.
- Mayer, D.J., Wolfe, T.L., Akil, H., Carder, B., Liebeskind, J.C., 1971. Analgesia from electrical stimulation in the brainstem of the rat. *Science* 174, 1351–1354.
- Miller, A.J., Roman, B., Norstrom, E.M., 2016. Protein electrophoretic migration data from custom and commercial gradient gels. *Data Brief* 9, 1–3.
- Munro, G., Storm, A., Hansen, M.K., Dyhr, H., Marcher, L., Erichsen, H.K., Sheykhzade, M., 2012. The combined predictive capacity of rat models of algogen-induced and neuropathic hypersensitivity to clinically used analgesics varies with nociceptive endpoint and consideration of locomotor function. *Pharmacol. Biochem. Behav.* 101, 465–478.
- Narita, M., Kuzumaki, N., Suzuki, M., Oe, K., Yamazaki, M., Yajima, Y., Suzuki, T., 2004. Increased phosphorylated- $\mu$ -opioid receptor immunoreactivity in the mouse spinal cord following sciatic nerve ligation. *Neurosci. Lett.* 354, 148–152.
- Nee, R.J., Butler, D., 2006. Management of peripheral neuropathic pain: integrating neurobiology, neurodynamics, and clinical evidence. *Phys. Ther.* 7, 36–49.
- Obara, Y., Yamachi, A., Takehara, S., Nemoto, W., Takahashi, M., Stork, P.J., Nakahata, N., 2009. ERK5 activity is required for nerve growth factor-induced neurite outgrowth and stabilization of tyrosine hydroxylase in PC12 cells. *J. Biol. Chem.* 284, 23564–23573.
- Padua, L., Coraci, D., Erra, C., Pazzaglia, C., Paolasso, I., Loreti, C., Caliendo, P., Hobson-Webb, L.D., 2016. Carpal tunnel syndrome: clinical features, diagnosis, and management. *Lancet Neurol.* 15, 1273–1284.
- Pailleux, F., Lemoine, J., Beaudry, F., 2012. Quantitative mass spectrometry analysis reveals that deletion of the TRPV1 receptor in mice alters substance P and neurokinin A expression in the central nervous system. *Neurochem. Res.* 37, 2678–2685.
- Paxinos, G., Watson, C., 2006. *The Rat Brain in Stereotaxic Coordinates*: Hard Cover Edition. Elsevier.
- Porreca, F., Tang, Q.B., Bian, D., Riedl, M., Elde, R., Lai, J., 1998. Spinal opioid mu receptor expression in lumbar spinal cord of rats following nerve injury. *Brain Res.* 795, 197–209.
- Sanderson Nydahl, K., Skinner, K., Julius, D., Basbaum, A.I., 2004. Co-localization of endomorphin-2 and substance P in primary afferent nociceptors and effects of injury: a light and electron microscopic study in the rat. *Eur. J. Neurosci.* 19, 1789–1799.
- Santos, F.M., Silva, J.T., Giardini, A.C., Rocha, P.A., Achermann, A.P., Alves, A.S., Britto, L.R., Chacur, M., Doolen, S., Blake, C., 2012. Neural mobilization reverses behavioral and cellular changes that characterize neuropathic pain in rats. *Mol. Pain* 8, 57.
- Santos, F.M., Grecco, L.H., Pereira, M.C., Oliveira, M.E., Rocha, P.A., Silva, J.T., Martins, D.O., Miyabara, E.H., Chacur, M., 2014. The neural mobilization technique modulates the expression of endogenous opioids in the periaqueductal gray and improves muscle strength and mobility in rats with neuropathic pain. *Behav. Brain Funct.* 10, 19.
- Sapunar, D., Modric-Jednacak, K., Grkovic, I., Michalkiewicz, M., Hogan, Q.H., 2005. Effect of peripheral axotomy on pain-related behavior and dorsal root ganglion neurons excitability in NPY transgenic rats. *Brain Res.* 1063, 48–58.
- Sapunar, D., Kostic, S., Banozic, A., Puljak, L., 2012. Dorsal root ganglion – a potential new therapeutic target for neuropathic pain. *J. Pain Res.* 5, 31–38.
- Schmid, A.B., Elliott, J.M., Stradwick, M.W., Little, M., Coppiters, M.W., 2012. Effect of splinting and exercise on intraneural edema of the median nerve in carpal tunnel syndrome – an MRI study to reveal therapeutic mechanisms. *J. Orthop. Res.* 30, 1343–1350.
- Shacklock, M., 1995. *Neurodynamics*. Physiotherapy 81, 9–16.
- Sicuteri, F., Rainò, L., Geppetti, P., 1983. Substance P and endogenous opioids: how and where they could play a role in cluster headache. *Cephalalgia* 3, 143–145.
- Snedecor, G.W., Sokal, R.R., Rohlf, F.J., 1946. *Statistical Methods Biometry*. Iowa State University Press, New York.
- Stein, C., Millan, M.J., Vassouridis, A., Herz, A., 1988. Antinociceptive effects of  $\mu$ - and  $\kappa$ -agonists in inflammation are enhanced by a peripheral opioid receptor-specific mechanism. *Eur. J. Pharmacol.* 155, 255–264.
- Steinhoff, M., Stander, S., Seeliger, S., Ansel, J.C., Schmelz, M., Luger, T., 2003. Modern aspects of cutaneous neurogenic inflammation. *Arch. Dermatol.* 139, 1479–1488.
- Svensson, C.I., Tran, T.K., Fitzsimmons, B., Yaksh, T.L., Hua, X.Y., 2006. Descending serotonergic facilitation of spinal ERK activation and pain behavior. *FEBS Lett.* 580, 6629–6634.
- Thomson, J.G., 2017. Diagnosis and treatment of carpal tunnel syndrome. *Lancet Neurol.* 16, 263.
- Tominaga, M., Caterina, M.J., Malmberg, A.B., Rosen, T.A., Gilbert, H., Skinner, K., Raumann, B.E., Basbaum, A.I., Julius, D., 1998. The cloned capsaicin receptor integrates multiple pain-producing stimuli. *Neuron* 21, 531–543.
- Truong, W., Cheng, C., Xu, Q.G., Li, X.Q., Zochodne, D.W., 2003.  $\mu$  opioid receptors and analgesia at the site of a peripheral nerve injury. *Ann. Neurol.* 53, 366–375.
- Ueda, H., 2006. Molecular mechanisms of neuropathic pain-phenotypic switch and initiation mechanisms. *Pharmacol. Ther.* 109, 57–77.
- van Sloten, T.F., Savelberg, H.H., Duimel-Peters, J.G., Meijer, K., Henry, R., Stehouwer, C.D., Schaper, N.C., 2011. Peripheral neuropathy, decreased muscle strength and obesity are strongly associated with walking in persons with type 2 diabetes without manifest mobility limitations. *Diabetes Res. Clin. Pract.* 91, 32–39.
- Vilceanu, D., Honore, P., Hogan, Q.H., Stucky, C.L., 2010. Spinal nerve ligation in mouse upregulates TRPV1 heat function in injured IB4-positive nociceptors. *J. Pain* 11, 588–599.
- Wu, X.N., Zhang, T., Qian, N.S., Guo, X.D., Yang, H.J., Huang, K.B., Luo, G.Q., Xiang, W., Deng, W.T., Dai, G.H., Peng, K.R., Pan, S.Y., 2015. Antinociceptive effects of endomorphin-2: suppression of substance P release in the inflammatory pain model rat. *Neurochem. Int.* 82, 1–9.
- Xie, W.R., Deng, H., Li, H., Bowen, T.L., Strong, J.A., Zhang, J.M., 2006. Robust increase of cutaneous sensitivity, cytokine production and sympathetic sprouting in rats with localized inflammatory irritation of the spinal ganglia. *Neuroscience* 142, 809–822.
- Yaksh, T., Jessell, T., Gamse, R., Mudge, A., Leeman, S., 1980. Intrathecal morphine inhibits substance P release from mammalian spinal cord in vivo.
- Yaksh, T.L., 1988. Substance P release from knee joint afferent terminals: modulation by opioids. *Brain Res.* 458, 319–324.
- Zhang, Y., Chen, S.R., Launet, G., Chen, H., Pan, H.L., 2016. Nerve injury diminishes opioid analgesia through lysine methyltransferase-mediated transcriptional repression of  $\mu$ -opioid receptors in primary sensory neurons. *J. Biol. Chem.* 291, 8475–8485.
- Zimmermann, M., 1983. Ethical guidelines for investigations of experimental pain in conscious animals. *Pain* 16, 109–110.



## Effect of photobiomodulation on mitochondrial dynamics in peripheral nervous system in streptozotocin-induced type 1 diabetes in rats

Igor Rafael Correia Rocha<sup>1</sup> · Edward Perez-Reyes<sup>2</sup> · Marucia Chacur<sup>1</sup>

Received: 14 October 2020 / Accepted: 2 February 2021 / Published online: 18 February 2021  
 © The Author(s), under exclusive licence to European Photochemistry Association, European Society for Photobiology 2021

### Abstract

There is no effective treatment to halt peripheral nervous system damage in diabetic peripheral neuropathy. Mitochondria have been at the center of discussions as important factors in the development of neuropathy in diabetes. Photobiomodulation has been gaining clinical acceptance as it shows beneficial effects on a variety of nervous system disorders. In this study, the effects of photobiomodulation (904 nm, 45 mW, 6.23 J/cm<sup>2</sup>, 0.13 cm<sup>2</sup>, 60 ns pulsed time) on mitochondrial dynamics were evaluated in an adult male rat experimental model of streptozotocin-induced type 1 diabetes. Results presented here indicate that photobiomodulation could have an important role in preventing or reversing mitochondrial dynamics dysfunction in the course of peripheral nervous system damage in diabetic peripheral neuropathy. Photobiomodulation showed its effects on modulating the protein expression of mitofusin 2 and dynamin-related protein 1 in the sciatic nerve and in the dorsal root ganglia neurons of streptozotocin-induced type 1 diabetes in rats.

**Keywords** Dorsal root ganglia · Dynamin-related protein 1 · Laser therapy · Mitofusin-2 · Sciatic nerve

### Abbreviations

CTRL	Control
DRP-1	Dynamin-related protein 1
DRG	Dorsal root ganglia
i.p	Intraperitoneal
MFN-2	Mitofusin-2
PBM	Photobiomodulation
SN	Sciatic nerve
STZ	Streptozotocin

### 1 Introduction

Diabetes mellitus, which has become a considerable global health-care problem of the twenty-first century is a group of metabolic diseases characterized by chronic hyperglycemia resulting from decreased insulin secretion, insulin action, or both [1, 2]. According to the International Diabetes Federation (IDF—Diabetes Atlas) it was estimated that in 2017 there were 425 million people aged between 20 and 79 years with diabetes worldwide and that those numbers are expected to increase to 629 million by the year of 2045 [3]. There are two main types of diabetes. Type 1 diabetes mellitus is an autoimmune disorder characterized by the destruction of the insulin-producing  $\beta$ -cells [4] and type 2 diabetes in which defective insulin secretion and reduced insulin sensitivity are the main pathophysiological features responsible for the development of hyperglycemia [5].

Regardless of the type of diabetes, the majority of diabetic individuals will develop chronic complications due to persistent hyperglycemia [6]. Among the most prevalent diabetic complications are kidney disease, blindness, amputations, central and peripheral neuropathy, with no available therapies to prevent them to occur only to slow their progression [6–8]. Diabetic peripheral neuropathy (DPN) is the most common clinical form of diabetic neuropathy, affecting

✉ Marucia Chacur  
 chacurm@icb.usp.br  
 Igor Rafael Correia Rocha  
 ircrocha@yahoo.com.br  
 Edward Perez-Reyes  
 ebp8n@virginia.edu

<sup>1</sup> Department of Anatomy, Biomedical Sciences Institute, University of Sao Paulo, Avenue Lineu Prestes 2415, Room 007, Sao Paulo, SP 05508-900, Brazil

<sup>2</sup> Department of Pharmacology, School of Medicine, University of Virginia, Charlottesville, VA, USA

more than 90% of the patients [9]. The pathogenesis of DPN is not fully understood, and several theories have been proposed to explain how it develops [10–12].

Of note, Brownlee proposed a unifying mechanism for the development of diabetes complications [13]. According to Brownlee, hyperglycemia increases superoxide production by the mitochondria through the over-activation of tricarboxylic acid cycle [13]. Moreover, the overproduction of superoxide by the electron transport chain during hyperglycemia inhibits glyceraldehyde 3-phosphate dehydrogenase (GAPDH), leading to the activation of the four deleterious pathways involved in diabetic neuropathy [13]. Of note, mitochondrial dysfunction has gained much attention as an etiological factor implicated in the development of diabetic neuropathy [14, 15].

Mitochondria are highly dynamic organelles that play a vital role in metabolic processes by making energy in the form of ATP through the oxidative phosphorylation system [16]. Mitochondria continuously undergo fission and fusion, which are necessary processes for cell survival, adaptation to changing environment and maintaining mitochondrial integrity and quality control [17]. Mitochondrial fission is regulated by dynamin-related protein 1 (DRP-1), the central player for mitochondria fragmentation [18, 19]. DRP-1 is a dynamin GTPase superfamily protein mostly found in the cytosol, and therefore the second class of mitochondrial surface proteins is needed to efficiently recruit DRP-1 for fission [20, 21]. Such a process is required to create new mitochondria, to maintain the mitochondrial network and to segregate damaged mitochondria in the cell environment [16, 20, 22].

Mitochondrial fusion on the other hand, is regulated by mitofusin-2 (MFN-2) located in the outer mitochondrial membrane [23, 24]. MFN-2 is also a GTPase superfamily protein and it plays a vital role in mitochondrial energy metabolism [25]. Moreover, mitochondrial fusion allows these organelles to have an appropriate shape, function, and distribution within the cell [23]. In addition, mitochondrial fusion plays an important role in mitochondria trafficking [26]. Of note, MFN-2 plays a crucial role in several cell pathways [24, 27–29] as well as in the pathogenesis of neurodegenerative diseases and metabolic disorders [30]. Unfortunately, there is a lack of research on the effect of type 1 diabetes in mitochondrial dynamics. However, a common feature of mitochondrial morphology in type 2 diabetes is an increased mitochondrial fragmentation (fission) through activation/upregulation of DRP1 and/or downregulation of MFN2 levels [31].

Persistent hyperglycemia has a major role in the development of long-term pathology of diabetic peripheral neuropathy and peripheral nerve fibers are especially dependent on efficient mitochondrial dynamics to fulfill their energy needs due to their unique morphology [23, 32]. Excess glucose plays a significant role in mitochondrial dysfunction by

modifying their shape and size, increasing reactive oxygen species production, suppressing complex II dependent respiration and depressing mitochondrial bioenergetic reserve capacity [33, 34]. Due to their role in metabolism regulation, mitochondrial dysfunction in axons, Schwann cells, and DRG neurons has been proposed as a unifying mechanism for the development of diabetic peripheral neuropathy [33].

Surprisingly there is no effective available treatments to prevent mitochondrial dysfunction in diabetic neuropathy [35]. Strict glycemic control ameliorates, but does not prevent or reverse, diabetic neuropathy in type 1 diabetic patients and it is relatively ineffective in preventing the development of diabetic neuropathy in type 2 diabetes [36, 37]. In this study, we focused on the possible beneficial effects of photobiomodulation (PBM) on mitochondrial dynamics. PBM previously known as low-level laser (light) therapy (LLLT) involves the use of low-powered red and near-infrared (NIR) light from a laser or light-emitting diode (LED) to stimulate, heal, and regenerate damaged or dying tissues [38]. There is a substantial amount of data on the usage of PBM in preventing and reversing pain/inflammation, its use in neurodegenerative diseases, wound healing, and in musculoskeletal disorders [39–43].

Moreover, all the beneficial effects of PBM are regarded as a result from the direct interaction between light and mitochondria [44–46]. PBM involves absorption of the light through the mitochondria, leading to an increase in membrane potential, electron transport, oxygen consumption, and ATP synthesis [47]. Since the nervous system is heavily dependent on mitochondrial activity, it is not surprising that PBM has been extensively tested to treat various nervous system disorders [48]. Previous studies from our group have shown favorable results in using photobiomodulation as a tool to treat trigeminal neuralgia, chronic pain and diabetic peripheral neuropathy [49–51].

Interestingly, Wang et al. [52], showed that PBM dramatically reduced mitochondrial fragmentation in the global cerebral ischemic brain. PBM regulatory effect on mitochondrial fragmentation in the brain was associated with and likely due in part to (1) reduced Drp1 GTPase fission protein activity (2) increased mitochondrial location of fusion proteins (mitofusins), and (3) decreased mitochondrial targeting of fission proteins (Mff and Fis1) in neurons [52]. Moreover, Jose Carlos Tatmatsu-Rocha et al., [53] showed that PBM increased MFN2 scores in wounded streptozotocin-induced diabetic rats. Jose Carlos Tatmatsu-Rocha et al. proposes that the possible mechanism of action of PBM on the wound healing process is the regulation of the balance between mitochondrial fusion and fission [53].

The primary goal of our study was to show the effects of PBM on mitochondrial dynamics in diabetic peripheral neuropathy in streptozotocin-induced type 1 diabetes in rats. Mitofusin-2 (MFN-2) and dynamin-related protein 1

(DRP-1) were quantified in the rat sciatic nerve (SN) and in the dorsal root ganglia neurons (DRG) by western blot assay.

## 2 Materials and methods

### 2.1 Animals

A total of fifteen adult male Wistar rats, 8 weeks of age (200–220 g), were purchased from the Central Animal House at Biomedical Sciences Institute and kept in the local vivarium in the Department of Anatomy. Animals were socially housed in standard cages (3 rats per cage) in a 12-h light/12-h dark and temperature (23–25 °C) controlled condition, with the food and water ad libitum. After 3 days of acclimatization, rats were randomized into the Control (CTRL,  $n=5$ ), diabetic (STZ,  $n=5$ ) and diabetic treated with photobiomodulation groups (STZ + PBM,  $n=5$ ). It was used naive animals as a control group. Initially, before the division of groups and STZ (86 mg/kg) i.p injection, we had a total of 20 rats. Five rats were control (naive) and 15 rats were injected with STZ. After STZ ip injection, five rats died along the experimental timeline (60 days). At the end of the study, we had 5 rats per group.

### 2.2 Streptozotocin-induced type 1 diabetes mellitus

We injected a single dose of STZ (85 mg/Kg + 500  $\mu$ L Saline 0.9%) intraperitoneally (i.p) at time "0" and then we waited for 24 h to confirm hyperglycemia. After confirming that the rats were diabetic, we waited for 60 days to start PBM treatment. Rats were maintained in hyperglycemic conditions for 60 days because we have previously shown (transmission electron microscopy) that after 60 days in hyperglycemic condition rats had developed the most severe peripheral nerve damage [51]. After 60 days in hyperglycemic condition, we started PBM session that was performed every other day totaling 10 sessions. We show in Fig. 1 a 60 days of blood glucose evaluation to show blood glucose alteration in diabetic animals and unaltered blood glucose levels in normal rats.

### 2.3 Photobiomodulation protocol

PBM treatment was performed every other day, totaling 10 sessions. Treatment started on the sixtieth day after the induction of type 1 diabetes mellitus. After sterilization, the laser probe was placed on the skin surface on the right thigh directly above the course of the rat sciatic nerve. Animals were irradiated with gallium arsenide laser (Laserpulse—Ibramed Brazil) emitting a wavelength of 904 nm, an output power of 45mW, irradiance of 0.34 mW/cm<sup>2</sup>, a spot area of

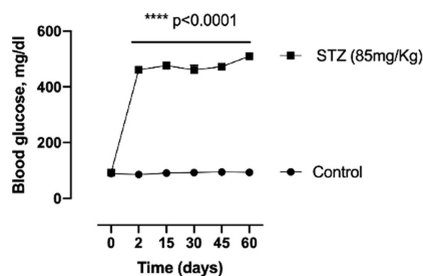


**Fig. 1** Effect of streptozotocin on rat blood glucose. At day "0" all rats had their initial ad libitum body weight and blood glucose assessed. According to their body weight 10 rats were injected one single dose of streptozotocin (85 mg/kg) intraperitoneally. 5 rats were kept as control (naive). 48 h after STZ injection (day 2) rats were confirmed hyperglycemic. Blood glucose levels were higher than 300 mg/dl in STZ group compared to Control (\*\*\*\* $p<0.0001$ ). The graph shows the effectiveness of a single intraperitoneal dose of streptozotocin on maintaining high blood glucose levels throughout the experiment time of 60 days

0.13cm<sup>2</sup>, a frequency of 9500 Hz, a pulse time of 60 ns, and an energy density of 6.23 J/cm<sup>2</sup> according to Rocha et al. [51] (Table 1). Each session included the stimulation of nine points along the sciatic nerve, each point lasting 18 s with 7.29 J of energy. All ten sessions had a total of 72.9 J.

### 2.4 Western blot assay

Western blot analyses were performed on samples from individual animals euthanized at the end of the last (10th) PBM session. Control (naive), diabetic (STZ) and diabetic rats treated with PBM (STZ + PBM) were euthanized by decapitation. The rats were previously placed in a plexiglass chamber with 5% isoflurane (Cristalia, Sao Paulo, Brazil) for 5 min and decapitated when fully sedated. Immediately after decapitation, SN and DRG were quickly removed and transferred to a tube containing 100  $\mu$ L extraction buffer (100 mM of Tris, pH 7.4, 1% SDS, 10 mM of EDTA, 2 mM of PMSF, and 10  $\mu$ g/mL of aprotinin) in ice-cold (4° C). Tissues (sciatic nerve and dorsal root ganglia) were separately homogenized using an ultrasonic processor (Sonics & Materials, Newtown, PA). The homogenates were then centrifuged at 12,000 rpm at 4 °C for 20 min, and the protein concentration of the supernatant was determined using the Bradford protein assay with albumin as a standard (Bio-Rad, USA) [54]. Samples containing 20  $\mu$ g of protein were loaded on acrylamide gradient gel [55] and transferred by electrophoresis to nitrocellulose membranes using a Bio-Rad miniature transfer apparatus for 1.5 h at 120 V. After transfer, the membranes were treated for 2 h at room temperature with a blocking solution containing 5% powdered milk, washed and

**Table 1** Photobiomodulation parameters

Protocol for the use of photobiomodulation	
Irradiation parameters	Treatment parameters
Emitter type: Gallium-Arsenide (GaAs)	Beam spot size at target (cm <sup>2</sup> ): 0.13 cm <sup>2</sup>
Wavelength (nm): 904 nm	Exposure duration (seconds): 18 s/point
Operating mode: Pulsed	Radiant exposure (J/cm <sup>2</sup> ): 6.23 J/cm <sup>2</sup>
Frequency (Hz): 9500 Hz	Radiant energy (J): 0.81 J/point
Pulse on duration (nanoseconds): 60 ns	Irradiated area (cm <sup>2</sup> ): 1.17 cm <sup>2</sup>
Beam shape: Circular	Total radiant energy (J): 7.29 J/session

**Table 2** Primary antibodies used in western blot assay

Antibody	Molecular weight	Host species	Dilution	RRID
Mitofusin-2	80 KDa	Rabbit	1:500	AB_2800025
DRP-1	80 KDa	Rabbit	1:500	AB_10950498
GAPDH	37 KDa	Rabbit	1:5000	AB_307275

incubated overnight at 4 °C with primary antibodies (Table 2). The membranes were then washed and incubated for 2 h at room temperature with a peroxidase-conjugated anti-rabbit secondary antibody diluted in 1:5000 (ZIMED Laboratories Inc). In every immunoblotting experiment GAPDH (anti-GAPDH antibody 1:5000; Abcam) was used as an internal control. Antibody bounding was visualized using a chemiluminescence kit (Clarity Max Western ECL Substrate, BIO-RAD Laboratories; Italy). The bands were corrected by the optical density of GAPDH (1:5000, Abcam) considering samples from control animals as the standard for normalization. For quantification, densitometry was performed using the NIH-Scion Image 4.0.2, quantified by optical densitometry of the developed autoradiographs (Scion Corporation, USA).

### 2.5 Statistical analysis

Results are presented as the mean  $\pm$  standard error of the mean (SEM). Statistical analyses of data were generated using GraphPad Prism, version 8.4 (Graph Pad Software Inc., San Diego, CA, USA). Statistical comparison of more than two groups was performed using analysis of variance (ANOVA), followed by Tukey's multiple comparisons test. Significance was defined as  $p < 0.05$ .

## 3 Results

### 3.1 Effect of streptozotocin on rat blood glucose level

The damage to insulin-producing B-cells in the pancreas caused by the toxic effects of STZ was verified through the

measurements of blood glucose levels. Forty-eight hours after a single intraperitoneal injection of STZ (85 mg/Kg) the blood samples of STZ group presented high levels of glucose in relation to the Control group ( $p < 0.0001$ ) (Fig. 1). Throughout the time course of the experiment blood glucose levels average in Control rats was 90 mg/dl while in STZ rats the average was 480 mg/dl. No additional injections of STZ were needed to complete the study.

### 3.2 Effect of photobiomodulation on mitochondrial fission in the rat sciatic nerve

There was a decrease in the protein expression of DRP-1 in the rat sciatic nerve in STZ group ( $p < 0.0001$ ) when compared to Control (Fig. 2). It may indicate a reduction in mitochondrial fission in peripheral nerve fibers of diabetic rats in response to an increase in the fission activity in the DRG neurons. Furthermore, diabetic rats treated with PBM (STZ + PBM) had also a decrease in the protein expression of DRP-1 ( $p < 0.0001$ ) in their sciatic nerve when compared to STZ group (Fig. 2).

### 3.3 Effect of photobiomodulation on mitochondrial fusion in the rat sciatic nerve

Concerning mitochondrial fusion, there were no statistical difference between STZ and Control group regarding the protein expression of MFN-2 in the rat peripheral nerve fibers (Fig. 3). It may suggest an imbalance between mitochondrial fusion and fission activity in the diabetic peripheral nerve fibers in response to hyperglycemia. Moreover, STZ + PBM group had an increase ( $p < 0.001$ ) in the levels of protein expression of MFN-2 in their peripheral nerve fibers when compared to STZ and to the Control group (Fig. 3). Such data may suggest that PBM could have a potential role in preventing or reversing a probable fusion/fission imbalance in the diabetic peripheral nerve fibers.

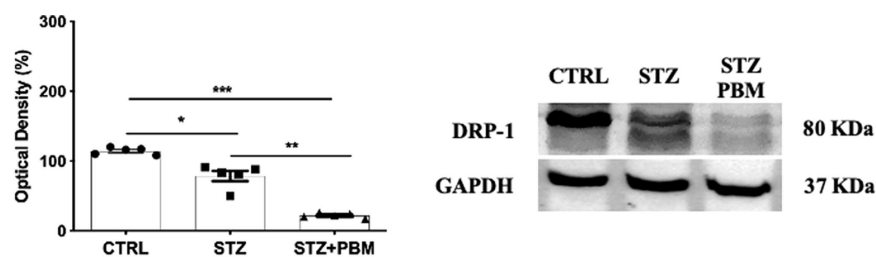


**Fig. 2** Effect of photobiomodulation on mitochondrial fission in the rat sciatic nerve. Western blot protein analysis of dynamin-related protein 1 (DRP-1) in the rat sciatic nerve. \* $p < 0.0001$  in comparison between STZ and Control animals. \*\* $p < 0.0001$  in comparison between STZ+PBM and STZ. \*\*\* $p < 0.0001$  in comparison between STZ+PBM and Control. 5 rats per group

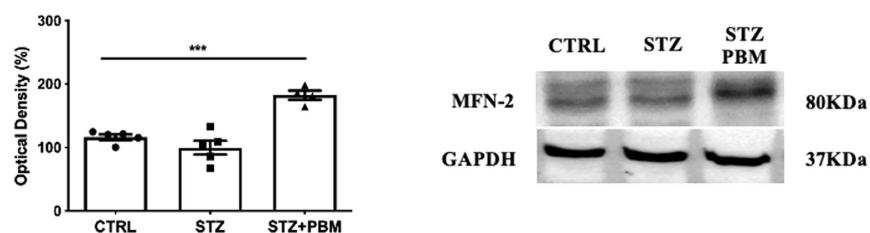


**Fig. 3** Effect of photobiomodulation on mitochondrial fusion in the rat sciatic nerve. Western blot protein analysis of mitofusin-2 (MFN-2) in the rat sciatic nerve. \*\*\* $p < 0.0001$  in comparison between STZ+PBM and STZ. Statistical difference was also observed

between STZ and Control animals. \*\* $p < 0.0001$  in comparison between STZ+PBM and STZ. \*\*\* $p < 0.0001$  in comparison between STZ+PBM and Control. 5 rats per group

between STZ+PBM and Control ( $p < 0.0001$ ). No statistical difference was observed between diabetic (STZ) and Control (CTRL) rats. 5 rats per group

### 3.4 Effect of photobiomodulation on mitochondrial fission in the rat dorsal root ganglia

Results revealed an increase in the protein expression levels of DRP-1 in the DRG neurons in STZ group ( $p < 0.003$ ) when compared to Control (Fig. 4). This data may corroborate the result observed in the sciatic nerve where it was shown a decrease in DRP-1 levels in STZ group. It may probably occur higher mitochondrial fission activity in the DRG neurons of diabetic rats when compared to peripheral fibers. Furthermore, PBM decreased the protein levels of DRP-1 in STZ+PBM group ( $p < 0.0001$ ) when compared to STZ. In addition, there was also a decrease between STZ+PBM and Control  $p < 0.0023$  (Fig. 4) regarding DRP-1 protein expression levels.

### 3.5 Effect of photobiomodulation on mitochondrial fusion in the rat dorsal root ganglia

In contrast to DRP-1, STZ group showed a decrease in the protein expression levels MFN-2 in the DRG neurons when compared to Control  $p < 0.0001$  (Fig. 5). Such difference in the protein expression levels of MFN-2 and DRP-1 in the DRG neurons may suggest altered mitochondrial fusion and fission activity in a hyperglycemic environment. Moreover, STZ+PBM group had an increase in the protein levels of MFN-2 in the DRG neurons ( $p < 0.0001$ ) when compared to STZ. It was also observed an increase in MFN-2 protein expression levels in the DRG neurons between STZ+PBM and Control group ( $p < 0.0001$ ) (Fig. 5).



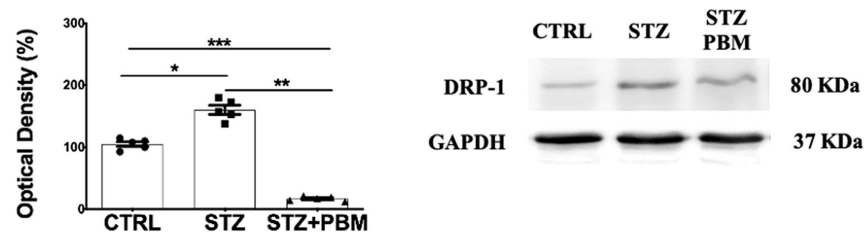


**Fig. 4** Effect of photobiomodulation on mitochondrial fission in the rat dorsal root ganglia. Western blot protein analysis of dynamin-related protein 1 (DRP-1) in the rat dorsal root ganglia. \* $p < 0.003$  in

comparison between STZ and Control (CTRL) animals. \*\* $p < 0.0001$  in comparison between STZ+PBM and STZ. \*\*\* $p < 0.0001$  in comparison between STZ+PBM and Control (CTRL). 5 rats per group

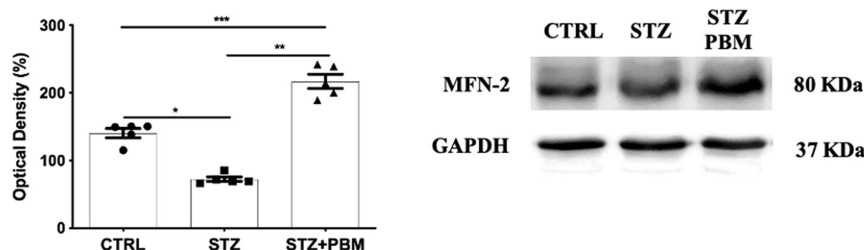


**Fig. 5** Effect of photobiomodulation on mitochondrial fusion in the rat dorsal root ganglia. Western blot protein analysis of mitofusin 2 (MFN-2) in the rat dorsal root ganglia. \* $p < 0.0001$  in comparison

between STZ and Control (CTRL) animals. \*\* $p < 0.0001$  in comparison between STZ+PBM and STZ. \*\*\* $p < 0.0001$  in comparison between STZ+PBM and Control. 5 rats per group

#### 4 Discussion

In this study, we evaluated the effect of PBM on mitochondrial dynamics *in vivo*. MFN-2 and DRP-1 protein expression levels were quantified in the peripheral nerve fibers and in the DRG neurons of diabetic rats through western blot assay. Diabetic peripheral neuropathy was developed by STZ-induced type 1 diabetes mellitus. PBM modulates the expression of those proteins involved in mitochondrial dynamics (MFN-2, DRP-1) in the SN and in the DRG neurons of diabetic rats treated with PBM. In addition, results presented herein demonstrated that one single dose of STZ (85 mg/kg) via intraperitoneal effectively induced the development of diabetic peripheral neuropathy in rats.

STZ is a naturally occurring diabetogenic compound that has been widely used to induce diabetes due to its particular toxicity to the insulin-producing  $\beta$ -cells of the pancreas [56, 57]. Of note, chronic hyperglycemia as a result of  $\beta$ -cells destruction induces the development of diabetic complications [58]. STZ toxic effects per se

does not induce the development of diabetic neuropathy [59, 60]. In this study, rats had their blood glucose levels increased (hyperglycemia) 24 h after STZ (i.p) injection. Rats that were STZ injected had a significant decrease in body weight and also developed all the characteristics signs of diabetic complications as polyuria, polydipsia, polyphagia, and cataracts (data not shown here). Control animals had no significant changes in their blood glucose levels, body weight or developed any of the signs throughout the whole experiment.

Rats were maintained in hyperglycemia condition for 60 days with free access to food and water and they had their cages cleaned daily due to excess urine. PBM treatment in diabetic rats started at the sixtieth (60) day after induction of diabetes. A total of ten (10) PBM sessions were applied every other day in the diabetic rat right hind paw and on the next day after the last PBM session all groups of rats (Control, STZ, STZ+PBM) were euthanized and had their SN and DRG collected for protein expression analysis of MFN-2 (fusion) and DRP-1 (fission) by western blot.



Interestingly, the data presented here showed that DRP-1 involved in mitochondrial fission had a decrease in the sciatic nerve of STZ rats but a significant increase in its protein level in the DRG neurons of STZ rats compared to Control group. Our results corroborate the findings in the literature that indicate hyperglycemia as a primary cause of DRG neuron injury in diabetic neuropathy [61]. In addition, mitochondrial fission is a prominent response during hyperglycemia and excessive mitochondrial fission may result in dysregulation of energy production and subsequent DRG neuron injury [62]. Moreover, hyperglycemia stimulates an increase of the Drp1/Bax complexes, which mediate apoptotic mitochondrial fragmentation in diabetic polyneuropathy [35]. Furthermore, PBM had a significant role in decreasing the protein expression of DRP-1 in both tissue (sciatic nerve, DRG) in diabetic rats treated with photobiomodulation (STZ + PBM). Thus, revealing that PBM may have a protective role against hyperglycemia in the peripheral nervous system.

No statistical difference was observed between STZ and Control rats regarding the protein expression of MFN-2 in the rat sciatic nerve. While DRG neurons of STZ group showed a decrease in the protein levels of MFN-2 in the DRG neurons in STZ rats when compared to control animals. This result notably indicates hyperglycemia as a detrimental factor that impairs mitochondrial biogenesis and exacerbates the imbalance between mitochondrial fusion and fission [63]. Additionally, PBM was able to increase the protein expression levels of MFN-2 in the DRG neurons and in the SN of diabetic rats treated with photobiomodulation (STZ + PBM) when compared to diabetic rats (STZ). The increase of MFN-2 protein levels in the DRG neurons of STZ + PBM treated group was also statistically different from the Control group. Such a result may suggest that PBM might overexpress the levels of MFN-2 in the DRG to protect DRG neurons from injury during hyperglycemia.

The beneficial effects of photobiomodulation on a variety of diseases has been proved to be as a result of the direct interaction between light and mitochondria [48, 53, 64–66]. Unfortunately, little is known about the effects of phototherapy in altering mitochondrial dynamics. Yujiao Lu et al. [67] showed that low-level laser irradiation remarkably suppressed the protein levels of fission proteins (DRP-1, Fis-1, Mff, and Mief) in the rat hippocampus of Alzheimer's Disease. Tatmatsu-Rocha [53], demonstrated higher expression of mitofusin-2 (MFN-2) in rat diabetic wounds treated with photobiomodulation. Moreover, there is a lack of studies that investigate mitochondrial dynamics in type 1 diabetes. Hopefully, we can start changing this scenario.

## 5 Conclusion

In conclusion, our data demonstrate that photobiomodulation exhibits an effective and reliable role in mitochondrial dynamics through the modulation of mitofusin-2 and dynamin-related protein 1 in an animal model of diabetic peripheral neuropathy. According to our results, photobiomodulation may protect dorsal root ganglia neurons and peripheral nerve fibers from the deleterious effects of chronic hyperglycemia. Photobiomodulation may have the ability to restore the balance between mitochondrial fusion and fission in the DRG neurons in a toxic environment (hyperglycemia). Further studies are necessary to elucidate the beneficial effects of photobiomodulation on the peripheral nervous system, especially with regard to diabetic peripheral neuropathy and mitochondrial dynamics.

**Acknowledgements** Funding for this work was generously provided by Sao Paulo Research Foundation—FAPESP (grant number 2017/25,554-0; 2017/05,218-5).

## Compliance with ethical standards

**Conflict of interest** The authors declare that they have no conflict of interest.

**Ethical approval** All procedures of the study were conducted in accordance with the ethical guidelines set by Institutional Animal Care Committee of the University of Sao Paulo. Protocol number 123/2015. The funding agency plays no role in the design of the study, data collection, analysis, interpretation of the data, or in writing the manuscript.

## References

- Juster-Switlyk, K., & Smith, A. G. (2016). *Updates in diabetic peripheral neuropathy*. *F1000Res*, 5.
- Kharroubi, A. T., & Darwish, H. M. (2015). Diabetes mellitus: the epidemic of the century. *World Journal of Diabetes*, 6(6), 850–867.
- Cho, N. H., et al. (2018). IDF Diabetes Atlas: global estimates of diabetes prevalence for 2017 and projections for 2045. *Diabetes Research and Clinical Practice*, 138, 271–281.
- Zaccardi, F., et al. (2016). Pathophysiology of type 1 and type 2 diabetes mellitus: a 90-year perspective. *Postgraduate Medical Journal*, 92(1084), 63–69.
- Ostenson, C. G. (2001). The pathophysiology of type 2 diabetes mellitus: an overview. *Acta Physiologica Scandinavica*, 171(3), 241–247.
- Forbes, J. M., & Cooper, M. E. (2013). Mechanisms of diabetic complications. *Physiological Reviews*, 93(1), 137–188.
- Selvarajah, D., et al. (2011). Central nervous system involvement in diabetic neuropathy. *Current Diabetes Reports*, 11(4), 310–322.
- Yagihashi, S., Mizukami, H., & Sugimoto, K. (2011). Mechanism of diabetic neuropathy: where are we now and where to go? *Journal of Diabetes Investigation*, 2(1), 18–32.

9. Schreiber, A. K., et al. (2015). Diabetic neuropathic pain: pathophysiology and treatment. *World Journal of Diabetes*, 6(3), 432–444.
10. Tesfaye, S., Boulton, A. J., & Dickenson, A. H. (2013). Mechanisms and management of diabetic painful distal symmetrical polyneuropathy. *Diabetes Care*, 36(9), 2456–2465.
11. Iqbal, Z., et al. (2018). Diabetic peripheral neuropathy: epidemiology, diagnosis, and pharmacotherapy. *Clinical Therapeutics*, 40(6), 828–849.
12. Callaghan, B. C., et al. (2012). Diabetic neuropathy: clinical manifestations and current treatments. *The Lancet. Neurology*, 11(6), 521–534.
13. Brownlee, M. (2005). The pathobiology of diabetic complications: a unifying mechanism. *Diabetes*, 54(6), 1615–1625.
14. Fernyhough, P., Huang, T. J., & Verkhatsky, A. (2003). Mechanism of mitochondrial dysfunction in diabetic sensory neuropathy. *Journal of the Peripheral Nervous System*, 8(4), 227–235.
15. Fernyhough, P., Roy Chowdhury, S. K., & Schmidt, R. E. (2010). Mitochondrial stress and the pathogenesis of diabetic neuropathy. *Expert Review of Endocrinology & Metabolism*, 5(1), 39–49.
16. Suarez-Rivero, J. M., et al. (2017). Mitochondrial dynamics in mitochondrial diseases. *Diseases*, 5(1), 1. <https://doi.org/10.3390/diseases5010001>
17. Amchenkova, A. A., et al. (1988). Coupling membranes as energy-transmitting cables. I. Filamentous mitochondria in fibroblasts and mitochondrial clusters in cardiomyocytes. *Journal of Cell Biology*, 107(2), 481–495.
18. Frank, S., et al. (2001). The role of dynamin-related protein 1, a mediator of mitochondrial fission, in apoptosis. *Developmental Cell*, 1(4), 515–525.
19. Vantaggiato, C., et al. (2019). The fine tuning of Drp1-dependent mitochondrial remodeling and autophagy controls neuronal differentiation. *Frontier Cell Neuroscience*, 13, 120.
20. Fonseca, T. B., et al. (2019). Mitochondrial fission requires DRP1 but not dynamin. *Nature*, 570(7761), E34–E42.
21. Chan, D. C. (2012). Fusion and fission: interlinked processes critical for mitochondrial health. *Annual Review of Genetics*, 46, 265–287.
22. Ni, H. M., Williams, J. A., & Ding, W. X. (2015). Mitochondrial dynamics and mitochondrial quality control. *Redox Biology*, 4, 6–13.
23. Filadi, R., Pendin, D., & Pizzo, P. (2018). Mitofusin 2: from functions to disease. *Cell Death & Disease*, 9(3), 330.
24. Chen, K. H., et al. (2014). Role of mitofusin 2 (Mfn2) in controlling cellular proliferation. *The FASEB Journal*, 28(1), 382–394.
25. Mourier, A., et al. (2015). Mitofusin 2 is required to maintain mitochondrial coenzyme Q levels. *Journal of Cell Biology*, 208(4), 429–442.
26. Chen, H., & Chan, D. C. (2009). Mitochondrial dynamics—fusion, fission, movement, and mitophagy—in neurodegenerative diseases. *Human Molecular Genetics*, 18(R2), R169–R176.
27. Xue, R., et al. (2018). Mitofusin2 induces cell autophagy of pancreatic cancer through inhibiting the PI3K/Akt/mTOR signaling pathway. *Oxidative Medicine and Cellular Longevity*, 2018, 2798070.
28. Peng, C., et al. (2015). Mitofusin 2 ameliorates hypoxia-induced apoptosis via mitochondrial function and signaling pathways. *International Journal of Biochemistry & Cell Biology*, 69, 29–40.
29. Pawlikowska, P., Gajkowska, B., & Orzechowski, A. (2007). Mitofusin 2 (Mfn2): A key player in insulin-dependent myogenesis in vitro. *Cell and Tissue Research*, 327(3), 571–581.
30. Cerveny, K. L., et al. (2007). Regulation of mitochondrial fusion and division. *Trends in Cell Biology*, 17(11), 563–569.
31. Woo, D. H., et al. (2018). Activation of astrocytic  $\mu$ -opioid receptor elicits fast glutamate release through TREK-1-containing K2P channel in hippocampal astrocytes. *Frontiers in Cellular Neuroscience*, 12, 319.
32. Pareyson, D., et al. (2013). Peripheral neuropathy in mitochondrial disorders. *Lancet Neurology*, 12(10), 1011–1024.
33. Chandrasekaran, K., et al. (2019). Role of mitochondria in diabetic peripheral neuropathy: Influencing the NAD(+)-dependent SIRT1-PGC-1 $\alpha$ -TFAM pathway. *International Review of Neurobiology*, 145, 177–209.
34. Dassanayaka, S., et al. (2015). High glucose induces mitochondrial dysfunction independently of protein O-GlcNAcylation. *The Biochemical Journal*, 467(1), 115–126.
35. Sifuentes-Franco, S., et al. (2017). The role of oxidative stress, mitochondrial function, and autophagy in diabetic polyneuropathy. *Journal of Diabetes Research*, 2017, 1673081.
36. Russell, J. W., & Zilliox, L. A. (2014). Diabetic neuropathies. *Continuum (Minneapolis, Minn)*, 20(5 Peripheral Nervous System Disorders), 1226–1240.
37. Callaghan, B. C., et al. (2012). Enhanced glucose control for preventing and treating diabetic neuropathy. *Cochrane Database Systematic Review*, 6, CD007543.
38. Salehpour, F., & Hamblin, M. R. (2020). Photobiomodulation for Parkinson's disease in animal models: A systematic review. *Biomolecules*, 10(4), 610.
39. Kingsley, J. D., Demchak, T., & Mathis, R. (2014). Low-level laser therapy as a treatment for chronic pain. *Frontiers in Physiology*, 5, 306.
40. Alves, A. C., et al. (2013). Effect of low-level laser therapy on the expression of inflammatory mediators and on neutrophils and macrophages in acute joint inflammation. *Arthritis Research & Therapy*, 15(5), R116.
41. Song, S., Zhou, F., & Chen, W. R. (2012). Low-level laser therapy regulates microglial function through Src-mediated signaling pathways: implications for neurodegenerative diseases. *Journal of Neuroinflammation*, 9, 219.
42. Kajagar, B. M., et al. (2012). Efficacy of low level laser therapy on wound healing in patients with chronic diabetic foot ulcers—a randomised control trial. *Indian Journal of Surgery*, 74(5), 359–363.
43. Song, H. J., et al. (2018). Effectiveness of high-intensity laser therapy in the treatment of musculoskeletal disorders: a systematic review and meta-analysis of randomized controlled trials. *Medicine (Baltimore)*, 97(51), e13126.
44. Salehpour, F., et al. (2017). Transcranial low-level laser therapy improves brain mitochondrial function and cognitive impairment in D-galactose-induced aging mice. *Neurobiology of Aging*, 58, 140–150.
45. de Freitas, L. F., & Hamblin, M. R. (2016). Proposed mechanisms of photobiomodulation or low-level light therapy. *IEEE Journal of Selected Topics in Quantum Electronics*, 22(3), 7000417. <https://doi.org/10.1109/JSTQE.2016.2561201>
46. Souza, N. H., et al. (2014). Effect of low-level laser therapy on the modulation of the mitochondrial activity of macrophages. *Brazilian Journal of Physical Therapy*, 18(4), 308–314.
47. Chung, H., et al. (2012). The nuts and bolts of low-level laser (light) therapy. *Annals of Biomedical Engineering*, 40(2), 516–533.
48. Hamblin, M. R. (2016). Shining light on the head: photobiomodulation for brain disorders. *BBA Clinical*, 6, 113–124.
49. Martins, D. O., et al. (2017). Neuropeptide expression and morphometric differences in crushed alveolar inferior nerve of rats: effects of photobiomodulation. *Lasers in Medical Science*, 32(4), 833–840.
50. Oliveira, M. E., et al. (2017). Low level laser therapy alters satellite glial cell expression and reverses nociceptive behavior in rats with neuropathic pain. *Photochemical & Photobiological Sciences*, 16(4), 547–554.

51. Rocha, I. R., et al. (2017). Photobiostimulation reverses allodynia and peripheral nerve damage in streptozotocin-induced type 1 diabetes. *Lasers in Medical Science*, 32(3), 495–501.
52. Wang, R., et al. (2019). Photobiomodulation for global cerebral ischemia: targeting mitochondrial dynamics and functions. *Molecular Neurobiology*, 56(3), 1852–1869.
53. Tatmatsu-Rocha, J. C., et al. (2018). Mitochondrial dynamics (fission and fusion) and collagen production in a rat model of diabetic wound healing treated by photobiomodulation: Comparison of 904 nm laser and 850nm light-emitting diode (LED). *Journal of Photochemistry and Photobiology B: Biology*, 187, 41–47.
54. Bradford, M. M. (1976). A rapid and sensitive method for the quantitation of microgram quantities of protein utilizing the principle of protein-dye binding. *Analytical Biochemistry*, 72, 248–254.
55. Miller, A. J., Roman, B., & Norstrom, E. M. (2016). Protein electrophoretic migration data from custom and commercial gradient gels. *Data Brief*, 9, 1–3.
56. Wu, J., & Yan, L. J. (2015). Streptozotocin-induced type 1 diabetes in rodents as a model for studying mitochondrial mechanisms of diabetic beta cell glucotoxicity. *Diabetes, Metabolic Syndrome and Obesity: Targets and Therapy*, 8, 181–188.
57. Eleazu, C. O., et al. (2013). Review of the mechanism of cell death resulting from streptozotocin challenge in experimental animals, its practical use and potential risk to humans. *Journal of Diabetes Metabolic Disorders*, 12(1), 60.
58. American Diabetes, A. (2009). Diagnosis and classification of diabetes mellitus. *Diabetes Care*, 32(Suppl 1), S62–S67.
59. Davidson, E., et al. (2009). The roles of streptozotocin neurotoxicity and neutral endopeptidase in murine experimental diabetic neuropathy. *Experimental Diabetes Research*, 2009, 431980.
60. Campos, C. (2012). Chronic hyperglycemia and glucose toxicity: pathology and clinical sequelae. *Postgraduate Medicine*, 124(6), 90–97.
61. Schmeichel, A. M., Schmelzer, J. D., & Low, P. A. (2003). Oxidative injury and apoptosis of dorsal root ganglion neurons in chronic experimental diabetic neuropathy. *Diabetes*, 52(1), 165–171.
62. Vincent, A. M., et al. (2010). Mitochondrial biogenesis and fission in axons in cell culture and animal models of diabetic neuropathy. *Acta Neuropathologica*, 120(4), 477–489.
63. Kumari, S., et al. (2012). Hyperglycemia alters mitochondrial fission and fusion proteins in mice subjected to cerebral ischemia and reperfusion. *Translational Stroke Research*, 3(2), 296–304.
64. Farivar, S., Malekshahabi, T., & Shiari, R. (2014). Biological effects of low level laser therapy. *Journal of Lasers in Medical Sciences*, 5(2), 58–62.
65. de la Torre, J. C. (2017). Treating cognitive impairment with transcranial low level laser therapy. *Journal of Photochemistry and Photobiology B: Biology*, 168, 149–155.
66. Hamblin, M. R. (2017). Mechanisms and applications of the anti-inflammatory effects of photobiomodulation. *AIMS Biophysics*, 4(3), 337–361.
67. Lu, Y., et al. (2017). Low-level laser therapy for beta amyloid toxicity in rat hippocampus. *Neurobiology of Aging*, 49, 165–182.



## Modulatory effects of photobiomodulation in the anterior cingulate cortex of diabetic rats

Igor Rafael Correia Rocha<sup>1</sup> · Marucia Chacur<sup>1</sup>

Received: 12 March 2021 / Accepted: 25 May 2021 / Published online: 30 May 2021  
 © The Author(s), under exclusive licence to European Photochemistry Association, European Society for Photobiology 2021

### Abstract

Anterior Cingulate Cortex (ACC) has a crucial contribution to higher order pain processing. Photobiomodulation (PBM) has been used as integrative medicine for pain treatment and for a variety of nervous system disorders. This study evaluated the effects of PBM in the ACC of diabetic rats. Type 1 diabetes was induced by a single dose of streptozotocin (85 mg/Kg). A total of ten sessions of PBM (pulsed gallium-arsenide laser, 904 nm, 9500 Hz, 6.23 J/cm<sup>2</sup>) was applied to the rat peripheral nervous system. Glial fibrillary acidic protein (GFAP), mu-opioid receptor (MOR), glutamate receptor 1 (GluR1), and glutamic acid decarboxylase (GAD65/67) protein level expression were analyzed in the ACC of diabetic rats treated with PBM. Our data revealed that PBM decreased 79.5% of GFAP protein levels in the ACC of STZ rats. Moreover, STZ + PBM rats had protein levels of MOR increased 14.7% in the ACC. Interestingly, STZ + PBM rats had a decrease in 70.7% of GluR1 protein level in the ACC. Additionally, PBM decreased 45.5% of GAD65/67 protein levels in the ACC of STZ rats.

**Keywords** Diabetes · Hyperglycemia · Neuropathy · Phototherapy · Streptozotocin · Western blot

### Abbreviations

ACC Anterior cingulate cortex  
 i.p Intraperitoneal  
 PBM Photobiomodulation  
 STZ Streptozotocin

### 1 Introduction

The anterior cingulate cortex (ACC) plays relevant role in pain perception [1], and despite its involvement in chronic pain development following peripheral nerve injury [2], however, the contribution of ACC to the experience of chronic pain in diabetic peripheral neuropathy (DPN) remains unclear. The ACC along with thalamus, insular cortex, prefrontal cortex, and somatosensory cortex is one of the main components of the pain matrix [3, 4]. Pain-related studies with animals have shown that ACC mediates

responses to inflammatory pain, neuropathic pain, spontaneous pain in the formalin test, and formalin-induced conditioned place avoidance [5–8].

According to the International Diabetes Federation (IDF), there are approximately 463 million adults (20–79 years) living with diabetes worldwide, and by 2045, this will rise to 700 million (IDF ATLAS). This increase in the number of people with diabetes will be accompanied by an increase in the prevalence of diabetes complications [9]. Half of people living with diabetes develop DPN [10, 11], one of the leading causes of neuropathy worldwide [12]. DPN is characterized by the progressive loss of peripheral nerve fibers [13], and painful neuropathy is the main clinical consequences of this complex syndrome related to diabetes [14, 15]. Additionally, there is no effective treatment that prevents peripheral nerve fiber degeneration in DPN [16], except tight glycaemic control [17].

Painful DPN is characterized by tingling, burning, sharp, shooting, and lancinating pain [18]. Pain can be constant and cutaneous allodynia may be present [19, 20], negatively affecting diabetic people mood [21, 22]. Furthermore, people living with painful DPN may also remove themselves from social activities and eventually develop depression [23, 24]. Given ACC involvement in the affective/motivational aspects of pain [25, 26] and its involvement in the glucose-monitoring network in the brain [27], it is of great

✉ Marucia Chacur  
 chacurm@icb.usp.br

Igor Rafael Correia Rocha  
 irrocha@usp.br

<sup>1</sup> Departamento de Anatomia, Instituto de Ciências Biomédicas, Universidade de São Paulo, Avenue Lineu Prestes 2415, room 007, São Paulo 05508-900, Brazil

importance to develop research that aims to investigate the ACC participation in processing pain in DPN, which is still unknown. Recalling what has already been mentioned, no single pharmacological treatment exists to prevent pain or provide total pain relieve in painful DPN [28].

Astrocyte activation or astrogliosis in ACC has been linked with chronic or neuropathic pain [29, 30]. Astrocytes are the most numerous non-neuronal cells in the brain involved in modulateg a variety of neuronal activities [31, 32], including glucose metabolism [33, 34]. Astrocytes were reported to highly express  $\mu$ -opioid receptor (MOR) [35], one of the three subtypes of opioid receptors that play important role in modulating pain behavior and antinociception [36]. Moreover, MOR are also efficacious mood enhancers and are involved in the activation of dopamine reward pathway [37, 38].

ACC is composed of both excitatory and inhibitory neurons [39, 40], and GABAergic transmission in the ACC plays a critical role in modulating nociception and chronic pain in humans and animal [41]. Glutamatergic AMPA ( $\alpha$  amino-3-hydroxy-5-methylisoxazole-4-propionic acid) receptors (GluR1, GluR2, GluR3, and GluR4) involved in a variety of central nervous system functions [42–44], including pain modulation [45], mediate the majority of excitatory synaptic transmission in the brain [46]. However, the roles of glutamatergic receptors in ACC during pain receive few attentions [6]. Additionally, changes in GABA content have recently been described in the central nervous system [47], including ACC of chronic pain patients [48, 49].

Based on the information presented here, the present study aimed to assess whether photobiomodulation (PBM) applied to the peripheral nervous system would have modulatory effects on the ACC in animal model of streptozotocin-induced DPN. PBM has been used as complementary medicine for chronic and neuropathic pain treatment [50, 51], nerve fibre regeneration [52], and a variety of diseases [53–57]. Of note, it is well known the beneficial effects of PBM on the central nervous system [58–61].

## 2 Materials and methods

### 2.1 Animals

The experiments were carried out in accordance with the CONCEA guidelines (CONCEA, Brazil), a constituent body of the Ministry of Science, Technology, and Innovation (MCTI, Brazil). All protocols, including STZ-induction type 1 diabetes and photobiomodulation therapy, were approved by the Animal Research Ethics Committee (CEUA) of the Biomedical Sciences Institute of the University Sao Paulo (protocol number: CEUA 2269190619). All animals were handled according to the guidelines for

the use of laboratory animals [62]. The study used a total of 30 adult male Wistar rats (250–300 g) supplied by the central animal facility of the Biomedical Sciences Institute of University of Sao Paulo. Rats were kept at room temperature of  $22 \pm 2$  °C with light/dark cycle (12:12 h). Food and water were provided ad libitum. The rats were allowed to acclimatize for at least 5 days prior to the onset of the study. They were randomly divided into three groups: (1) Naive rats were used as control animals (CTRL); (2) STZ animals, which were intraperitoneally injected with streptozotocin (STZ, 85 mg/kg), and (3) STZ + PBM animals, which were injected with streptozotocin (STZ, 85 mg/kg) and treated with photobiomodulation (PBM). After STZ i.p injection, three rats died along the experimental timeline. At the end of the study, we had nine rats per group.

#### 2.1.1 Streptozotocin-induced type 1 diabetes

For the STZ-induced type 1 diabetes, a single dose of streptozotocin (85 mg/kg; S0130-1G, Sigma-Aldrich) diluted in 500  $\mu$ L of 0.9% Saline were injected in the peritoneal cavity [63]. Blood glucose levels were assessed 48H after STZ intraperitoneal injection to confirm hyperglycemia. Plasma glucose levels higher than 300 mg/dl were considered indicative of diabetes [64]. Glycemic control was assessed once a week using an ULTRAMINI® I ONETOUCH® blood glucose-monitoring system. A single administration of streptozotocin induced insulin-dependent diabetes mellitus within 48H by the destruction of pancreatic islet cells [65].

### 2.2 Photobiomodulation

Rats in the STZ + PBM group were irradiated with a GaAs laser (Gallium Arsenide, Laserpulse-Laser, Ibramed, Brazil) emitting a wavelength of 904 nm, output power of 45 mW, 0.13 cm<sup>2</sup> beam area, 9500 Hz frequency, duty cycle (DC) 0.0617%, pulse time of 65 ns, and 6.23 J/cm<sup>2</sup> fluence (Table 1). CTRL and STZ groups were not submitted to PBM. PBM initiated 60 days after diabetes induction. This time point was chosen, because we showed in a previous study that pain-related behavior (allodynia) and degeneration of peripheral nerve fibers were increased during persistent hyperglycaemia in the long term (60 days) [63]. The PBM treatment was performed under anesthesia with isoflurane (Cristalia, MG, Brazil) every other day totalling ten sessions. After sterilization, the laser probe was lightly placed on the unshaved skin surface of the rat's right thigh. Nine points in the region of the sciatic nerve were irradiated for 18 s each (Fig. 1). Points were irradiated between intervals of 30 s.

**Table 1** Photobiomodulation parameters

Irradiation parameters	
Wavelength (nm)	904 nm
Operating mode	Pulsed
Frequency (Hz)	9500 Hz
Pulse on duration (nanoseconds)	65 ns
Beam shape	Circular
Treatment parameters	
Beam spot size at target (cm <sup>2</sup> )	0.13 cm <sup>2</sup>
Exposure duration (seconds)	18 s/point
Radiant exposure (J/cm <sup>2</sup> )	6.23 J/cm <sup>2</sup>
Radiant energy (J)	0.81/point
Number of points irradiated	9
Irradiated area (cm <sup>2</sup> )	1.17 cm <sup>2</sup>
Application technique	Skin contact
Number and frequency of treatment	10 sessions performed every other day
Total radiant energy (J)	7.29 J/ session. 72.9 J total sessions

(GluR1), and Glutamic Acid Decarboxylase (GAD65/67) protein levels were quantified in the rat ACC. For total protein extraction, ACC was immersed in lysis buffer (90 mM KCl, 10 mM Hepes, 3 mM MgCl<sub>2</sub>, 5 mM EDTA, 1% glycerol, 1 mM DTT, 0.04% SDS, 20 mM Aprotinin, 20 mM Pepstatin, 20 mM Leupeptin, 40 μM PMSF, 100 mM Orthovanadate). The total protein concentration was obtained by Bradford method [66]. Subsequently, 40 μg (ACC) of total protein underwent polyacrylamide gradient gel (4 and 20%) [67] electrophoresis and transferred to nitrocellulose membrane (Bio-Rad). The membrane was subsequently stained with Ponceau solution to evaluate the similarity of protein concentration between the samples and for data normalization. Following Ponceau washing with TBST (20 mM TRIS, 148 mM NaCl, Tween 20 0.1%), membrane was incubated with primary antibodies shown in Table 2 under constant agitation at 4 °C overnight. After washing with TBST, the membrane was incubated with the peroxidase-conjugated anti-rabbit (1:5000) secondary antibodies for MOR, GluR1, and GAD65/67 and with the anti-mouse (1:5000) secondary antibodies for GFAP and β-Actin, at room temperature for

### 2.3 Protein expression analysis: Western blotting

On the next day after the last PBM session (10th session), all the rats were anesthetized with 5% isoflurane and decapitated when fully sedated. The animals' brains (anterior cingulate cortex) were removed for analysis of protein levels by Western blot assay. ACC were pooled from three rats of each group. Glial fibrillary acidic protein (GFAP), μ-Opioid receptor (MOR), Glutamate Receptor 1

**Table 2** List of primary antibodies used for Western Blotting

Antibody	Host species	Molecular weight	Dilution	RRID
GFAP	Mouse	50 KDa	1:1000	AB_477010
MOR	Rabbit	50 KDa	1:1000	AB_2156520
GluR1	Rabbit	106 KDa	1:1000	AB_2113602
GAD65/67	Rabbit	65/67 KDa	1:1000	AB_90715
Beta-Actin	Mouse	42 KDa	1:5000	AB_476743

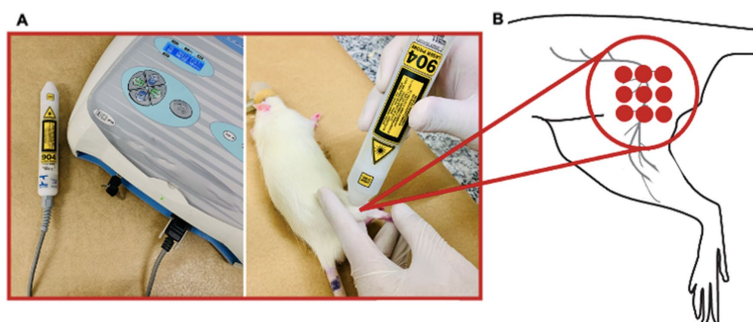


**Fig. 1** Photobiomodulation session **a** Represents laser device and laser probe (904 nm). PBM sessions were applied to the rat peripheral nerve fibers by superficial skin contact—rats were anesthetized

(O<sub>2</sub>/Isoflurane) to receive PBM therapy. **b** Nine points were irradiated with PBM (904 nm) on the rat right leg

90 min. The membrane was then washed again with TBST and submitted to chemiluminescence detector (UviTec Gel Doc Systems). The bands corresponding to the protein of interest were quantified by optical densitometry using the ImageJ software (NIH; USA), and the values were expressed as percentage [68]. For GFAP, MOR, GluR1, and GAD65/67, protein expression in the ACC, the same nitrocellulose membrane was used after stripping process for each antibody, and then,  $\beta$ -actin data were the same for all antibodies.

### 3 Statistical analysis

Statistical analyses of data were generated using GraphPad Prism, version 8 (GraphPad Software Inc., San Diego, CA). For Western blot analysis statistical comparison among groups was performed using one-way analysis of variance; differences between means were tested by Bonferroni's multiple comparison test. In all cases,  $p < 0.05$  was considered statistically significant.

## 4 Results

### 4.1 Type 1 diabetes onset through a single dose of STZ evaluated by blood glucose levels

One single intraperitoneal injection of STZ (85 mg/kg) diluted in 500  $\mu$ L of Saline 0.9% was used to induce type 1 diabetes in male Wistar rats. The difference between means (STZ and CTRL) was 292.3 md/dl in ad libitum blood glucose level. STZ group had a mean blood glucose level of 387.7 mg/dl compared to CTRL, 95.40 mg/dl. STZ revealed a significant blood glucose level increase compared to CTRL [ $F(3,16) = 313.6$ ;  $p < 0.0001$ ] (Fig. 2).

### 4.2 Effect of photobiomodulation on Glial Fibrillary Acidic Protein (GFAP) in the Anterior Cingulate Cortex (ACC)

STZ group revealed an increase in GFAP protein expression in the ACC of diabetic rats, compared to CTRL and STZ+PBM groups (Fig. 3) [ $F(2,6) = 2859$ ;  $p = 0.0001$ ]. Western blotting data also revealed that PBM significantly decreased GFAP protein expression in the ACC in STZ+PBM group compared to STZ and CTRL groups ( $p < 0.0001$ ). PBM decreased 138.52% of GFAP protein expression in the ACC of STZ+PBM group compared to STZ and 79.49% compared to CTRL (Fig. 3).

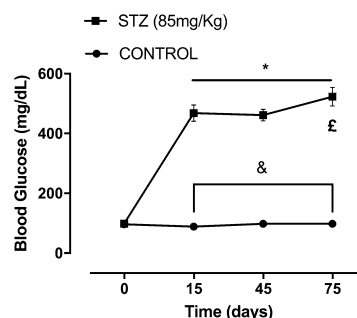


**Fig. 2** Blood Glucose Effect of STZ on ad libitum blood glucose levels. & $p < 0.0001$  between Control and STZ. \* $p < 0.0001$  among 15, 45, 75 and day 0 in STZ. £ $p < 0.0001$  among 75 and 45, 15 days in STZ

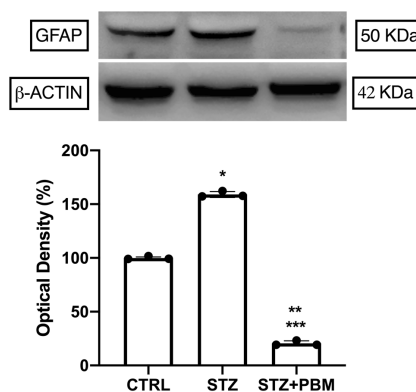


**Fig. 3** Glial fibrillary acidic protein. Western blotting analysis of PBM on GFAP in the rat ACC. \* $p < 0.0001$  STZ/CTRL; \*\* $p < 0.0001$  STZ+PBM/STZ; \*\*\* $p < 0.0001$  STZ+PBM/CTRL. Each black point in the graph represents a pool of three rats

### 4.3 Effect of photobiomodulation on $\mu$ -Opioid Receptor (MOR) in the Anterior Cingulate Cortex (ACC)

STZ group revealed a decrease in MOR protein expression in the ACC of diabetic rats, compared to CTRL and STZ+PBM groups (Fig. 4) [ $F(2,6) = 39.05$ ;  $p = 0.0004$ ]. Western blotting data also revealed that PBM increased MOR protein expression in the ACC of STZ+PBM group compared to STZ ( $p < 0.0049$ ) group. PBM increased 14.77%

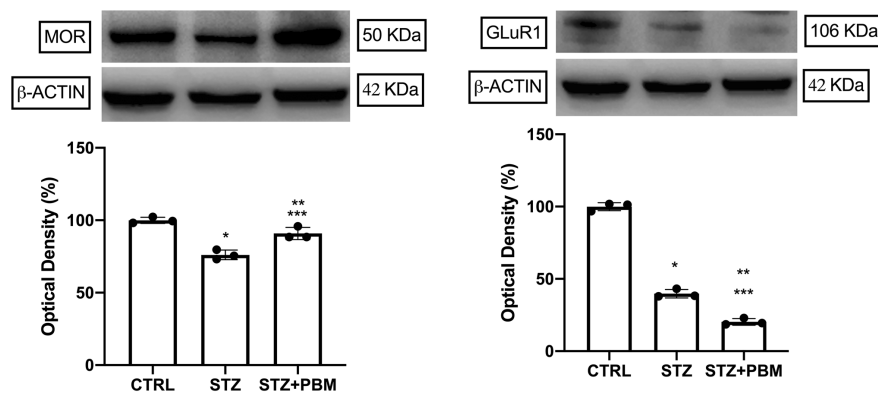


**Fig. 4** Mu-opioid receptor. Western blotting analysis of PBM on MOR in the rat ACC. \* $p < 0.0004$  STZ/CTRL; \*\* $p < 0.0049$  STZ+PBM/STZ; \*\*\* $p < 0.0467$  STZ+PBM/CTRL. Each black point in the graph represents a pool of three rats

of MOR protein expression in the ACC of STZ+PBM group compared to STZ group (Fig. 4).

#### 4.4 Effect of photobiomodulation on Glutamate Receptor 1 (GluR1) in the Anterior Cingulate Cortex (ACC)

STZ group revealed a decrease in GluR1 protein expression in the ACC of diabetic rats, compared to CTRL group (Fig. 5) [ $F(2,6) = 724.4$ ;  $p = 0.0001$ ]. Western blotting data also revealed an even greater decrease in STZ+PBM group compared to both groups. PBM decreased 10.48% of GluR1 protein expression in the ACC of STZ+PBM group compared to STZ and 70.7% compared to CTRL (Fig. 5). STZ group had a decrease of 60.22% of GluR1 protein expression compared to CTRL.

#### 4.5 Effect of photobiomodulation on Glutamic Acid Decarboxylase (GAD65/67) in the Anterior Cingulate Cortex (ACC)

STZ group revealed a decrease in GAD65/67 protein expression in the ACC compared to CTRL group (Fig. 6) [ $F(2,6) = 103.6$ ;  $p = 0.0001$ ]. After PBM treatment, our western blotting data revealed that PBM also decreased GAD65/67 protein expression in STZ+PBM group compared CTRL ( $p < 0.0001$ ). STZ group had a decreased of 47.51% of GAD65/67 protein expression compared to CTRL and STZ+PBM had a decreased of 45.51% compared to CTRL (Fig. 6). No statistical difference was found

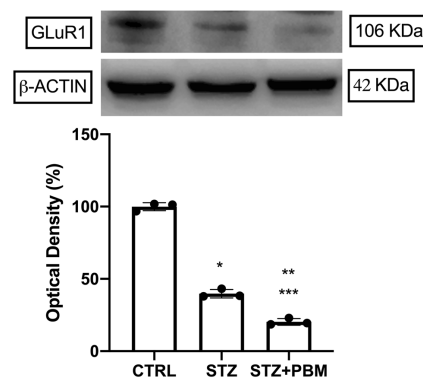


**Fig. 5** Glutamate receptor 1. Western blotting analysis of PBM on GluR1 in the rat ACC. \* $p < 0.0001$  STZ/CTRL; \*\* $p < 0.0003$  STZ+PBM/STZ; \*\*\* $p < 0.0001$  STZ+PBM/CTRL. Each black point in the graph represents a pool of three rats

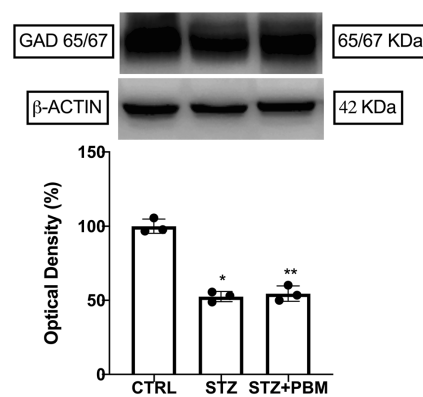


**Fig. 6** Glutamic acid decarboxylase. Western blotting analysis of PBM on GAD65/67 in the rat ACC. \* $p < 0.0001$  STZ/CTRL; \*\*\* $p < 0.0001$  STZ+PBM/CTRL. No statistical significance was found between STZ+PBM and STZ. Each black point in the graph represents a pool of three rats



between STZ + PBM and STZ regarding protein expression of GAD65/67 in the rat ACC.

## 5 Discussion

In the present study, we investigated the effects of PBM on the supraspinal brain region involved in the cognitive and emotional processing of peripheral painful sensation, ACC. In our study, we used rat model of diabetic peripheral neuropathy induced by a single dose of streptozotocin (STZ, 85 mg/kg) injected in the peritoneal cavity (intraperitoneal, i.p.). Rats that were injected with STZ developed hyperglycemia 24 h after STZ i.p. injection. Furthermore, STZ-induced diabetic rats developed the most common signs of diabetic neuropathy. It includes severe weight loss, polyuria, polyphagia and, in some cases, cataracts (data not shown). Additionally, we have previously shown that one single dose of STZ (85 mg/kg) induced allodynia in rat model of diabetic peripheral neuropathy and that PBM restore pain threshold in those rats [63]. Streptozotocin-induced diabetic rats had an average blood glucose level of 387.7 mg/dl. Control (CTRL) rats developed no signs of diabetic neuropathy and had an average blood glucose level of 95.40 mg/dl throughout the experimental timeline (12 weeks).

Currently, there is an increasing body of evidence showing the involvement of ACC in the perception of physical and affective components of pain [69–73]. Of note, little is known about the direct effects of hyperglycemia (diabetes) on ACC. Moreover, there is a limited but growing body of evidence concerning the effects of PBM on the brain [58, 60, 61, 74]. Furthermore, less is known about how PBM that was applied to the peripheral nervous system has the potential to modulate protein levels in supraspinal segments in the central nervous system. We present here the modulatory effects of photobiomodulation on (1) glial fibrillary acidic protein (GFAP), (2)  $\mu$ -opioid receptor (MOR), and (3) glutamate receptor (GluR1) protein levels in the ACC of diabetic rats in streptozotocin-induced diabetic peripheral neuropathy.

Initially, our results showed that hyperglycemia increases GFAP protein levels in the ACC of diabetic rats (STZ) when compared to control (CTRL) group. It must be mentioned that one of the major roles played by astrocytes is their direct involvement in energy storage and supply for the brain [33, 75, 76]. Moreover, Coleman et al. [77] and Saraiva et al. [78] demonstrated changes in GFAP expression in the central nervous system (CNS) in rodent diabetes model. However, the effects of high glucose on astrocytes metabolism and function remains unclear [75]. Of note, we showed here that diabetic rats treated with PBM (STZ + PBM) had a significant decrease of GFAP protein levels in the ACC when

compared to STZ group. There was also statistical difference between STZ + PBM and CTRL group.

It was also presented here that PBM increased  $\mu$ -opioid receptor (MOR) in the ACC of diabetic rats (STZ + PBM) when applied to the peripheral nervous system. STZ rats had a decrease in MOR protein levels when compared to CTRL group. Opioid receptors comprise four members, the classical  $\mu$  (MOR),  $\delta$  (DOR), and  $\kappa$  (KOR) receptors, and the non-classical nociceptin/orphanin FQ (NOP) receptor [79]. MOR receptors are the most important class of receptors clinically, playing an important role in pain treatment [36, 80, 81]. Interestingly, MOR was reported to be highly expressed in the central nervous system astrocytes [82]. However, the role of astrocytic MOR has not been investigated [82, 83]. Furthermore, little is known about the role of astrocytes and MOR in diabetic peripheral neuropathy, especially regarding ACC.

In the present study, we also showed that hyperglycemia decreased glutamate receptor (GluR1) protein levels in the ACC of diabetic rats (STZ) compared to control (CTRL). Surprisingly, PBM decreased even further GluR1 protein levels in the diabetic rats (STZ) that were treated with PBM. Glutamate is the main excitatory neurotransmitter in the mammalian brain where astrocytes play an important role in removing 90% of such neurotransmitter from the synapse in the central nervous system [84, 85]. Bolo et al. [86] and Wieggers et al. [87] demonstrated elevated brain glutamate levels in people with type 1 diabetes, but they did not correlate such results with ionotropic glutamate receptor 1 (GluR1). Moreover, Andersen et al. [84] showed impaired glutamate and glutamine metabolism in the hippocampus of mouse model of type 2 diabetes but did not make any correlation between this finding and GluR1.

Additionally, we evaluated the effects of PBM on the modulation of protein levels of glutamic acid decarboxylase (GAD65/67) on the ACC of diabetic rats (STZ). GAD65/67 plays an important role in the synthesis of gamma-aminobutyric acid (GABA) in the central nervous system (CNS) [88]. GABA is the principal inhibitory transmitter in the CNS, including the spinal dorsal horn and ACC [88, 89]. Our results demonstrated that diabetic rats (STZ) had a significant decrease in the levels of GAD65/67 in the ACC compared to control rats. Interestingly, PBM had no effect in GAD65/67 protein levels of diabetic rats. The effects of hyperglycemia on GAD65/67 protein modulation should be further investigated.

Regarding the abscopal effects of PBM our data summarized here corroborates the findings presented by Mitrofanis et al. [90]. Mitrofanis and colleagues showed that ten consecutive days of remote PBM had neuroprotective effects in mice model of Parkinson's disease (PD) [90]. According to their study, remote PBM produces modest but widespread changes in the brain transcriptome [90]. With respect

to working memory and cognitive functions in which ACC plays an important role, Salehpour et al. [91] demonstrated in a case report that an individual affected by Alzheimer's disease (AD) treated with transcranial e intranasal PBM had improvements in cognitive abilities, working memory, as well as in quality of life [91]. Another interesting finding with respect to indirect effects of PBM was demonstrated by Kern et al. [92]. In STZ-induced diabetes in mice, PBM attenuated diabetes-induced retinopathy by improving diabetic-changes in superoxide generation, leukostasis, and expression of ICAM-1 [92]. Kern and colleagues showed that such significant results were achieved with the mice's head protected from the light therapy, the retina itself did not receive PBM directly [92].

## 6 Conclusion

In conclusion, the present study demonstrated the abscopal effects of PBM on the ACC of diabetic rats. Interestingly, hyperglycemia had expressive modulatory effect on the protein levels of GFAP, MOR, GluR1, and GAD65/67 on the ACC of diabetic rats. Surprisingly, PBM applied to the peripheral nervous system of these diabetic animals modulated the protein levels of GFAP, MOR, and GluR1 on the ACC. PBM had no effect on the modulation of GAD65/67. Our results suggest that PBM applied to the periphery may have interesting effects on supraspinal brain regions, especially on the ACC. We must further investigate the effects of hyperglycemia in this brain region and why and how PBM that was applied to the peripheral nervous system elicits its effect on supraspinal brain region.

**Acknowledgements** This study was supported by Sao Paulo Research Foundation (FAPESP, Sao Paulo, Brazil). Igor Rafael Correia Rocha was the recipient of a FAPESP PhD scholarship (2017/25554-0). Marucia Chacur was the recipient of an FAPESP (2017/05218-5)/CNPq (405853/2018-1) fellowship. Igor Rafael Correia Rocha and Marucia Chacur have contributed equally to this work.

**Funding** This study was supported by Sao Paulo Research Foundation (FAPESP), grant number 2017/25554-0. The funding agency plays no role in the design of the study, data collection, analysis, interpretation of the data, or in writing the manuscript.

## Declarations

**Conflict of interest** The authors declare no financial or commercial conflict of interest.

## References

- Zhuo, M. (2014). Long-term potentiation in the anterior cingulate cortex and chronic pain. *Philosophical Transactions of the Royal Society of London. Series B, Biological sciences*, 369(1633), 20130146. <https://doi.org/10.1098/rstb.2013.0146>
- Zhao, R., Zhou, H., Huang, L., Xie, Z., Wang, J., Gan, W. B., et al. (2018). Neuropathic pain causes pyramidal neuronal hyperactivity in the anterior cingulate cortex. *Frontiers in Cellular Neuroscience*, 12, 107. <https://doi.org/10.3389/fncel.2018.00107>
- Um, S. W., Kim, M. J., Leem, J. W., Bai, S. J., & Lee, B. H. (2019). Pain-relieving effects of mTOR inhibitor in the anterior cingulate cortex of neuropathic rats. *Molecular Neurobiology*, 56(4), 2482–2494. <https://doi.org/10.1007/s12035-018-1245-z>
- Chai, S. C., Kung, J. C., & Shyu, B. C. (2010). Roles of the anterior cingulate cortex and medial thalamus in short-term and long-term aversive information processing. *Molecular Pain*, 6, 42. <https://doi.org/10.1186/1744-8069-6-42>
- Wu, L. J., Steenland, H. W., Kim, S. S., Isiegas, C., Abel, T., Kaang, B. K., et al. (2008). Enhancement of presynaptic glutamate release and persistent inflammatory pain by increasing neuronal cAMP in the anterior cingulate cortex. *Molecular Pain*, 4, 40. <https://doi.org/10.1186/1744-8069-4-40>
- Xu, H., Wu, L. J., Wang, H., Zhang, X., Vadakkan, K. I., Kim, S. S., et al. (2008). Presynaptic and postsynaptic amplifications of neuropathic pain in the anterior cingulate cortex. *Journal of Neuroscience*, 28(29), 7445–7453. <https://doi.org/10.1523/JNEUROSCI.1812-08.2008>
- Fuchs, P. N., Balinsky, M., & Melzack, R. (1996). Electrical stimulation of the cingulum bundle and surrounding cortical tissue reduces formalin-test pain in the rat. *Brain Research*, 743(1–2), 116–123. [https://doi.org/10.1016/s0006-8993\(96\)01035-9](https://doi.org/10.1016/s0006-8993(96)01035-9)
- Johansen, J. P., Fields, H. L., & Manning, B. H. (2001). The affective component of pain in rodents: direct evidence for a contribution of the anterior cingulate cortex. *Proceedings of the National Academy of Sciences USA*, 98(14), 8077–8082. <https://doi.org/10.1073/pnas.141218998>
- Iqbal, Z., Azmi, S., Yadav, R., Ferdousi, M., Kumar, M., Cuthbertson, D. J., et al. (2018). Diabetic peripheral neuropathy: epidemiology, diagnosis, and pharmacotherapy. *Clinical Therapeutics*, 40(6), 828–849. <https://doi.org/10.1016/j.clinthera.2018.04.001>
- Albers, J. W., & Pop-Busui, R. (2014). Diabetic neuropathy: mechanisms, emerging treatments, and subtypes. *Current Neurology and Neuroscience Reports*, 14(8), 473. <https://doi.org/10.1007/s11910-014-0473-5>
- Young, M. J., Boulton, A. J., MacLeod, A. F., Williams, D. R., & Sonksen, P. H. (1993). A multicentre study of the prevalence of diabetic peripheral neuropathy in the United Kingdom hospital clinic population. *Diabetologia*, 36(2), 150–154. <https://doi.org/10.1007/BF00400697>
- Schreiber, A. K., Nones, C. F., Reis, R. C., Chichorro, J. G., & Cunha, J. M. (2015). Diabetic neuropathic pain: physiopathology and treatment. *World Journal of Diabetes*, 6(3), 432–444. <https://doi.org/10.4239/wjd.v6.i3.432>
- Tesfaye, S., Boulton, A. J., & Dickenson, A. H. (2013). Mechanisms and management of diabetic painful distal symmetrical polyneuropathy. *Diabetes Care*, 36(9), 2456–2465. <https://doi.org/10.2337/dc12-1964>
- Boulton, A. J., Kirsner, R. S., & Vileikyte, L. (2004). Clinical practice. Neuropathic diabetic foot ulcers. *New England Journal of Medicine*, 351(1), 48–55. <https://doi.org/10.1056/NEJMc032966>
- Kaur, S., Pandhi, P., & Dutta, P. (2011). Painful diabetic neuropathy: an update. *Annals of Neurosciences*, 18(4), 168–175. <https://doi.org/10.5214/ans.0972-7531.1118409>
- Boucek, P. (2006). Advanced diabetic neuropathy: a point of no return? *The Review of Diabetic Studies*, 3(3), 143–150. <https://doi.org/10.1900/RDS.2006.3.143>
- Ang, L., Jaiswal, M., Martin, C., & Pop-Busui, R. (2014). Glucose control and diabetic neuropathy: lessons from recent large

- clinical trials. *Current Diabetes Reports*, 14(9), 528. <https://doi.org/10.1007/s11892-014-0528-7>
18. Bansal, V., Kalita, J., & Misra, U. K. (2006). Diabetic neuropathy. *Postgraduate Medical Journal*, 82(964), 95–100. <https://doi.org/10.1136/pgmj.2005.036137>
  19. Marchettini, P., Lacerenza, M., Mauri, E., & Marangoni, C. (2006). Painful peripheral neuropathies. *Current Neuropharmacology*, 4(3), 175–181. <https://doi.org/10.2174/157015906778019536>
  20. Aslam, A., Singh, J., & Rajbhandari, S. (2014). Pathogenesis of painful diabetic neuropathy. *Pain Research and Treatment*, 2014, 412041. <https://doi.org/10.1155/2014/412041>
  21. Girach, A., Julian, T. H., Varrassi, G., Paladini, A., Vadalouka, A., & Zis, P. (2019). Quality of life in painful peripheral neuropathies: a systematic review. *Pain Research & Management*, 2019, 2091960. <https://doi.org/10.1155/2019/2091960>
  22. Selvarajah, D., Cash, T., Sankar, A., Thomas, L., Davies, J., Cachia, E., et al. (2014). The contributors of emotional distress in painful diabetic neuropathy. *Diabetes & Vascular Disease Research*, 11(4), 218–225. <https://doi.org/10.1177/1479164114522135>
  23. Jain, R., Jain, S., Raison, C. L., & Maletic, V. (2011). Painful diabetic neuropathy is more than pain alone: examining the role of anxiety and depression as mediators and complicators. *Current Diabetes Reports*, 11(4), 275–284. <https://doi.org/10.1007/s11892-011-0202-2>
  24. Vileikyte, L., Peyrot, M., Gonzalez, J. S., Rubin, R. R., Garrow, A. P., Stickings, D., et al. (2009). Predictors of depressive symptoms in persons with diabetic peripheral neuropathy: a longitudinal study. *Diabetologia*, 52(7), 1265–1273. <https://doi.org/10.1007/s00125-009-1363-2>
  25. Fuchs, P. N., Peng, Y. B., Boyette-Davis, J. A., & Uhelski, M. L. (2014). The anterior cingulate cortex and pain processing. *Frontiers in Integrative Neuroscience*, 8, 35. <https://doi.org/10.3389/fnint.2014.00035>
  26. Huang, J., Zhang, Z., & Zamponi, G. W. (2020). Pain: integration of sensory and affective aspects of pain. *Current Biology*, 30(9), R393–R395. <https://doi.org/10.1016/j.cub.2020.02.056>
  27. Hormay, E., Laszlo, B., Szabo, I., Ollmann, T., Nagy, B., Pecze, L., et al. (2019). The effect of loss of the glucose-monitoring neurons in the anterior cingulate cortex: physiologic challenges induce complex feeding-metabolic alterations after local streptozotocin microinjection in rats. *Neuroscience Research*, 149, 50–60. <https://doi.org/10.1016/j.neures.2019.01.005>
  28. Javed, S., Petropoulos, I. N., Alam, U., & Malik, R. A. (2015). Treatment of painful diabetic neuropathy. *Therapeutic Advances in Chronic Disease*, 6(1), 15–28. <https://doi.org/10.1177/2040622314552071>
  29. Masocha, W. (2015). Astrocyte activation in the anterior cingulate cortex and altered glutamatergic gene expression during paclitaxel-induced neuropathic pain in mice. *PeerJ*, 3, e1350. <https://doi.org/10.7717/peerj.1350>
  30. Kuzumaki, N., Narita, M., Narita, M., Hareyama, N., Niikura, K., Nagumo, Y., et al. (2007). Chronic pain-induced astrocyte activation in the cingulate cortex with no change in neural or glial differentiation from neural stem cells in mice. *Neuroscience Letters*, 415(1), 22–27. <https://doi.org/10.1016/j.neulet.2006.12.057>
  31. Maragakis, N. J., & Rothstein, J. D. (2006). Mechanisms of disease: astrocytes in neurodegenerative disease. *Nature Clinical Practice Neurology*, 2(12), 679–689. <https://doi.org/10.1038/ncpneuro0355>
  32. Seifert, G., Schilling, K., & Steinhauser, C. (2006). Astrocyte dysfunction in neurological disorders: a molecular perspective. *Nature Reviews Neuroscience*, 7(3), 194–206. <https://doi.org/10.1038/nrn1870>
  33. Deitmer, J. W., Theparambil, S. M., Ruminot, I., Noor, S. I., & Becker, H. M. (2019). Energy dynamics in the brain: contributions of astrocytes to metabolism and pH homeostasis. *Frontiers in Neuroscience*, 13, 1301. <https://doi.org/10.3389/fnins.2019.01301>
  34. Belanger, M., Allaman, I., & Magistretti, P. J. (2011). Brain energy metabolism: focus on astrocyte-neuron metabolic cooperation. *Cell Metabolism*, 14(6), 724–738. <https://doi.org/10.1016/j.cmet.2011.08.016>
  35. Woo, D. H., Bae, J. Y., Nam, M.-H., An, H., Ju, Y. H., Won, J., et al. (2018). Activation of astrocytic  $\mu$ -opioid receptor elicits fast glutamate release through TREK-1-containing K2P channel in hippocampal astrocytes. *Frontiers in Cellular Neuroscience*. <https://doi.org/10.3389/fncel.2018.00319> Original Research.
  36. Al-Hasani, R., & Bruchas, M. R. (2011). Molecular mechanisms of opioid receptor-dependent signaling and behavior. *Anesthesiology*, 115(6), 1363–1381. <https://doi.org/10.1097/ALN.0b013e318238bba6>
  37. Lutz, P. E., & Kieffer, B. L. (2013). Opioid receptors: distinct roles in mood disorders. *Trends in Neurosciences*, 36(3), 195–206. <https://doi.org/10.1016/j.tins.2012.11.002>
  38. Le Merrer, J., Becker, J. A., Befort, K., & Kieffer, B. L. (2009). Reward processing by the opioid system in the brain. *Physiological Reviews*, 89(4), 1379–1412. <https://doi.org/10.1152/physrev.00005.2009>
  39. Kang, S. J., Kim, S., Lee, J., Kwak, C., Lee, K., Zhuo, M., et al. (2017). Inhibition of anterior cingulate cortex excitatory neuronal activity induces conditioned place preference in a mouse model of chronic inflammatory pain. *The Korean Journal of Physiology & Pharmacology*, 21(5), 487–493. <https://doi.org/10.4196/kjpp.2017.21.5.487>
  40. Yang, Z., Tan, Q., Cheng, D., Zhang, L., Zhang, J., Gu, E. W., et al. (2018). The changes of intrinsic excitability of pyramidal neurons in anterior cingulate cortex in neuropathic pain. *Frontiers in Cellular Neuroscience*, 12, 436. <https://doi.org/10.3389/fncel.2018.00436>
  41. Koga, K., Shimoyama, S., Yamada, A., Furukawa, T., Nikaido, Y., Furue, H., et al. (2018). Chronic inflammatory pain induced GABAergic synaptic plasticity in the adult mouse anterior cingulate cortex. *Molecular Pain*, 14, 1744806918783478. <https://doi.org/10.1177/1744806918783478>
  42. Ceprian, M., & Fulton, D. (2019). Glial cell AMPA receptors in nervous system health, injury and disease. *International Journal of Molecular Sciences*. <https://doi.org/10.3390/ijms20102450>
  43. Chater, T. E., & Goda, Y. (2014). The role of AMPA receptors in postsynaptic mechanisms of synaptic plasticity. *Frontiers in Cellular Neuroscience*, 8, 401. <https://doi.org/10.3389/fncel.2014.00401>
  44. Jones, E. V., Bernardinelli, Y., Zarruk, J. G., Chierzi, S., & Murai, K. K. (2018). SPARC and GluA1-containing AMPA receptors promote neuronal health following CNS injury. *Frontiers in Cellular Neuroscience*, 12, 22. <https://doi.org/10.3389/fncel.2018.00022>
  45. Bie, B., Brown, D. L., & Naguib, M. (2011). Increased synaptic GluR1 subunits in the anterior cingulate cortex of rats with peripheral inflammation. *European Journal of Pharmacology*, 653(1–3), 26–31. <https://doi.org/10.1016/j.ejphar.2010.11.027>
  46. Zhang, H., & Bramham, C. R. (2020). Bidirectional dysregulation of AMPA receptor-mediated synaptic transmission and plasticity in brain disorders. *Frontiers in Synaptic Neuroscience*, 12, 26. <https://doi.org/10.3389/fnsyn.2020.00026>
  47. Blom, S. M., Piister, J. P., Santello, M., Senn, W., & Nevian, T. (2014). Nerve injury-induced neuropathic pain causes disinhibition of the anterior cingulate cortex. *Journal of Neuroscience*, 34(17), 5754–5764. <https://doi.org/10.1523/JNEUROSCI.3667-13.2014>

48. Henderson, L. A., Peck, C. C., Petersen, E. T., Rae, C. D., Youssef, A. M., Reeves, J. M., et al. (2013). Chronic pain: lost inhibition? *Journal of Neuroscience*, *33*(17), 7574–7582. <https://doi.org/10.1523/JNEUROSCI.0174-13.2013>
49. Foerster, B. R., Petrou, M., Edden, R. A., Sundgren, P. C., Schmidt-Wilcke, T., Lowe, S. E., et al. (2012). Reduced insular gamma-aminobutyric acid in fibromyalgia. *Arthritis and Rheumatism*, *64*(2), 579–583. <https://doi.org/10.1002/art.33339>
50. Kingsley, J. D., Demchak, T., & Mathis, R. (2014). Low-level laser therapy as a treatment for chronic pain. *Frontiers in Physiology*, *5*, 306. <https://doi.org/10.3389/fphys.2014.00306>
51. de Andrade, A. L., Bossini, P. S., & Parizoto, N. A. (2016). Use of low level laser therapy to control neuropathic pain: a systematic review. *Journal of Photochemistry and Photobiology B: Biology*, *164*, 36–42. <https://doi.org/10.1016/j.jphotobiol.2016.08.025>
52. Wang, C. Z., Chen, Y. J., Wang, Y. H., Yeh, M. L., Huang, M. H., Ho, M. L., et al. (2014). Low-level laser irradiation improves functional recovery and nerve regeneration in sciatic nerve crush rat injury model. *PLoS ONE*, *9*(8), e103348. <https://doi.org/10.1371/journal.pone.0103348>
53. Posten, W., Wrone, D. A., Dover, J. S., Arndt, K. A., Silapunt, S., & Alam, M. (2005). Low-level laser therapy for wound healing: mechanism and efficacy. *Dermatologic Surgery*, *31*(3), 334–340. <https://doi.org/10.1111/j.1524-4725.2005.31086>
54. Lee, J. H., Chiang, M. H., Chen, P. H., Ho, M. L., Lee, H. E., & Wang, Y. H. (2018). Anti-inflammatory effects of low-level laser therapy on human periodontal ligament cells: in vitro study. *Lasers in Medical Science*, *33*(3), 469–477. <https://doi.org/10.1007/s10103-017-2376-6>
55. Angelova, A., & Ilieva, E. M. (2016). Effectiveness of high intensity laser therapy for reduction of pain in knee osteoarthritis. *Pain Research & Management*, *2016*, 9163618. <https://doi.org/10.1155/2016/9163618>
56. Cotler, H. B., Chow, R. T., Hamblin, M. R., & Carroll, J. (2015). The Use of Low Level Laser Therapy (LLLT) For Musculoskeletal Pain. *MOJ Orthopedics & Rheumatology*. <https://doi.org/10.15406/mojor.2015.02.00068>
57. Sun, G., & Tuner, J. (2004). Low-level laser therapy in dentistry. *Dental Clinics of North America*, *48*(4), 1061–1076. <https://doi.org/10.1016/j.cden.2004.05.004>
58. Hashmi, J. T., Huang, Y. Y., Osmani, B. Z., Sharma, S. K., Naeser, M. A., & Hamblin, M. R. (2010). Role of low-level laser therapy in neurorehabilitation. *PM & R: The Journal of Injury, Function, and Rehabilitation*, *2*(12 Suppl 2), S292–305. <https://doi.org/10.1016/j.pmrj.2010.10.013>
59. Rochkind, S., & Ouaknine, G. E. (1992). New trend in neuroscience: low-power laser effect on peripheral and central nervous system (basic science, preclinical and clinical studies). *Neurological Research*, *14*(1), 2–11. <https://doi.org/10.1080/01616412.1992.11740003>
60. Thunshelle, C., & Hamblin, M. R. (2016). Transcranial low-level laser (light) therapy for brain injury. *Photomedicine and Laser Surgery*, *34*(12), 587–598. <https://doi.org/10.1089/pho.2015.4051>
61. Hamblin, M. R. (2016). Shining light on the head: photobiomodulation for brain disorders. *BBA Clinical*, *6*, 113–124. <https://doi.org/10.1016/j.bbacli.2016.09.002>
62. Zimmermann, M. (1983). Ethical guidelines for investigations of experimental pain in conscious animals. *Pain*, *16*(2), 109–110. [https://doi.org/10.1016/0304-3959\(83\)90201-4](https://doi.org/10.1016/0304-3959(83)90201-4)
63. Correia Rocha, I. R., Ciena, A. P., Rosa, A. S., Martins, D. O., & Chacur, M. (2017). Photobiostimulation reverses allodynia and peripheral nerve damage in streptozotocin-induced type 1 diabetes. *Lasers in Medical Science*, *32*(3), 495–501. <https://doi.org/10.1007/s10103-016-2140-3>
64. Pandurangan, M., & Kim, D. H. (2016). Therapeutic potential of cyanobacteria against streptozotocin-induced diabetic rats. *3 Biotech*, *6*(1), 94. <https://doi.org/10.1007/s13205-016-0411-0>
65. Lenzen, S. (2008). The mechanisms of alloxan- and streptozotocin-induced diabetes. *Diabetologia*, *51*(2), 216–226. <https://doi.org/10.1007/s00125-007-0886-7>
66. Bradford, M. M. (1976). A rapid and sensitive method for the quantitation of microgram quantities of protein utilizing the principle of protein-dye binding. *Analytical Biochemistry*, *72*, 248–254. <https://doi.org/10.1006/abio.1976.9999>
67. Miller, A. J., Roman, B., & Norstrom, E. M. (2016). Protein electrophoretic migration data from custom and commercial gradient gels. *Data in Brief*, *9*, 1–3. <https://doi.org/10.1016/j.dib.2016.08.018>
68. Binda, K. H., Real, C. C., Ferreira, A. F. F., Britto, L. R., & Chacur, M. (2020). Antinociceptive effects of treadmill exercise in a rat model of Parkinson's disease: the role of cannabinoid and opioid receptors. *Brain Research*, *1727*, 146521. <https://doi.org/10.1016/j.brainres.2019.146521>
69. Li, W., Wang, P., & Li, H. (2014). Upregulation of glutamatergic transmission in anterior cingulate cortex in the diabetic rats with neuropathic pain. *Neuroscience Letters*, *568*, 29–34. <https://doi.org/10.1016/j.neulet.2014.03.038>
70. Han, M., Xiao, X., Yang, Y., Huang, R. Y., Cao, H., Zhao, Z. Q., et al. (2014). SIP30 is required for neuropathic pain-evoked aversion in rats. *Journal of Neuroscience*, *34*(2), 346–355. <https://doi.org/10.1523/JNEUROSCI.3160-13.2014>
71. Li, X. Y., Ko, H. G., Chen, T., Descalzi, G., Koga, K., Wang, H., et al. (2010). Alleviating neuropathic pain hypersensitivity by inhibiting PKMzeta in the anterior cingulate cortex. *Science*, *330*(6009), 1400–1404. <https://doi.org/10.1126/science.1191792>
72. Zhuo, M. (2008). Cortical excitation and chronic pain. *Trends in Neurosciences*, *31*(4), 199–207. <https://doi.org/10.1016/j.tins.2008.01.003>
73. Zhuo, M. (2006). Molecular mechanisms of pain in the anterior cingulate cortex. *Journal of Neuroscience Research*, *84*(5), 927–933. <https://doi.org/10.1002/jnr.21003>
74. Xuan, W., Vatanserver, F., Huang, L., Wu, Q., Xuan, Y., Dai, T., et al. (2013). Transcranial low-level laser therapy improves neurological performance in traumatic brain injury in mice: effect of treatment repetition regimen. *PLoS ONE*, *8*(1), e53454. <https://doi.org/10.1371/journal.pone.0053454>
75. Li, W., Roy Choudhury, G., Winters, A., Prah, J., Lin, W., Liu, R., et al. (2018). Hyperglycemia alters astrocyte metabolism and inhibits astrocyte proliferation. *Aging and Disease*, *9*(4), 674–684. <https://doi.org/10.14336/AD.2017.1208>
76. Prebil, M., Jensen, J., Zorec, R., & Kreft, M. (2011). Astrocytes and energy metabolism. *Archives of Physiology and Biochemistry*, *117*(2), 64–69. <https://doi.org/10.3109/13813455.2010.539616>
77. Coleman, E., Judd, R., Hoe, L., Dennis, J., & Posner, P. (2004). Effects of diabetes mellitus on astrocyte GFAP and glutamate transporters in the CNS. *Glia*, *48*(2), 166–178. <https://doi.org/10.1002/glia.20068>
78. Saravia, F. E., Revsin, Y., Gonzalez Deniselle, M. C., Gonzalez, S. L., Roig, P., Lima, A., et al. (2002). Increased astrocyte reactivity in the hippocampus of murine models of type 1 diabetes: the nonobese diabetic (NOD) and streptozotocin-treated mice. *Brain Research*, *957*(2), 345–353. [https://doi.org/10.1016/s0006-8993\(02\)03675-2](https://doi.org/10.1016/s0006-8993(02)03675-2)
79. Machelska, H., & Celik, M. O. (2020). Opioid receptors in immune and glial cells-implications for pain control. *Frontiers in Immunology*, *11*, 300. <https://doi.org/10.3389/fimmu.2020.00300>
80. Pasternak, G., & Pan, Y. X. (2011). Mu opioid receptors in pain management. *Acta Anaesthesiologica Taiwanica*, *49*(1), 21–25. <https://doi.org/10.1016/j.aat.2010.12.008>

81. Ehrlich, A. T., Kieffer, B. L., & Darq, E. (2019). Current strategies toward safer mu opioid receptor drugs for pain management. *Expert Opinion on Therapeutic Targets*, 23(4), 315–326. <https://doi.org/10.1080/14728222.2019.1586882>
82. Woo, D. H., Bae, J. Y., Nam, M. H., An, H., Ju, Y. H., Won, J., et al. (2018). Activation of astrocytic mu-opioid receptor elicits fast glutamate release through TREK-1-containing K2P channel in hippocampal astrocytes. *Frontiers in Cellular Neuroscience*, 12, 319. <https://doi.org/10.3389/fncel.2018.00319>
83. Nam, M. H., Han, K. S., Lee, J., Won, W., Koh, W., Bae, J. Y., et al. (2019). Activation of astrocytic mu-opioid receptor causes conditioned place preference. *Cell Reports*, 28(5), 1154–1166.e5. <https://doi.org/10.1016/j.celrep.2019.06.071>
84. Andersen, J. V., Nissen, J. D., Christensen, S. K., Markussen, K. H., & Waagepetersen, H. S. (2017). Impaired hippocampal glutamate and glutamine metabolism in the db/db mouse model of type 2 diabetes mellitus. *Neural Plasticity*, 2017, 2107084. <https://doi.org/10.1155/2017/2107084>
85. Mahmoud, S., Gharagozloo, M., Simard, C., & Gris, D. (2019). Astrocytes maintain glutamate homeostasis in the CNS by controlling the balance between glutamate uptake and release. *Cells*. <https://doi.org/10.3390/cells8020184>
86. Bolo, N. R., Jacobson, A. M., Musen, G., Keshavan, M. S., & Simonson, D. C. (2020). Acute hyperglycemia increases brain pregenual anterior cingulate cortex glutamate concentrations in type 1 diabetes. *Diabetes*, 69(7), 1528–1539. <https://doi.org/10.2337/db19-0936>
87. Wieggers, E. C., Rooijackers, H. M., van Asten, J. J. A., Tack, C. J., Heerschap, A., de Galan, B. E., et al. (2019). Elevated brain glutamate levels in type 1 diabetes: correlations with glycaemic control and age of disease onset but not with hypoglycaemia awareness status. *Diabetologia*, 62(6), 1065–1073. <https://doi.org/10.1007/s00125-019-4862-9>
88. Kami, K., Taguchi Ms, S., Tajima, F., & Senba, E. (2016). Improvements in impaired GABA and GAD65/67 production in the spinal dorsal horn contribute to exercise-induced hypoalgesia in a mouse model of neuropathic pain. *Molecular Pain*. <https://doi.org/10.1177/1744806916629059>
89. Levar, N., van Leeuwen, J. M. C., Puts, N. A. J., Denys, D., & van Wingen, G. A. (2017). GABA concentrations in the anterior cingulate cortex are associated with fear network function and fear recovery in humans. *Frontiers in Human Neuroscience*, 11, 202. <https://doi.org/10.3389/fnhum.2017.00202>
90. Ganesan, V., Skladnev, N. V., Kim, J. Y., Mitrofanis, J., Stone, J., & Johnstone, D. M. (2019). Pre-conditioning with remote photobiomodulation modulates the brain transcriptome and protects against MPTP insult in mice. *Neuroscience*, 400, 85–97. <https://doi.org/10.1016/j.neuroscience.2018.12.050>
91. Salehpour, F., Hamblin, M. R., & DiDuro, J. O. (2019). Rapid reversal of cognitive decline, olfactory dysfunction, and quality of life using multi-modality photobiomodulation therapy: case report. *Photobiomodulation, Photomedicine, and Laser Surgery*, 37(3), 159–167. <https://doi.org/10.1089/photob.2018.4569>
92. Saliba, A., Du, Y., Liu, H., Patel, S., Roberts, R., Berkowitz, B. A., et al. (2015). Photobiomodulation mitigates diabetes-induced retinopathy by direct and indirect mechanisms: evidence from intervention studies in pigmented mice. *PLoS ONE*, 10(10), e0139003. <https://doi.org/10.1371/journal.pone.0139003>